NIPAM-collagen I hybrid cell scaffolds for modeling lymphoid stromal networks

A Barnes[1-3], B Glaysher[1], J Lapworth[3], P Genever[2], S Rimmer[3] and M Coles[1].

[1]Centre for Immunology and Infection, [2] Biomedical Tissue Research Group, University of York, UK. [3]Department of Chemistry, University of Sheffield, UK.

INTRODUCTION: Both Collagen I and N-isopropylacrylamide (NIPAM) hydrogels undergo gelation at physiological temperatures and have been shown to be biocompatible. On their own both materials are less than ideal as cell scaffolds, collagen I is prone to cell contraction, whilst NIPAM gels undergo syneresis. Combining these two materials can overcome this and exploit the biocompatibility and cell adhesiveness of collagen I and the mechanical strength of NIPAM.

To demonstrate this we have used blends with high and low NIPAM content for tissue engineering applications of mesenchymal stem cells (MSCs). Within our group we have previously developed a 2D model of lymphoid stroma using adipose derived stem cells (ADSCs) and this is has been brought into 3D through utilising low NIPAM collagen I gels as scaffolds.

METHODS: Poly (NIPAM-*co*-styrene)-*graft*–poly(N-vinylpyrrolidone) (NSN) was synthesised as previously described [1]. Whilst collagen I was extracted from rat-tail tendon and solubilised in acetic acid. Hybrid gels were created by mixing the NSN hydrogel and collagen I at 4^{o} C and then gelled by incubating at 37^{o} C.

RESULTS: To assess the mechanical properties of the NSN gels rheological measurements were carried out. Collagen I gels at physiological concentration (3 mg/ml) have a low shear modulus of 66.6 Pa, Addition of 5 mg/ml NSN hydrogel, increases this to 122 Pa similar to soft biological tissues such as the mammary gland and the lymph node [2], highlighting the suitability of this blend for modeling the lymph node. Addition of higher concentrations of NSN have a more significant effect, 50 mg/ml increases the shear moduli to 11301 Pa.

The presence of NSN hydrogel also affects the microstructure of collagen I gels. SEM imaging shows a more porous, open network as the NSN content increases. Tan δ values; reinforce this showing the particle association within the gels reduces as the NSN content increases.

To mimic the lymphoid stromal network ADSCs were treated with inflammatory cytokines, which induced the expression of lymphoid stromal markers ICAM-1, VCAM-1 and podoplanin. The cells need to be maintained at high density to produce a suitable model, and in collagen alone this density contracts the gel. ADSCs can form uniform dense cellular networks within the low NSN content hybrid gels and remain viable for at least 5 days, without gel contraction.

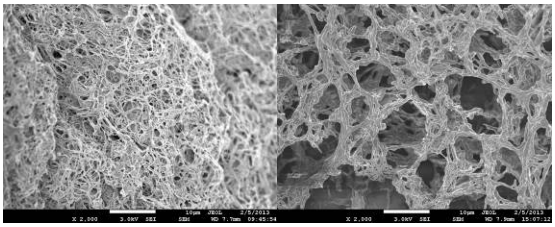

Fig. 1 SEM micrographs of collagen I (3 mg/ml) left, and collagen I (3 mg/ml) NSN (12.5 mg/ml) hybrid gel. The NSN containing gel is more open and porous.

Table 1. Tan δ values of hybrid gels

Collagen content (mg/ml)	NSN content (mg/ml)	Tan δ
3	50	0.77
3	5	0.12
3	0	0.10

DISCUSSION & CONCLUSIONS: In summary, hybrid gels of collagen I and NSN exploits the advantages of the individual materials producing an overall better cell scaffold. The presence of NSN within collagen I gels increases the mechanical properties of the material, thus improving the bio mimicry of the scaffold for various soft biological tissues. Low NSN content gels reflect the stiffness of the lymph node and can support the formation of lymphoid induced ADSC cell networks in-vitro.

REFERENCES: [1]J W Lapworth et al (2012) *Interface* **9**: 362-75. [2] I Levental, P C Georges and P A Janmey (2007) *Soft Matter* **3:**299-306

ACKNOWLEDGEMENTS: EPSRC and DTC TERM for funding and support in this research.

Influence of cell seeding and fluid flow on cell aggregate growth in a hollow fibre bioreactor

L A C Chapman[1,2], R J Shipley[3], M J Ellis[4], J P Whiteley[2], H M Byrne[1,2], S L Waters[1]

[1]*Math. Inst., Univ. of Oxford.* [2] *Dept. of Comp. Science, Univ. of Oxford.*[3] *Dept. of Mech. Eng., UCL.* [4]*Dept. of Chem. Eng., Univ. of Bath*

INTRODUCTION: A long-term goal of culturing cells in hollow fibre bioreactors (HFBs) is to expand cell populations to clinically useful numbers[1]. The cell yield depends on the seeded cell distribution and the flow environment, through nutrient delivery and fluid shear. We develop a simple 2D mathematical model of cell aggregates growing over the membrane in a HFB to explore the coupling between these features.

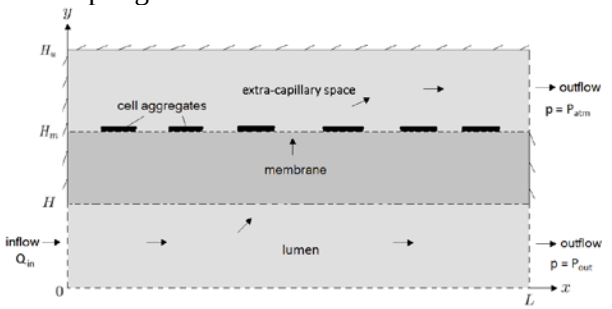

Fig. 1: Diagram of HFMB modelling set-up. p = fluid pressure, Q_{in} = inlet flow rate, P_{out} = lumen outlet pressure, P_{atm} = atmospheric pressure

METHODS: We exploit the small aspect ratio of the lumen to simplify the fluid and oxygen transport equations and solve them numerically for a prescribed initial aggregate distribution. Aggregates are assumed to increase/decrease in length at a rate which depends on the local oxygen concentration and shear stress[2,3] (see Fig. 2).

We use our model to simulate aggregate growth, over a period of 40 days with different initial aggregate distributions, lumen inlet flow rates (0.02-2.3ml/min) and outlet pressures (14.9-19psi). We record either the time at which the aggregates reach confluence or their total length after 40 days.

RESULTS: Increasing the inlet flow rate and lumen outlet pressure led to a monotonic increase in the oxygen concentration around and maximum shear stress over the aggregates (from 0.01Pa to 0.2Pa). For typical oxygen uptake rates for various cell types (10^{-18}-10^{-17}mol/s/cell), the oxygen concentration was well above the threshold for cell viability. Aggregate growth was highly sensitive to the shear tolerance of the cell type. Cell types able to withstand higher shear stresses (≥0.2Pa) reached confluence increasingly rapidly as the flow rate and outlet pressure were increased due to greater oxygen delivery and shear stimulation (Fig. 3). The initial aggregate distribution also had a major impact on the rate of aggregate growth, due to the non-uniform oxygen and shear stress distributions over the aggregates.

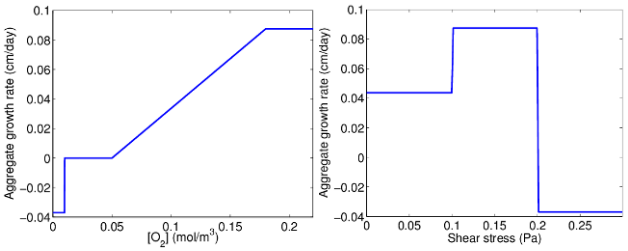

Fig. 2: Prescribed dependence of aggregate growth rate on oxygen concentration (left) and shear stress (right).

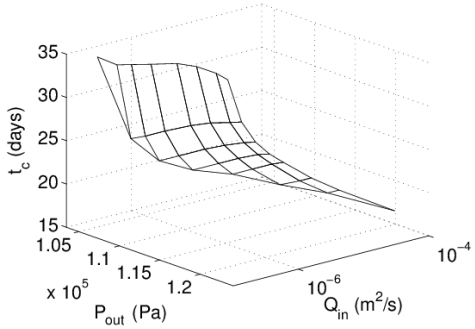

Fig. 3: Time taken, t_c, for aggregates of rat cardiomyocytes to reach confluence for different values of Q_{in} and P_{out}. (Results from numerical simulations).

DISCUSSION & CONCLUSIONS: Our results indicate that the optimum flow rate and outlet pressure for culturing cells in a HFB is highly specific to the cell type, and in particular how it responds to shear stress. Whilst increasing the flow rate and outlet pressure can reduce the time the cells take to reach confluence by increasing oxygen delivery and shear stimulation, care must be taken to avoid damaging or killing the cells by using too high a shear stress.

REFERENCES:

[1]M.J. Ellis, J.B. Chaudhuri (2007) *Biotech. and Bioeng.* **96**:177-187.

[2] R.J. Shipley, S.L. Waters (2012) *Math. Med. Biol.* **29**:329-359.

[3] R.D. O'Dea, S.L. Waters, H.M. Byrne (2010) *Math. Med. Biol.* **27**:95-127.

ACKNOWLEDGEMENTS: The authors thank the EPSRC for funding this work.

Spatial dependent mechanical properties of hydroxyapatite biopolymers composite for tissue engineering

J. Chen[1,2*], M. Capstick[1]

[1] *School of Mechanical and System Engineering, Newcastle University, UK.*

[2] *Arthritis Research UK Tissue Engineering Centre, Newcastle University, UK.*

*E-mail: Jinju.chen@ncl.ac.uk

INTRODUCTION: Composites of hydroxyapatite (HA) and biodegradable polymers such as poly(lactic acid) (PLA) have been used as scaffold materials for bone tissue engineering [1,2]. Nanocrystalline HA is preferred over the coarser crystals because it is expected to have better bioactivity and improved toughness. However, when the nano-HA particles were dispersed in the biopolymers they tend to form microscale or submicroscale agglomeration which is nearly spherical shape [3]. As the cell senses elastic properties of the matrix at nanoscale to microscale [4], it is important to investigate how the composite mechanical properties changes at different length scale. In this study, finite element (FE) simulations were used to study spatial dependent mechanical properties of HA-biopolymer composites.

METHODS: For simplicity**,** we consider an effective spherical HA particle cut through at mid-plane which was embedded in various biopolymers such as polylactic acid (PLA) and polyglycolic acid (PGA). Fig. 1 shows the FE mesh of indentation of HA embedded in biopolymer. The effective radius of 1μm was considered. The elastic-plastic properties of HA particle and biopolymer matrix taken from literature [5-6] were used as input values in the FE model. The indentation depth varies from 30nm to 100nm.

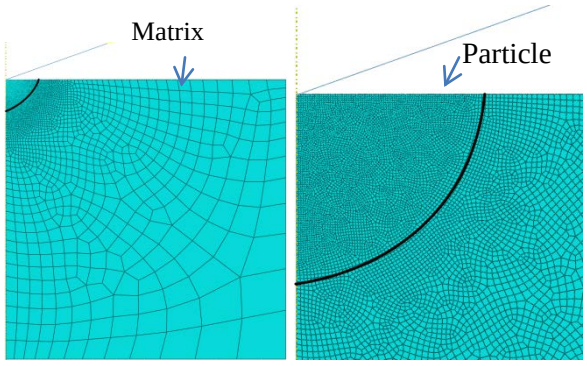

Fig. 1: Details of finite element mesh of indentation of HA embedded in biopolymer.

RESULTS: Fig. 2 shows von mises stress contour for indentation of HA particle embedded in PLA and PGA at penetration of 50nm. Fig. 3 shows how the elastic modulus and hardness of the HA-biopolymer composites vary with penetrations.

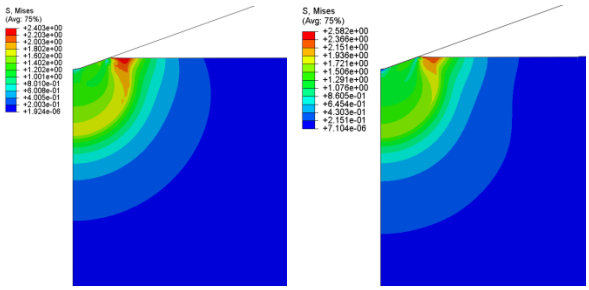

Fig. 2: Von mises stress contour for indentation of HA particle embedded in PLA and PGA at penetration of 50nm.

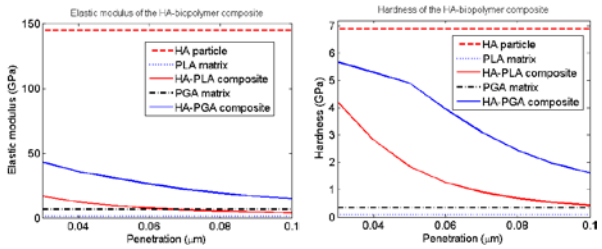

Fig. 3: Elastic modulus and hardness of HA – biopolymer composites at various indentation penetrations.

DISCUSSION & CONCLUSIONS: The elastic-plastic properties of matrices affect the stress magnitude and pattern in the HA-biopolymer composites. The elastic modulus decays with the penetration much quicker than the hardness due to the long range elastic stress field effect. The biopolymer matrix starts to contribute to the elastic-plastic properties of the composite even at the depth of 3% of the particle radius. This will provide useful information to understand how cells may sense the mechanical properties of the composite scaffold materials.

REFERENCES: [1]K.G.Marra, et al (1999) *J. Biomed. Mater. Res. A* **47**: 324-335. [2]C. Durucan and P.W. Brown (2000) *J. Biomed. Mater. Res. A* **51**: 726-734. [3]K. Sato, et al (2006) *J. Mater. Sci.* **41**: 5424-5428. [4]A.J. Engler, et al (2006) Cell. **126**: 677-689. [5]A.Zamiri and S. De (2011) J.Mech.Behav.Biomed. **4**:146-152. [6] K.V.de Velde and P. Kiekens, Polym.Test. (2002) **21**:433-442.

GDF6 drives discogenic differentiation of human mesenchymal stem cells encapsulated in type I collagen gels

L E Clarke[1], S M Richardson[1], J A Hoyland[1]

[1] *Centre of Regenerative Medicine, Institute of Inflammation and Repair, University of Manchester, Manchester, UK*

INTRODUCTION: Mesenchymal stem cells (MSCs) have been proposed as a suitable cell source for cell-based therapies aimed at repairing the degenerate IVD. Both bone marrow derived and adipose derived MSCs (BM-MSCs and AD-MSCs respectively) have demonstrated the capacity to proliferate and differentiate into multiple connective tissue lineages, including the NP phenotype[1]; however, at present there is no standard protocol to do this. We have previously demonstrated that GDF5 and GDF6 are expressed in human NP cells[2] and a recent study has demonstrated GDF5 can enhance the differentiation of bone marrow MSCs (BM-MSCs) to a discogenic phenotype[3]. Therefore the aim of this study was to investigate the effects of GDF5 and GDF6 on discogenic differentiation of both BM-MSCs and AD-MSCS.

METHODS: Patient matched human AD-MSCs and BM-MSCs (n=7) were seeded into type I collagen hydrogels (Devro) at a density of 4 x 10^6 /ml. Seeded hydrogels were then cultured in a differentiating media consisting of high glucose DMEM supplemented with 1% FCS, ITS (Gibco), 10^{-7} M dexamethasone. Differentiating media was further supplemented with TGF-β3 10ng/ml, GDF5 100ng/ml or GDF6 100ng/ml and media changed every 48 hours. After 14 days QPCR analysis of classic chondrogenic (SOX9, COL2 and ACAN) and novel NP (KRT8, 18, 19, CAXII, FOXF1, and T) markers was undertaken. PG content (n=3) of the construct and media components were analysed using the dimethylmethylene blue (DMMB) assay

RESULTS: Culture of AD-MSCs in the presence of GDF6 resulted in a significant increase in expression of all novel NP marker genes compared to culture with TGF-β or GDF5. Both GDF5 and GDF6 resulted in significantly higher ACAN expression in AD-MSCs than in cells cultured with TGF-β. Culture of BM-MSC in the presence of GDF6 resulted in a significant upregulation of all novel NP markers compared to culture with either GDF5 or TGF-β. When comparing between AD-MSC and BM-MSC for the GDF6 treatment groups gene expression was significantly higher for the discogenic makers in AD-MSCs. PG content was significantly greater in GDF6 treated AD-MSCs compared to GDF5 and TGF-β treatment (*Figure 1).*

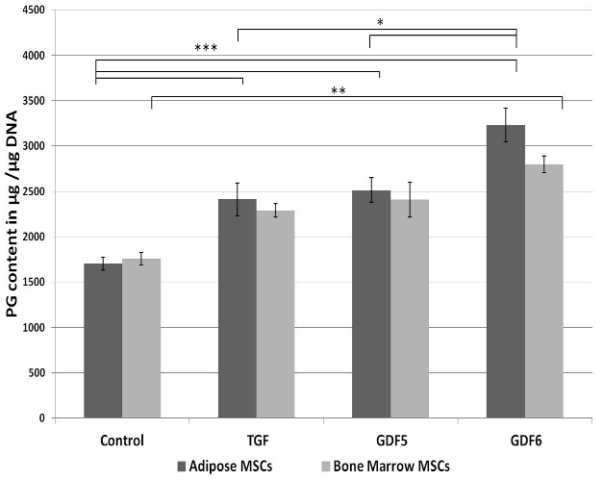

Fig. 1: DMMB analysis of PG content in both AD-MSCs and BM-MSCs.

DISCUSSION & CONCLUSIONS: Both AD-MSCs and BM-MSCs seeded in hydrogels and supplemented with GDF6 undergo discogenic differentiation. However AD-MSC and BM-MSC responded to GDF6 stimulation in a different manner, which resulted in a more discogenic phenotype in AD-MSCs. Treatment with GDF6 also resulted in a greater PG content in both cell types, particularly AD-MSCs suggesting the growth factor is inducing a matrix that is more akin to the native tissue. In conclusion AD-MSCs may be the preferred cell choice for regenerative strategies in the IVD and GDF6 may be an important factor for preconditioning or for incorporation into biomaterials to ensure discogenic differentiation of implanted cells.

REFERENCES: [1]Minogue et al., *Arthritis Rheum*, 2010,62: 3695-705 [2] Le Maitre et al., *Arthritis Res Ther*, 2009, 11:R137 [3]Stoyanov, J.V.et al. *Eur Cell Mater* 2011; 21: 1533-154

Decellularised rat liver and jejunum bioscaffolds for neovascularisation in tissue-engineered skin

L Dew[1], CK Chong[1], S MacNeil[1]

[1] *Kroto Research Institute, Department of Materials Science and Engineering, University of Sheffield, UK*

INTRODUCTION: Delays in developing new vasculature after tissue transplantation is a major problem in getting tissue-engineered (TE) skin to survive on the patient's wound bed[1,2]. To overcome this we aim to induce neovascularisation in TE skin using a bioreactor and 'pre-vascularised' skin, obtained by incorporating TE skin with a re-endothelialised biological vascular network. The work focuses on the decellularisation of rat liver and jejunum to establish the bioscaffolds with preserved vascular networks and discusses preliminary recellularisation results.

METHODS: *Decellularisation* - Rat liver and jejunum were harvested from fresh cadavers. The inferior vena cava (IVC) of the liver and main vessel of the mesentery were cannulated. The vasculatures were flushed thoroughly with heparin solution and distilled water before treatment of 1% Triton-X 100. Distilled water was then circulated to remove residual detergent and the resultant matrices were sterilised using 0.1% peracetic acid. Residual peracetic acid was removed with sterile PBS. Blue dye was then injected into the resultant matrices to assess vascular patency. Low magnification and confocal microscopies along with microCT imaging were used to further examine the networks. Histochemical and DAPI stainings were used to characterise the composition of the matrices.

Recellularisation - Dermal fibroblasts were injected through the IVC of the decellularised liver and subsequently perfused continuously with cell culture medium for 5 days at 37˚C. Samples were taken at days 1, 3 and 5 for histological analysis. Using a similar procedure, the jejunum was injected with oral fibroblasts that had been stained with CellTracker red. Samples were taken at days 1 and 3 for histological analysis, fluorescence microscopy and cell viability tests using the MTT assay.

RESULTS: *Decellularisation* - A well-defined vascular tree with multiple branching was visible from blue dye injection and imaging techniques. Histochemical analysis showed staining expected from proteinous ECM but no evidence of cells. The latter point was confirmed with DAPI staining.

Recellularisation – Histochemical analysis showed that in both cases the cells attached to the matrices and seemed to occupy the blood vessels. The use of the MTT assay showed the presence of viable cells within the matrices.

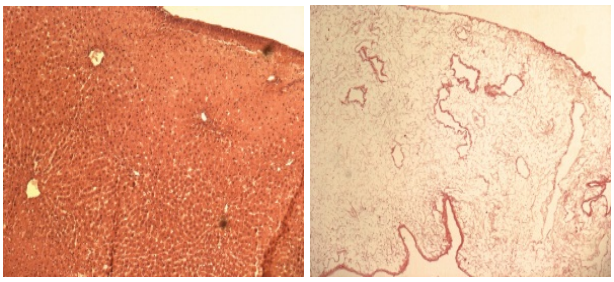

Fig. 1: H&E staining of intact liver (left) and decellularised liver (right)

DISCUSSION & CONCLUSIONS: The decellularisation procedure appears effective in preserving the architecture of the matrices whilst removing most of the cellular matter. Preliminary results from the recellularisation work shows that the cells attach to the matrices and are viable. The current protocols appear to be effective in establishing bioscaffolds with preserved vascular networks.

REFERENCES: [1] MacNeil, S., Progress and opportunities for tissue-engineered skin. *Nature, 2007*. **445**(7130): p. 874-880. [2] Sahota, P.S., et al., *Development of a reconstructed human skin model for angiogenesis.* Wound Repair and Regeneration, 2003. **11**(4): p. 275-284.

ACKNOWLEDGEMENTS: This work is funded by the EPSRC.

Switching Alginate/Collagen Hydrogels tailored for Human Pluripotent Stem Cell Self-renewal and Differentiation.

James E. Dixon[1*], Catherine Rogers[1], Disheet A. Shah[1], Stephen Hall[2], Chris Denning[3] and Kevin M. Shakesheff[1]

Wolfson Centre for Stem Cells, Tissue Engineering, and Modelling (STEM), Centre of Biomolecular Sciences, School of Pharmacy[1], School of Clinical Science[3], Medical Engineering Unit[2], University of Nottingham, Nottingham, UK.

INTRODUCTION: Human Pluripotent Stem cells (HPSCs) have the ability to generate any tissue given the correct developmental cues. Therefore Human Embryonic Stem cells (HESCs) or Induced Pluripotent Stem cells (HiPSCs; generated directly from patient cells) represent the ideal sources for tissue engineering and regenerative medicine. Hydrogel systems are proven matrices to culture and deliver cells in complex geometries however three-dimensional (3D) constructs quickly develop necrotic cores and no simple hydrogel has been described for HPSCs. Furthermore the matrix microenvironment ultimately needs to be suitable for cell self-renewal, and differentiation or switch between both if the potential of HPSCs is to be realised.

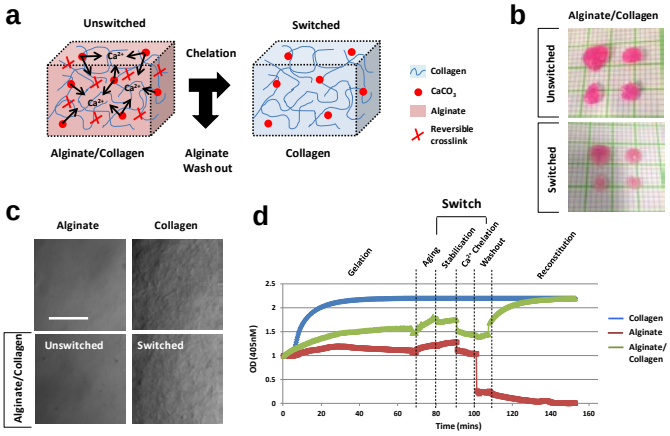

Figure 1 | The Alginate/Collagen Switching Micro-environment. **a**, Schematic of the switching hydrogel system. **b**, Example 3D geometries created using the Switching Hydrogel system. (grid; 1mm). **c**, Confocal analyses of collagen fibres with transmission imaging demonstrating that in the presence of alginate that collagen fibre formation is significantly inhibited (bar, 20µm). **d**, Spectroscopy measuring collagen fibre character during cross-linking and switching of hydrogels.

METHODS: Composite hydrogels were created by mixing and alginate was crosslinked/decrosslinked with $CaCO_3$/GDL and Citrate/EDTA, respectively.

RESULTS: Here, we generated a method to produce conditions (alginate/ collagen/ Matrigel™/PVA hydrogels) which are permissive for 3D self-renewal of HESCs in load-bearing complex geometries. Using mild ionic decross-linking hydrogel micro-environment may be switched to one permissive for differentiation and construct geometry is retained. Because the timing of this switching process can be varied we demonstrated that the switch may be tailored to the differentiation of HPSCs into specific lineages. We show the differentiation of HESC line, HUES7, into germ-layer lineages which may be directed by simple micro-environmental switching. Furthermore we exploit this system to control the efficiency of differentiation of HPSCs to cardiomyocytes by either by growth factor[1]- or transcription factor[2]-driven differentiation which is dependent on switching.

DISCUSSION & CONCLUSIONS: We have demonstrated that the alginate masking of collagen can be modified to allow the propagation of HPSCs which are exceptionally sensitive to culture conditions. Tailoring micro-environmental changes as well as growth factor[1]- and small molecule[2]-directed manipulation will be an important parameter when producing human engineered tissues. Our proof-of-principle demonstration of expansion of HPSCs into specific tissue geometries followed by *in situ* differentiation will aid future tissue engineering efforts for regenerative medicine applications.

REFERENCES:

Burridge et al. (2011). *PLoS one* **6**:e18293[1].
Paik, et al. (2012). *Biotech Bioeng* **109**:2630-41[2]

ACKNOWLEDGEMENTS: This work was funded by the BBSRC, ERC and Regentec.

A bilayered electrospun scaffold to replace the corneal stroma: the use of topography to guide cell phenotype

S Dunphy[1], HS Dua[2], AJ El Haj[3], A Hopkinson[2], FRAJ Rose[1]

[1]School of Pharmacy, University of Nottingham, UK. [2]Division of Ophthalmology and Visual Sciences, University of Nottingham, UK. [3]ISTM, Keele University, UK.

INTRODUCTION: Donor shortages and graft rejection have led to the search for a tissue-engineered alternative to corneal allografting. In this study, a bilayer of electrospun PLGA micron and sub-micron diameter fibres was used to mimic anatomical features of the anterior cornea: stroma and epithelium. The construct comprised a porous microfibrous layer (stroma) to allow infiltration of keratocytes and a dense layer of nanofibres on top to act as a *pseudo* basement membrane to support the epithelium.

METHODS: Scaffolds with fibre diameters in the nanometer range were manufactured by electrospinning 12 wt% solution of PLGA (75:25) in 1,1,1,3,3,3,hexafluoro-iso-propanol. Microfibres were produced using 25 wt% solution in dichloromethane. Primary human corneal stromal stem cells (hCSSC) and SV40-immortalised human corneal epithelial cells (ihCEC) were cultured on the scaffolds. Proliferation (Alamar blue), viability (LIVE/DEAD), phenotype (SEM, ICC), and gene expression (PCR) were assessed.

RESULTS: Scaffolds supported cell adhesion and proliferation. The microfibrous layer permitted ingrowth of hCSSC.

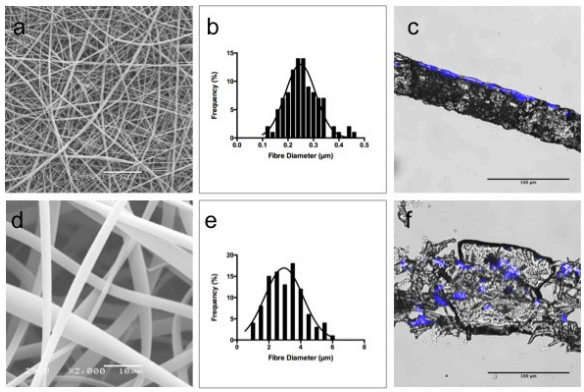

Fig. 1: Scanning electron micrographs showed the morphphology of (a) nanofibres and (d) microfibres. Corresponding fibre diameter distributions in (b) and (e), respectively. DAPI-stained cross-sections of ihCSSC showed level of cellular infiltration into (c) nanofibres and (f) microfibres.

The provision of a porous 3D microenvironment with important topographical cues had the ability to promote the keratocyte phenotype *in vitro*. Moreover, a more dendritic morphology was observed on the microfibres, with a reduction in stress fibres, and expression of keratocyte markers such as ALDH, Keratocan, and CD34.

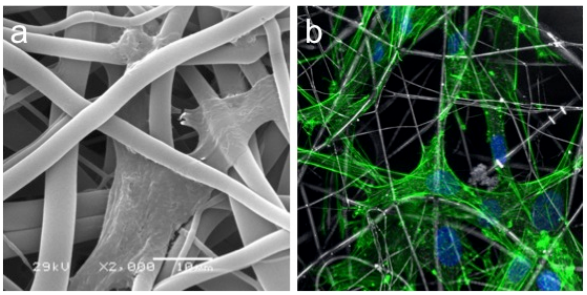

Fig. 2: hCSSC infiltrated the microfibres shown by (a) SEM, and (b) confocal microscopy of immunostaining for F-actin. Cell nuclei counterstained with DAPI. Cells attached to single fibres and appeared dendritic.

Formation of a confluent monolayer of ihCEC and the establishment of cellular junctions (E-caderin, ZO-1) was shown on the closely-packed nanofibres.

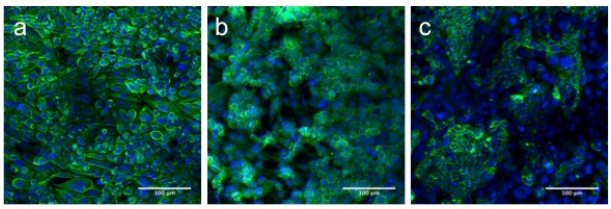

Fig. 3: Immunostaining of ihCEC on nanofibres. Formation of a confluent, stratified layer of ihCEC was established as evidenced by (a) F-actin, (b) ZO-1, and (c) E-cadherin. Cell nuclei counterstained with DAPI. Scale bar = 100 µm.

DISCUSSION & CONCLUSIONS: A bilayered scaffolding approach may be appropriate for corneal wound repair; a microfibrous or 'stromal-type' environment to allow infiltration of keratocytes and a dense fibrous layer as a *pseudo* basement membrane to promote rapid establishment of a stratified epithelium.

ACKNOWLEDGEMENTS: This research was funded by the EPSRC DTC for Regenerative Medicine. We gratefully thank the Manchester Eye Bank for their generous donation of tissue.

Comparing Engineered Neural Tissue formats within a peripheral nerve repair conduit

M Georgiou, AJ Loughlin, JP Golding, JB Phillips

Life, Health and Chemical Sciences, The Open University, Milton Keynes

INTRODUCTION: The current clinical gold standard treatment for peripheral nerve repair is the nerve autograft, in which only ~50% of cases result in full functional recovery. Tissue engineered cellular bridging devices could provide an attractive alternative to autografts. Sheets of engineered neural tissue (EngNT), which is formed from columns of Schwann cells within a 3D aligned collagen matrix, can promote directed neurite outgrowth *in vitro*. These sheets of EngNT can be arranged to form the 'endoneurium' of a repair device. Two different arrangements, rod- and sheet-based designs, were tested within a clinically approved tube, NeuraWrap™, in a 5mm gap in the rat sciatic nerve (fig 1).

METHODS: Three experimental constructs were tested in rat sciatic nerve to repair a 5mm gap, with a NeuraWrap™ sheath containing either (A) 2 EngNT rods; (B) 2 EngNT sheets; or (C) an empty conduit. For (B) the 2 EngNT sheets were used to line the tube prior to closure, maintaining a lumen. Animals were culled after 4 weeks and repaired nerves were excised. Cross sections were taken from the proximal part of the construct and stained to detect neurofilament, revealing where the axons were growing in relation to the EngNT structures (this was divided into 3 zones for the analysis, fig 2).

RESULTS: The axon density was significantly greater in zone 1 than in zone 3 in the devices ($P<0.05$, one-way ANOVA). The rod-based arrangement (A) gave a higher axon density in zone 1, 3350 ± 143 axons/mm^2 (mean ± SEM), compared to the sheet-based arrangement (B) (2920 ± 587 axons/mm^2).

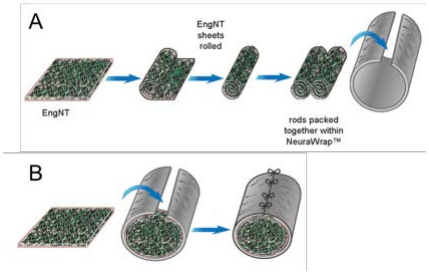

Fig. 1: The different device formats: (A) rod-based and (B) sheet-based.

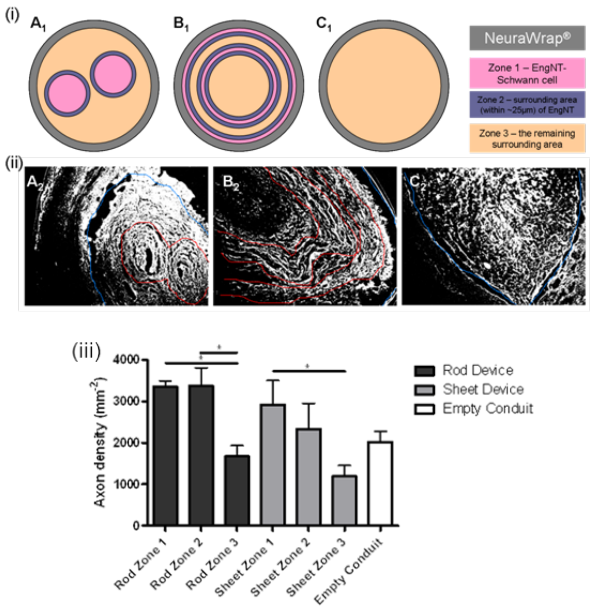

*Fig. 2: The different zones within a cross-section from an EngNT device post-implantation. (i) different zones within the different device designs: EngNT rods (A); EngNT sheets (B); and the empty NeuraWrap™ tube (C). (ii) Fluorescence micrographs showing cross-sections after 4 weeks in vivo, for 3 different device designs. The red outlines the EngNT material and the blue outlines the device core. (iii) One-way ANOVA with Tukey's post-test was used to compare three zones within each device group (*P<0.05). An empty conduit was also included. T-tests were performed to compare the equivalent zone between each of the two device designs (no significant differences). Data are means ± SEM, n=4.*

DISCUSSION & CONCLUSIONS: The rod-based arrangement was more stable; there were no observed changes to its structure or orientation as a result of surgical handling or limb movement post-implantation. The designs are modular and can be adapted for the repair of bigger nerves by, for example, having multiple rod structures in the core of outer tubes or sheath wraps. Aligned cellular EngNT rods can form the basis of a functional conduit for peripheral nerve repair.

ACKNOWLEDGEMENTS: This research was funded by an Open University Studentship.

Using acoustic tweezers to pattern Schwann cells for axon guidance

F Gesellchen[1], AL Bernassau[2], T Dejardin[1], DRS Cumming[2], MO Riehle[2]

[1]Centre for Cell Engineering, College of Medical Veterinary & Life Sciences, University of Glasgow [2]Microsystem Technology Group, School of Engineering, University of Glasgow

INTRODUCTION: Schwann cells (SC) play a central role in peripheral nerve repair by promoting and guiding neurite outgrowth[1]. This has been exploited in various scaffold-based tissue-engineering approaches that use topographical cues to align Schwann cells and guide regenerating axons[2,3]. Here we present a novel method to align Schwann cells with an acoustic tweezer device[4] to guide axon outgrowth from neonatal rat dorsal root ganglia (DRGs) without the need for microfabrication of polymer substrates.

METHODS: Schwann cells were isolated from neonatal rat sciatic nerve by positive selection with an anti-NGFR antibody followed by magnetic cell separation. The heptagon sonotweezer device used in this study is described elsewhere[4]. For SC patterning, a poly-L-lysine coated cover slip was placed in the centre of the device in 0.5 mL of SC growth medium (SCGM). Two non-adjacent piezoelectric transducers were activated to generate a pattern of parallel acoustic traps at the centre of the device before adding ~50,000 cells for patterning. Randomly seeded SC served as a control. After cells had adhered, cover slips were transferred to a 24-well plate and incubated for 16h at 37˚C. Freshly explanted rat DRGs were seeded onto patterned or randomly seeded SC in 200 µl of SCGM and incubated for a further 4-5 days to allow axon outgrowth. Cultures were fixed and stained with an anti-β3-tubulin antibody. The entire axon network was imaged on an Olympus BX51 fluorescence microscope equipped with a scanning stage. Image analysis was performed using the OrientationJ plug-in for ImageJ (http://bigwww.epfl.ch/demo/orientation/) to analyse directionality of axon growth on cover slips with patterned and randomly seeded SC.

RESULTS: Schwann cells patterned with the acoustic tweezer retained their parallel alignment for at least 16h (*Fig. 1A*). 24 h after seeding the DRGs the pattern was in most cases no longer discernible, due to outgrowth of cells and neurites from the DRG. Nonetheless, after 4 d in culture, axon outgrowth on patterned SC cultures displayed a preference in direction compared to randomly seeded cultures (*Fig. 1B*). The dominant direction of axon growth was found to be within ± 30˚ of the initial SC pattern while directionality varied randomly on non-patterned SC cultures. This suggests that the initial pattern of Schwann cells guided axon outgrowth from the DRG.

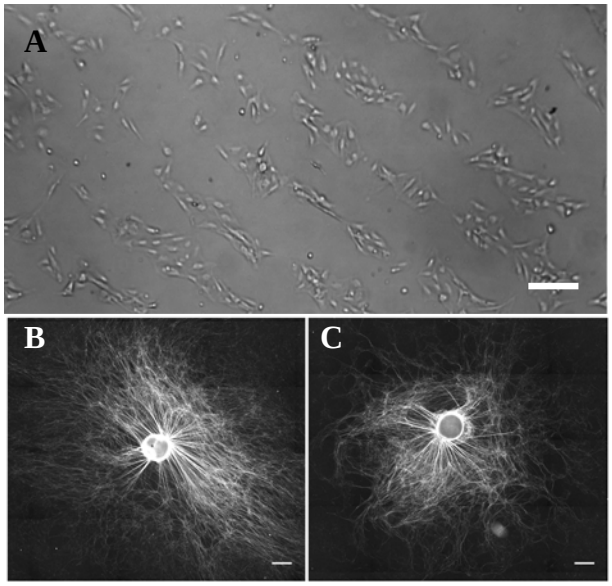

Fig. 1: (A) SC 16h after patterning. Scale=200µm (B, C) Axonal network (β3-tubulin) of regenerating DRG on patterned (B) and random (C) SC cultures. Scale=500µm

DISCUSSION & CONCLUSIONS: While patterning of SCs for nerve repair using micropatterned surfaces is well established, this is to our knowledge the first report of SCs patterned on a non-structured surface for successful axon guidance. With our device's capability to shift the position of acoustic traps, this scenario could easily be extended to generate a co-culture of SCs and fibroblasts to promote deposition of basal lamina. Patterning methods using acoustic force have the potential to become a valuable addition to the tissue engineering arsenal.

REFERENCES: [1]M.D. Ard, R.P. Bunge, and M. B. Bunge (1987) *J Neurocytol* **16**, 539–555. [2]D. M.Thompson, and H. M. Buettner (2004). *Ann Biomed Eng* **32**, 1120–1130. [3] K. E. Schmalenberg, and K. E. Uhrich, (2005) *Biomaterials* **26**, 1423–1430. [4] A.L. Bernassau, F. Gesellchen, et al. (2012) *Biomedical Microdevices* **14**(3), 559-564.

Development of novel, non-invasive stem cell imaging technologies

Glen A[1], Masia F[2], Curtis DJ[4], Hunter S[3], Borri P[3], Langbein W[2], Stephens P[1]

[1]Wound Biology Group, Tissue Engineering and Reparative Dentistry, Cardiff Institute of Tissue Engineering and Repair, School of Dentistry, [2]School of Astronomy and Physics and [3]School of Biosciences, Cardiff University, Cardiff, Wales (Email: GlenA@cf.ac.uk)

INTRODUCTION: A major barrier in the realisation of the therapeutic potential of embryonic stem (ES) cells has been the inability to easily, effectively and reproducibly track stem cells in an unlabelled, non-invasive and non-destructive manner in microenvironments more representative of three dimensional tissue structures. Hence, new imaging modalities are needed to advance this area of research.

METHODS: 3T3L1 cells were maintained in serum containing medium until confluent and induced to differentiate using 85nM Insulin and 2nM triiodothyronine. Mouse Embryonic Stem (mES) cells were differentiated based on a modified protocol developed by Dani *et al.* (1997). Cells were assessed both in 2D and 3D (type I collagen lattice) systems. Adipogenesis was validated using oil-o-red/fluorescent lipid staining (BODIPY 493/503) positivity (imaged by confocal laser scanning microscopy) and gene expression of PPARγ1/2, CEBPα, zfp423 and FABP4 (RT-PCR). Coherent Anti Stokes Raman Spectroscopy (CARS; a label free imaging technology) images were acquired using a micro-spectrometer with a femtosecond laser pulse. Samples for Scanning Electron Microscopy (SEM) were dried by sequentially dehydration with increasing percentages of ethanol and imaged.

RESULTS: 3T3L1 and mES cells were specified to adipocytes and imaged non-destructively (no exogenous label) by CARS in 2D (Figure 1). CARS can be utilized to differentiate between different cell types based on distinct spectral qualities (Figure 2). mES cells can be differentiated to adipocytes in 3D, imaged by CARS and additional data obtained about the surrounding 3D matrix by second harmonic generations (Figure 3).

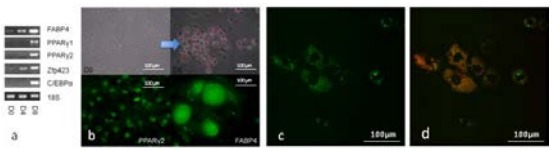

Fig. 1: Induction of 3T3L1 and mouse ES cells in 2D towards adipocytes with (a) molecular, (b) protein, (c) CARS validation [no exogenous staining] and (d) a combination of CARS and oil-o-red staining [CARS = green, oil-o-red = red].

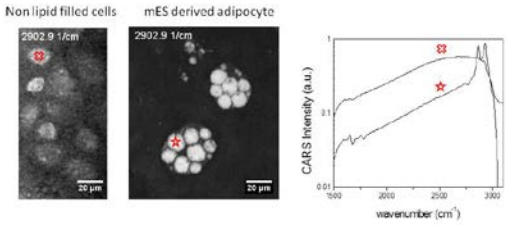

Fig. 2: mES derived adipocytes demonstrate differences in CARS spectra when compared to non lipid filled cells in the same sample.

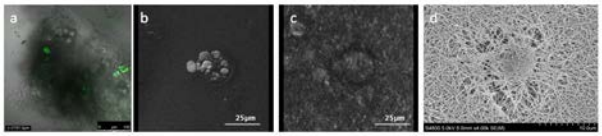

Fig 3: Induction of mES cells towards adipocytes in 3D. (a) A confocal image (stained with BODIPY 493/503) of adipocytes formed in a type I collagen matrix, (b) CARS imaging of adipocytes in 3D with (c) the surrounding collagen structure imaged via second harmonic generation. (d) The comparable collagen lattice structure as assessed by SEM.

DISCUSSION & CONCLUSIONS:

- Novel mES to adipocyte 3D protocols have been developed
- CARS can be utilised for non-destructive, non-invasive imaging of cells
- mES derived adipocytes demonstrate differences in spectral output when compared to adjacent non lipid filled cells
- CARS could be a useful non-destructive technique for the demonstration and delineation of stem cell lineage commitment/fate

REFERENCES: Dani et al. (1997). *J Cell Sci.* **110**: 1279-85

ACKNOWLEDGEMENTS: King Yim Osbert Cheung and N Badiei for assistance with SEM sample preparation.

Antibacterial graft copolymer gels

A.C. Harvey[1], S.P. Armes[1], C.W.I. Douglas[2] and S. MacNeil[3]
1- Department of Chemistry ,Dainton Building, University of Sheffield, Brook Hill, Sheffield
2-Department of Oral Pathology, School of Clinical Dentistry, University of Sheffield, Claremont Crescent ,Sheffield
3- The Kroto Research Institute, Department of Engineering Materials, University of Sheffield, Broad Lane ,Sheffield

INTRODUCTION: The aim of the current study is to explore the relationship between polymer composition and architecture, and how this affects antibacterial actions. This work continues and investigates the anti-bacterial activity towards *staphylococcus aureus* [SA] of various different thermo responsive copolymers based on 2-(meth acryloyloxy)ethylphosphorylcholine [MPC] and 2-hydroxy propyl methacrylate [PHPMA].[1,2] These gels did not reduce skin cell viability.

METHODS: Polymers were synthesized using either atom transfer radical polymerization [ATRP] or reversible addition-fragmentation [RAFT] polymerization and characterized via ^{1}H NMR, GPC and rheology.

Fluorescently-labeled copolymers were prepared to view their interactions with bacteria. Anti-bacterial activity was assessed using several well-known assays, including release of lactate dehydrogenase [LDH] and TEM imaging.

RESULTS:

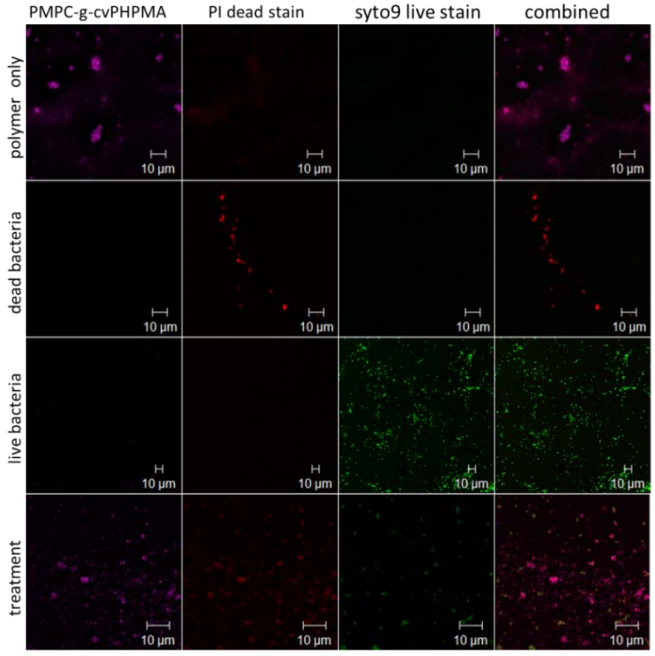

Fig. 1: Confocal fluorescent microscopy showing live/dead viability of SA after treatment with 10wt% PMPC-PHPMA graft copolymer.

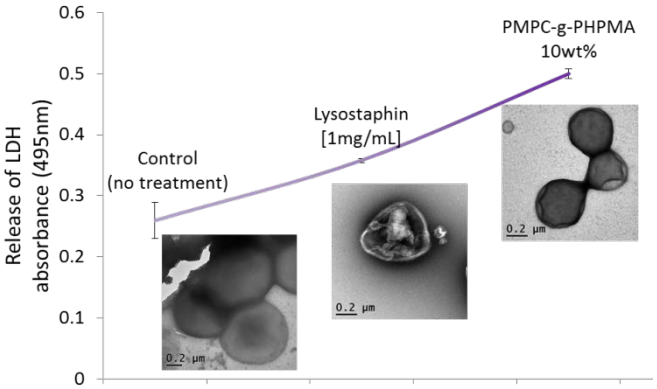

Fig. 2: MPC-g-PHPMA copolymer at 10wt% solution induced SA lysis and LDH release from SA after 24 hour treatment. Comparative data with lysostaphin and no treatment as shown. Inserts of TEM images.

DISCUSSION & CONCLUSIONS: Several physicochemical properties of the copolymer gel play an important part in the antimicrobial activity; the PHPMA 'chains' are thought to be a key component. The weakly hydrophobic properties of the PHPMA seem to be responsible for the thermo responsiveness, and possible antimicrobial activity of these copolymers. It is also possible that the PHPMA is causing selective "punching" through the membrane of the bacteria, responsible for LDH release, and subsequent effect on bacteria viability.

The composition of PMC and PHPMA alone does not predict gelation or antimicrobial activity. Architecture and concentration of the polymers has an effect on the overall activity which is very sensitive. The combination of anti-microbial activity with mammalian cell biocompatibility is unexpected for these polymers and suggests potential biomedical applications for these materials.

REFERENCES: ***1.*** *Madsen, J., et al. Journal of Materials Science, 2009. 44(23): p. 6233-6246*
2. *Bertal, K., et al, Biomacromolecules, 2008.* ***9****(8): p. 2265-75.*

ACKNOWLEDGEMENTS: BBSRC; Dr J Madsen, Dr J Rosselgong, Dr N Warren, Dr A Blanazs, Dr A Bullock, Dr N Green & Mr J Heath.

Amine functionalised synthetic hydrogels for corneal regeneration

ED Hassan[1], S Rimmer[2] F Claeyssens [1], S MacNeil [1]

[1] 1 Dept. of Materials Science & Engineering, The Kroto Research Institute, North Campus, University of Sheffield, Broad Lane, Sheffield, [2] Polymer and Biomaterials Chemistry Laboratories, Department of Chemistry, University of Sheffield, Sheffield,

INTRODUCTION: In cases of limbal stem cell deficiency conjunctival epithelial cells move over the cornea causing vascularisation and opacity. The underlying wound bed is often damaged and unresponsive to corneal transplants or limbal stem cell transplants. As a result a clinical challenge exists to develop a corneal inlay that can aid corneal re-epithelialization. Hydrogels are useful candidates for this purpose, they allow vital biomolecules to diffuse through their network and exhibit low immunogenicity due to their low interfacial tension. However traditional hydrated networks are usually non cell adhesive. The aim of this study was to overcome this limitation by developing amine functionalised synthetic hydrogels capable of selectively supporting the adhesion and proliferation of Limbal epithelial cells (LEC) to aid corneal regeneration.

METHODS: Monomers, Lauryl methacrylate, Glycerol monomethacrylate, Ethylene glycol dimethacrylate and Glycidyl methacrylate in varying ratios were dissolved in 4ml of isopropanol and purged from oxygen by bubbling Nitrogen for 20 minutes. Just before curing, 90 mg photoinitiator (1wt% monomers) was added. The solution was injected into a mould and cured under UV for 90 seconds on each side. Polymer sheets were washed in IPA to remove unreacted monomer and initiator, before functionalising in ethanolic alkyl amine solutions (250 cm^3, 5 vol%). The functional groups were ammonia, 1,2-diaminoethane, 1,3- diaminopropane, 1,4-diaminobutane or 1,6-diaminohexane.[1] Several hydrogel combinations produced optically clear gels and were assessed for cell adhesion and proliferation using rabbit limbal epithelial and stromal cells.

RESULTS: Rabbit limbal fibroblasts (RLFs) initially adhered well to 1,2 diamino ethane and 1,3 diamino propane functionalised hydrogels but detached rapidly over the next 72 hrs. In contrast, rabbit limbal epithelial cells (RLECs) adhered and proliferated on most aminated surfaces with 1,4 diamino butane performing as well as TCP over 4 days. Additionally 1,4 diaminobutane functionalised gels supported epithelial outgrowth from limbal explants.

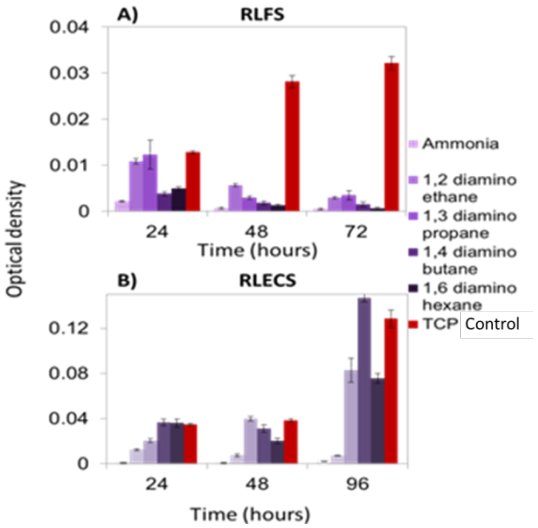

Fig. 1:MTT- assay of RLFs A) and RLECs B) on amine functional hydrogels

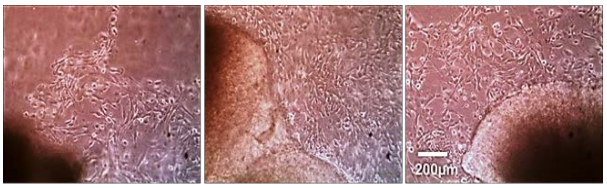

Fig. 2 Light microscopy images of epithelial outgrowth from limbal explants cultured on 1,4 diaminopropane functional hydrogels, after 6 days.

DISCUSSION & CONCLUSIONS: Using a combination of monomers that contribute specific properties it is possible to tune hydrogels to selectively support limbal epithelial cells for regenerating damaged corneas that lack residual limbal epithelial stem cells. Gels which had a higher water content and functionalised with 1,4 diamino butane were most successful at supporting RLEC adhesion and proliferation while inhibiting the growth and proliferation of RLFS. These materials also supported rapid limbal epithelial outgrowth from tissue explants.

REFERENCES: [1] Rimmer S, Johnson C, Zhao B, Collier J, Gilmore L, Sabnis S, et al. Epithelialization of hydrogels achieved by amine functionalization and co-culture with stromal cells. Biomaterials 2007 Dec; 28 (35):5319-5331.

Mechanotransduction via magnetic nanoparticles for injectable cell therpaies.

JR Henstock[1], M Rotherham[1], AJ El Haj[1]

[1] Institute for Science and Technology in Medicine, Keele University, UK.

INTRODUCTION: Injectable hydrogels present a useful method by which stem cells and biomaterials can be effectively delivered to wound sites. In this investigation we have used microinjections into the developing chick foetal femur to examine the potential for promoting osteogenesis in introduced mesenchymal stem cells by stimulating mechanotransduction via the TREK1 ion channel using remotely-controlled magnetic nanoparticles[1,2,3]. Repeating these experiments in a cell-seeded collagen hydrogel allowed for further analysis of enhanced mineralisation in tissue engineered constructs.

METHODS: [1] Human MSCs and TREK1 antibody-conjugated magnetic nanoparticles were introduced into the cartilagenous epiphyses of an organotypically cultured *ex vivo* chick foetal femur using a glass capilliary needle. 20nl of material was injected containing 10^3 cells per injection, whilst injecting unlabelled (nanoparticle-free) hMSCs was used as a control. The femurs were cultured organotypically for a period of 14 days in the presence of an oscillating magnetic field for one hour per day to remotely activate TREK1 signalling. [2] The above conditions were also replicated using 2mg.ml^{-1} collagen hydrogels seeded with hMSCs and cultured for 28 days.

RESULTS:

[1] Control (unlabelled) hMSC injected femurs were shown to mineralise in the bone collar (diaphysis) only, whilst secondary mineralisation sites were observed in the epiphyses of the femurs injected with TREK1-labelled hMSCs (fig. 1).

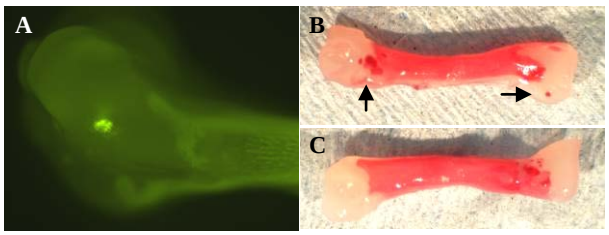

Fig. 1. (a) The location of DiL-labelled hMSCs in the epiphyseal injection site within the chick foetal femur. Following 14 days in vitro culture, the sites in which the TREK1-nanoparticle labelled cells were injected become mineralised (arrowed, Alizarin red staining), (b), whereas those injected with unlabelled hMSCs did not (c).

[2] Seeding these same hMSCs into collagen hydrogels (and culturing for 28 days) revealed that nanoparticle activation of TREK1 resulted in significant ($p < 0.05$) increases in mineralisation (3.8-fold, n=9), revealed by quantified µCT reconstruction of the mineralised phase of the construct and calcium staining (Alizarin red, followed by partial destain, fig. 2).

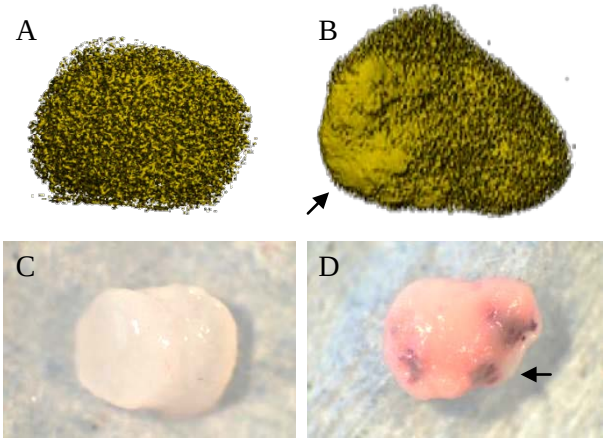

Fig. 2. X-ray microtomography (top) and dissecting microscope images (bottom) of collagen hydrogels seeded with hMSC (a, c) and nanoparticle labelled-hMSC (b, d). Large mineralised regions are formed within the gels containing cells in which the mechanosensitive ion channel TREK1 was activated using magentic nanoparticles (arrowed).

DISCUSSION & CONCLUSIONS: In these experiments we have demonstrated the effectiveness of targetting the TREK1 ion channel to remotely activate mechanotransduction and promote osteogenic effects at injection sites in an organotypically cultured chick foetal femur. Further research has shown that this method has the potential to act synergistically with other tissue engineering approaches, such as growth factor delivery, and can be used to drive osteogenic differentiation of hMSCs in hydrogel constructs.

REFERENCES: [1]Kanczler JM, Sura HS, Magnay J, Green D, Oreffo RO, Dobson JP, El Haj AJ (2010). *Tissue Eng Part A* **16**: 3241-50.

[2]Smith EL, Kanczler JM, Roberts CA, Oreffo ROC (2012) *Tissue Eng. Part C* **18**: 984-994.

[3]Henstock JR, Rotherham M, Rose JB, El Haj AJ (2013) *Bone* **53**: 468-77.

Assessment of ocular cell-matrix interactions in three-dimensions.

E Koudouna[1], RD Young[1], M Ueno[2], T Starborg[3], KE Kadler[3], C Knupp[1], AJ Quantock[1]

[1] School of Optometry & Vision Sciences, Cardiff University, Cardiff, CF24 4LU, UK.[2] Department of Ophthalmology, Kyoto Prefectural University of Medicine, Kyoto 602-0841, JAPAN. [3] Wellcome Trust Centre for Cell-Matrix Research, Faculty of Life Sciences, University of Manchester, Michael Smith Building, Oxford Road, Manchester, M13 9PT, UK.

INTRODUCTION: Three-dimensional (3D) structural information is essential in the field of biomedical sciences in order to gain a deeper understanding of the interactions between cells and extracellular tissue components. Here, we report two examples where structures in the eye were investigated in three dimensions using the new technique of serial block-face scanning electron microscopy. Keratocyte-collagen interactions were studied in the chick cornea during development to determine how cells associate with collagen fibril bundles which they organise into lamellae during the transition of an opaque embryonic matrix into a transparent functional mature tissue. In addition, we examined the 3D arrangement of extracellular matrix in the human trabecular meshwork, where changes in outflow pathways are thought to contribute to elevated intraocular pressure and visual impairment in glaucoma.

METHODS: Embryonic chick corneas were isolated at embryonic day (E) 12, and biopsies of human trabecular meshwork were carefully dissected from two donor eyes obtained for research purposes from Bristol Eye Bank. Samples were fixed in glutaraldehyde, passed through a series of solutions -- including osmium ferricyanide, tannic acid, osmium tetroxide and uranyl acetate -- to increase backscatter electron contrast and embedded in Araldite resin. Tissue blocks were transferred to a FEI Quanta FEG ESEM equipped with a Gatan 3View system, where automated block-face imaging alternating with serial sectioning at 100-125 nm was performed. Stacks of several hundred serial images were obtained and 3D reconstructions were generated using ImageJ and EM3D software.

RESULTS: Serial block face scanning electron microscopy facilitated the reconstruction of 3D tissue nanostructure, over large tissue volumes, in the embryonic chick cornea and the human trabecular meshwork. At E12, corneal keratocytes displayed lamellipodia and novel filopodia-like structures, we term 'keratopodia', extending many microns from the cell surface. Noticeably, primary cilia were abundant in nearly all cells at this developmental stage. Collagen fibrils appeared within cell involutions that ultimately opened into fibril bundles, detaching from the cell surface into the extracellular matrix. Moreover, small numbers of collagen fibrils were found in membrane-bound intracellular compartments. In trabecular meshwork, the ultrastructure of the Schlemm's canal inner wall and the juxtacanalicular tissue was examined. Schlemm's canal endothelial outpouchings led to the formation of giant vacuoles which were discernable along the inner wall of the canal, often encircled by the cytoplasm of trabecular cells. In the underlying juxtacanalicular tissue, a complex array of elastic fibers was observed. Also, in this region, empty spaces were visible, reminiscent of separation between cell-cell and cell-matrix, and which are likely to serve an outflow pathway for aqueous humour.

DISCUSSION & CONCLUSIONS: Our findings illustrate the potential of serial block face scanning electron microscopy for the acquisition of large image series for 3D reconstruction of cell-matrix interactions at electron microscopy resolution. In developing cornea the extent of cellular processes, *keratopodia*, which associate with collagen bundles during lamellogenesis has become evident. These structures appear important for long-range cellular control over the assembling matrix. In the trabecular meshwork, the complexity of the outflow pathways and the elastic matrix component of the juxtacanalicular tissue has become evident for the first time in 3D. These observations provide a useful baseline against which to compare changes accompanying glaucoma in future studies.

Development of novel tissue constructs using hydrogel-3D stem cell technologies

D Limonovs[1], S Rimmer[2], P Genever[1]

[1] *Department of Biology, University of York* [2] *Department of Chemistry, University of Sheffield*

INTRODUCTION: *In vivo*, tissues exist in a 3D environment, being surrounded by numerous biochemical and mechanical cues. In order to mimic such a complex environment *in vitro*, we have designed a "smart" thermoresponsive poly (N-isopropylacrylamide)-based hydrogel, that enables mesenchymal stromal/stem cell (MSC) encapsulation and analysis of MSC morphology and differentiation.

METHODS:
Highly branched poly (N-isopropylacrylamide) (PNIPAM) was synthesised by the reversible addition-fragmentation (RAFT) method, followed by carboxylic acid functional end group addition. Tri-arginine (RRR) peptide, synthesised in-house, was covalently attached to highly-branched PNIPAM polymer by succinimide group addition[1]. Change in lower critical solution temperature (LCST) was observed by UV-Vis spectrophotometer. Mechanical properties of the hydrogel were determined by rheological studies. Solution-gel phase transition was evaluated by differential scanning calorimetry (DSC) and Fourier transform infrared spectroscopy (FTIR). Particle diameter and zeta potential measurements of PNIPAM+RRR solutions were also performed.

Hydrogel architecture in deionized water and MSC culture media was investigated by scanning electron microscopy (SEM).

Viability of encapsulated MSCs was determined by staining encapsulated cells with calcein-AM and ethidium homodimer 1, where cell morphology and motility was assessed by pre-staining cells with cell tracking dyes and analysed by multiphoton microscopy.

Osteogenic and adipogenic differentiation potential of encapsulated MSCs was evaluated by alkaline phosphatase (ALP) activity, von-Kossa-stained mineralisation and staining for lipid droplets.

RESULTS: In this study, highly branched PNIPAM was successfully synthesised, followed by functionalisation with tri-arginine (RRR) peptide. Peptide functional group attachment improved polymer solubility and water retention after gelation.

Particle diameter analysis at corresponding temperatures confirmed expected polymer particle transition from open highly-branched conformation to a collapsed globule (see *Table 1*). Where zeta potential analysis suggests colloidal stability of the system at biologically relevant temperature (see *Table 1*).

Temperature (C°)	Particle diameter (nm)	Zeta Potential (mV)
20	460.37	19.202
37	238.13	31.496

Table 1. Particle diameter and zeta potential measurement of PNIPAM+RRR solutions.

Gelled PNIPAM+RRR structures provided a porous 3D environment (see *Fig. 1*) for encapsulated MSCs, where high cell viability was observed after 14 days of culture.

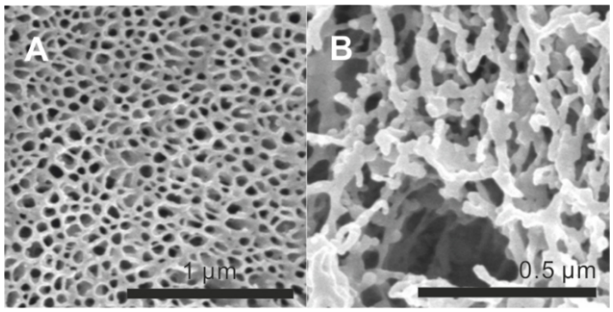

Fig.1: SEM analysis of the inner structure of 5wt% PNIPAM+RRR hydrogel prepared in (A) deionised water and (B) MSC culture media containing 10% foetal bovine serum.

ALP activity was used as a marker of osteogenesis in monolayer and hydrogel-encapsulated cultures, where in both osteo-inductive and basal conditions ALP-positive cells were observed after 21 days in culture with extensive mineral deposition. Whereas, adipogenesis was not observed in MSC-loaded hydrogels in both adipo-inductive and basal conditions.

DISCUSSION & CONCLUSIONS: The hydrogel designed in this study allows MSC encapsulation with high cell viability and enhanced osteogenic differentiation capacity with limited adipogenesis. PNIPAM+RRR hydrogels provide a promising platform for studying cell interaction and differentiation, as well as possibility of minimally-invasive cell delivery for tissue repair.

REFERENCES: [1]S. Hopkins, S.R. Carter, J.W. Haycock et al (2009) *Soft Matter* **5**: 4928-4937

Fibrinogen, riboflavin, and UVA to immobilize a corneal flap—conditions for tissue adhesion and molecular mechanisms.

SL Littlechild[1,2], G Brummer[1,2], Y Zhang[2], JM Tomich[3], GW Conrad[1,2]

[1] *Division of Biology, Kansas State University, Manhattan, Kansas, USA;* [2] *Mount Desert Island Biological Laboratory, Salisbury Cove, Maine, USA;* [3] *Department of Biochemistry, Kansas State University, Manhattan, Kansas, USA.*

INTRODUCTION: Laser in situ keratomileus (LASIK) is an eye surgery aimed at correcting common vision conditions such as nearsightedness, farsightedness, and astigmatism. A caveat to this procedure is that it creates a permanent flap that remains non-attached to the underlying laser-modified corneal stroma. This lack of permanent adhesion is a liability. To immobilize a corneal flap, a protocol using fibrinogen (FIB), riboflavin (RF), and ultraviolet (UVA) light (FIB+RF+UVA) was devised to re-adhere the flap to the stroma.[1] In addition, several covalent and noncovalent interactions between these classes of macromolecules are studied.[2]

METHODS: A model flap was created using rabbit (*Oryctolagus cuniculus*) and shark (*Squalus acanthias*) corneas. Solutions containing FIB and RF were applied between corneal strips as glue. Experimental corneas were irradiated with long wavelength (365 nm) UVA. To quantify adhesive strength between corneal strips, the glue-tissue interface was subjected to a constant force while a digital force gauge recorded peak tension. SDS-PAGE and Western blot techniques were used to identify covalent interactions between tissue glue molecules and corneal ECM molecules in either the presence or absence of RF and UVA, in vitro and ex vivo. Surface plasmon resonance (SPR) was used to characterize noncovalent interactions, and obtain k(a), k(d), and K(D) binding affinity values.

RESULTS: In the presence of FIB, substantive non-covalent interactions occurred between rabbit corneal strips. Adhesiveness was augmented if RF and UVA also were applied, suggesting formation of covalent bonds. Additionally, exposing both sides of rabbit corneas to UVA generated more adhesion than exposure from one side, suggesting that RF in the FIB solution catalyzes formation of covalent bonds at only the interface between stromal molecules and FIB closest to the UVA. In contrast, in the presence of FIB, shark corneal strips interacted non-covalently more substantively than those of rabbits, and adhesion was not augmented by applying RF+UVA, from either or both sides. Residual RF could be rinsed away within 1 hour. SDS-PAGE and Western blot analyses indicated that covalent interactions occurred between neighboring FIB molecules, as well as between FIB and collagen type I (Coll-I) proteins (in vitro and ex vivo). These interactions occurred only in the presence of RF and UVA. SPR data demonstrated the ability of FIB to bind noncovalently to corneal stroma molecules, Coll-I, decorin, dermatan sulfate, and corneal basement membrane molecules, laminin and heparan sulfate--only in the presence of Zn(2+).

DISCUSSION & CONCLUSIONS: Glue solution containing FIB and RF, together with UVA treatment, may aid immobilization of a corneal flap, potentially reducing risk of flap dislodgement. Covalent and (zinc-mediated) noncovalent mechanisms involving FIB and stromal ECM molecules contribute to the adhesion created by FIB + RF + UVA.

REFERENCES: [1] S.L. Littlechild, G. Brummer, Y. Zhang, et al (2012) *Invest Ophthalmol Vis Sci* **53**:4011-20. [2] S.L. Littlechild, J.M. Tomich, Y. Zhang, et al (2012) *Invest Ophthalmol Vis Sci* **53**: 5991-6003.

ACKNOWLEDGEMENTS: The authors thank those who funded and supported this work: an Undergraduate Outreach Fellowship from the NIH/NCRR Maine IDeA Network of Biomedical Research Excellence (ME-INBRE: 2-P20-RR016463); Johnson Center for Basic Cancer Research, Kansas State University; K-INBRE Award Number P20-RR016475 from the National Center for Research Resources; National Institutes of Health-National Eye Institute (NIH-NEI) Grant NIH EY0000952 (GWC); and Lillian J. Brychta Fund.

Dynamic mechanical characterisations of collagen/HAp composite scaffolds

Chaozong Liu[1,2], Simon Partridge[2], Kenny Dalgarno[1,2], Mark Birch[2], Andrew McCaskie[2,3]
[1] *Arthritis Research UK Tissue Engineering Centre, Institute of Cellular Medicine, Newcastle University*
[2] *School of Mechanical & Systems Engineering, Newcastle University*
[3] *Orthopaedic Surgery, Freeman Hospital, Newcastle, UK*

INTRODUCTION: Both Collagen and hydroxyapatite (HA) have merits as scaffold materials for bone regeneration [1]. Researches have shown that a combination of collagen and HA would provide an appropriate scaffold materials for bone tissue culture [2]. The *in vitro* performance of collagen-hydrodyapatite composite has well be documented, however, its dynamic mechanical properties at simulated environment has not yet sufficiently established. This work is to study the dynamic properties of the collagen-hydroxyapatite composite at physiological environment in order to determine the physical environment that the scaffold could provide in vivo.

METHODS: The collagen-hydroxyapatite composite scaffolds were prepared by an established in-site hydroxyapatite precipiration integrated freeze-drying method as reported elsewhere [3]. The microstructure and composition scaffolds were examined using SEM and XPS, respectively. Dynamic mechanical properties of the scaffolds were analyzed by using a dynamic mechanical analyzer (DMA8000, PerkinElmer). The dynamic stress scan and frequency scan methods in shear mode were performed on scaffolds in both dry and wet condition at 30^{o}C. The changes in modules and tan delta as a function of shear deformation were monitored. Compressive tan delta

RESULTS: SEM and TEM examinations revealed that nano-HAp precipitate onto and guided by the collagen fibers to form a composite with porous structure. Dynamic mechanical spectra for various collagen-hydroxyapatite composite scaffolds tested in wet condition at 37^{o}C under share mode are shown in Figure 1 a & b, respectively. It was observed that addition of hydroxyapatite into collagen matrix resulted in increase of the storage modulus of the scaffolds The higher the HAp content (within the range of study), the higher the modulus is. It was also observed that with the increase of modulus, the tan delta value of the scaffold decreased with the addition of HAp for both shear and compressive tests. The 1% collagen scaffold has a shear tan delta of 0.27, this decreased to 0.1 for the scaffold contains 75% (mass%) HAp. Correspondingly, 1% collagen scaffold has a tan delta of 0.35, this decreased to 0.104 for specimen contains 75% HAp.

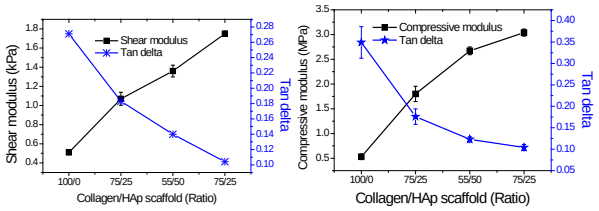

（a） (b)

Fig. 1: Variation of modulus of collagen-HAp scaffold with addition of HAp. (a) Shear modulus and (b) compressive modulus.

DISCUSSION & CONCLUSIONS: The structure of collagen scaffold consisting of a complex mass of randomly knitted chains or large arrays of fibers. Under stress, the chains are stretched. The strain is a combination of inelastic and elastic strains. The viscoelastic behaviour of collagen is a combination of the elastic components and viscous component. With the addition of HAp, it increased the elastic component of the scaffold as evidenced by the increase of modulus and decrease of tan delta value. The influence of HAp on the dynamic property was dependent on the ration of collagen/HAp ratio.

REFERENCES: [1] M. Achilli, D. Mantovani (2010) Polymer 2: 664-680. [2] E. Andronescu, G. Voicu et al (2011) J Electron Microscopy 60: 253-259. 3 C Liu, Z. Xia et al. (2008) JBMR: 85B:519-528.

ACKNOWLEDGEMENTS: The authors would like to acknowledge the support of Arthritis Research UK (Award 19429) and the FP7 RESTORATION project (Award CP-TP 280575-2).

Osteogenic Differentiation and Self-Organisation of Mesenchymal Stem Cells and Endothelial Cells in 3D Co-culture

J Marshall[1], X Yang[2], P Genever[1]

[1] BTR, Department of Biology, The University of York. [2] Biomaterials and Tissue Engineering Group, Department of Oral Biology, The University of Leeds.

INTRODUCTION: Mesenchymal stromal/stem cells (MSCs) have a variety of intrinsic properties which make them a popular candidate for cellular therapies. However, little is known about the *in vivo* environment in which they reside. It has been proposed that MSCs reside within a perivascular niche due to their close association with the vasculature system and endothelial cells [1]. Here, we have used a 3D in vitro co-culture model to investigate the effects of MSC human umbilical vein endothelial cell (HUVEC) self-organisation and osteogenesis.

METHODS:

3D co-culture spheroids totalling 30,000 cells at different ratios of human MSCs and HUVECs were produced using non-adherent U-bottomed 96 well plates in appropriate medium containing 0.25% (w/v) methyl cellulose (Fig 1).

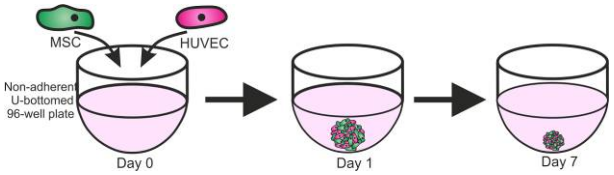

Fig 1: A random cell suspension of fluorescently labelled MSCs and HUVECs were placed in non-adherent U-bottomed 96 well plates. Within 24 hours the cells aggregate and form spheroids.

RESULTS:

3D co-culture of fluorescent labelled MSCs (green) and HUVECs (red) were tracked during spheroid initiation over 16 hours (Fig 2-A). HUVECs self-organised into discrete assemblies and preferentially towards the exterior (Fig 2-A section). Calcium depletion from the media to quantify osteogenic status by mineral incorporation increased from days 8 to 16 in 3D co-culture under osteogenic conditions, and to a less extent in basal media. Similar calcium depletion was observed in the 2D MSCs cultured in osteogenic conditions only (Fig 2-B). The 3D co-culture shown represents 50:50 MSC:HUVEC spheroids, however over a range of different ratios it was found that 65:35 (MSC:HUVEC) spheroids had the greatest calcium depletion. Staining for alkaline phosphatase (ALP) activity confirmed osteogenesis in basal and osteo-induction media in 3D co-culture, with prominent staining towards the periphery. However, using 2D MSCs, only the osteogenic condition samples were positive for ALP staining (Fig 2-C).

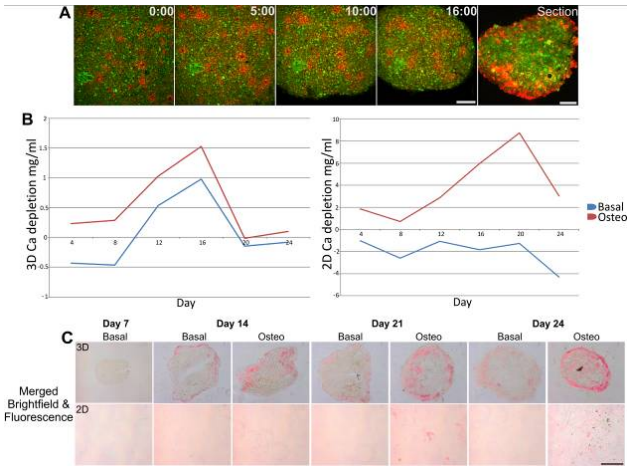

Fig 2: A – Self-assembly of a labelled spheroid over 16 hours using a multi-photon confocal microscope and a 24 hours section MSC:HUVEC. B - Quantification of calcium depletion from 3D spheroids and 2D MSCs under basal (blue) and osteogenic conditions (red). C – Spheroid sections and 2D MSCs stained with ALP. Scale bars = 250 μm.

DISCUSSION & CONCLUSIONS:

A random suspension of MSCs and HUVECs successfully aggregated and formed a spheroid within 24 hours. The mixed cells self-organised to reveal non-random MSC:HUVEC distributions and established HUVEC-dense peripheral assemblies. This simplified in vitro model can be used to analyse relevant heterotypic cell-cell interactions and signalling activities that regulate MSC behaviour in vivo, including an apparent positive influence of endothelial cells on MSC osteogenic specification.

REFERENCES: [1]M. Crisan *et al.* (2008) *A perivascular origin for mesenchymal stem cells in multiple human organs*, Cell Stem Cell **3**(3).

ACKNOWLEDGEMENTS: The authors would like to thank the EPSRC for funding.

Dental pulp stem cells differentiated towards Schwann cell-like cells enhance and guide neurite outgrowth in a 3D environment

W Martens[1*], K Sanen[2], M Georgiou[3], J B Phillips[3], M Ameloot[2] and I Lambrichts[1]

[1]Department of Morphology, BIOMED Hasselt University, Diepenbeek, Belgium; [2] Department of Biophysics, BIOMED Hasselt University, Diepenbeek, Belgium; [3] Department of Life, Health and Chemical Sciences, The Open University, Milton Keynes, United Kingdom

INTRODUCTION: Trauma, surgical procedures or accidents can often result in peripheral nerve injury. Although short gap lesions can regenerate spontaneously, large gap injuries require, artificial bridging. Recently, a new cell-based technique has been developed to efficiently and reproducibly align cells in a collagen type I hydrogel, thereby mimicking the environment required for nerve regeneration.[1] In this study, human dental pulp stem cells (hDPSC) were differentiated towards Schwann-like cells (d-hDPSC). We found that these cells align within a collagen type I hydrogel and can be stabilised to form engineered neural tissue (EngNT). Their potential to promote and direct neurite outgrowth of DRG in this 3D environment was determined.

METHODS: Following differentiation, Schwann-like cells (d-hDPSC) were characterized via immunocytochemistry for p75, integrin β4 and GFAP. In 2D cultures, the influence of conditioned medium (CM) from d-hDPSC on survival and neurite outgrowth of adult rat DRG neurons was evaluated. 3D constructs (EngNT) were made consisting of d-hDPSC seeded into a tethered collagen type I hydrogel and allowed to align overnight. After stabilization of the gel, DRG neurons were seeded on top of the EngNT and left in culture for 3 days. Immunocyctochemical analysis was performed for S100 and β-III-tubulin to determine the angle of neurite outgrowth compared to the direction of aligned d-hDPSC.

RESULTS: d-hDPSC expressed the typical Schwann cell markers p75, integrin β4 and GFAP. In 2D cultures, CM from d-hDPSC promoted neuronal survival and neurite outgrowth of DRG neurons (fig 1). In 3D, aligned d-hDPSC guided neurite growth of DRG seeded on top of EngNT (fig 2). Live/dead staining showed that d-hDPSC survived in the EngNT and that these cells maintained their alignment after the stabilization process to form sheets.

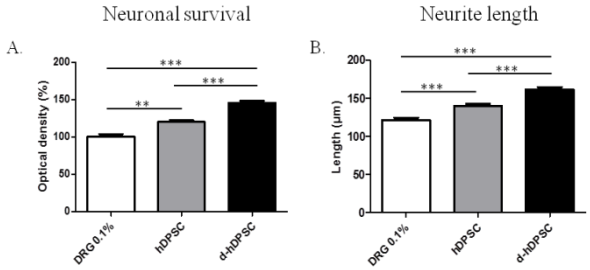

*Fig 1: Neuronal survival (n=7)(A) and neurite length (n=4) (B) was significantly increased after the addition of CM from hDPSC and d-hDPSC. Medium containing 0.1%FCS (DRG 0.1%) was used as control. (** $p \leq 0.01$; *** $p \leq 0.001$)*

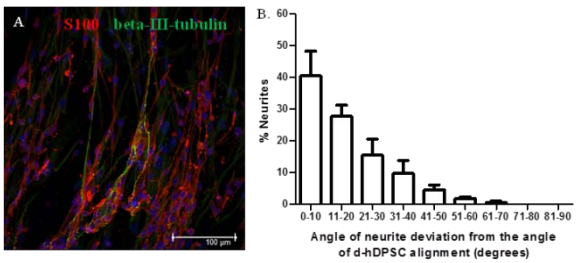

Fig 2: Guided neurite growth in EngNT containing d-hDPSC. (A) Confocal image showing neurites (green) and d-hDPSC (red). (B) Frequency distribution of neurite angles relative to d-hDPSC alignment (mean ± SEM; n=4; Scale bar=100µm).

DISCUSSION & CONCLUSIONS: d-hDPSC exerted positive effects on neuronal survival and neurite outgrowth in 2D and 3D environments. The ability of d-hDPSC to align within EngNT can be beneficial in the field of neuroregenerative medicine. A possible application of the EngNT construct is to provide an alternative therapy for bridging large gaps in peripheral nerve injury.

REFERENCES: [1] www.jamesphillips.org

ACKNOWLEDGEMENTS: This study was funded by grants of the FWO and Boehringer Ingelheim. Thanks to Prof. Politis for providing pulp tissues.

The effect of isolation and culture methods on epithelial stem cell populations and their progeny for clinical application

C Rogers[1], C Lenihan[2], D Fistouris[2], Y Martin[2]

[1] Brighton and Sussex Medical School, Brighton, UK [2] Blond McIndoe Research Foundation, Queen Victoria Hospital, East Grinstead, UK

INTRODUCTION: Severe burns present a significant clinical challenge. The application of cultured autologous epithelial keratinocytes to augment wound healing is well established, but current culture methods use lethally irradiated feeder cells and other xenobiotic components in the medium[1], which pose a potential risk to the patient.

METHODS: Split-thickness skin was separated using dispase. Keratinocytes were released from the epidermis using 0.5% trypsin. Cells were seeded at $2x10^6$ per T75 flasks, and sub-cultured at $5x10^5$ per T75 flask. Medium was replaced thrice weekly. Media used were (Table 1): Rheinwald and Green medium (R&G) (3:1 DMEM:Ham's F12,10% FCS, 10 ng/ml human recombinant EGF, 10 nM cholera toxin, 0.4 mg/ml hydrocortisone); PAA Celloneer KC Defined Medium (CKCD); EpiLife with defined EDGS supplement (EDGS); EpiLife with xenobiotic-free S7 supplement (S7). Cells in R&G were grown with lethally irradiated murine 3T3 cells, cells in EpiLife-based media were grown on rat tail collagen I.

RESULTS: Shorter incubation times in trypsin (5 – 10 min) yielded significantly greater numbers of stem cells (Fig 1). All three commercially available feeder-free media supported the growth of keratinocytes in culture, although growth rates varied (Fig 2). The numbers of stem and transiently amplifying (TA) daughter cells were not significantly affected by the different media (Fig 3).

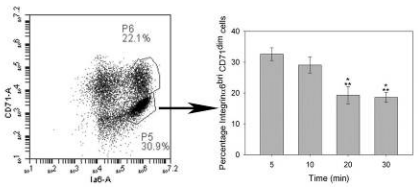

Fig. 1: Flow cytometry of epithelial stem cells (Integrin $\alpha6^{bri}$ $CD71^{dim}$) shows significant effect of incubation time in trypsin during isolation ($p = 0.05$).

Table 1. List of media

	R&G	CKCD	EDGS	S7
Feeder cells	Yes	No	No	No
Xenobiotics	Yes	Defined	Defined	No

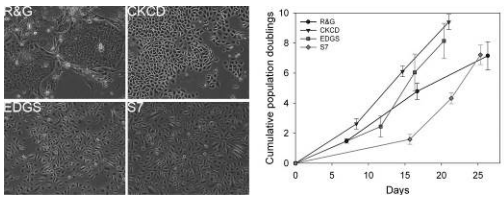

Fig.2 Light microscopy shows differences in morphology. Cumulative population doubling shows growth rates in the four media.

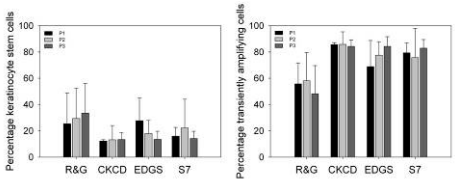

Fig. 3: Flow cytometry of epithelial stem cells and TA cells in the four media. No statistically significant differences were observed.

DISCUSSION & CONCLUSIONS: Adjusting incubation time in trypsin can lead to significantly greater yield of epithelial stem cells during isolation. Both epithelial stem and TA cells harbour significant long-term tissue regenerative capacities[2]. All media tested supported the growth of keratinocyte stem and TA cells, although the growth rates varied. Dispensing with lethally irradiated feeder cells and reducing the use of xenobiotic substances in culture media will improve the safety of patients treated with autologous keratinocytes.

REFERENCES: [1]JG. Rheinwald and H. Green (1975) *Cell* 6(3):331-343. [2]H Schlüter, et al (2011) *Stem Cells* 29(8):1256-1268

ACKNOWLEDGEMENTS: This work was supported by charitable donations to the Blond McIndoe Research Foundation.

Delivery of Therapeutically Active siRNA against c-Myc in Bone Cancer Cells

M.McCully[1], Yulan Hernandez [2], Jesus M. de la Fuente [2] M.J.Dalby[1], C.C.Berry[1]

[1] *Centre for Cell Engineering, College of Medical Veterinary and Life Sciences, University of Glasgow, Scotland*

[2]*Instituto de Nanociencia de Aragon, University of Zaragoza, C/Mariano Esquillor s/n Zaragoza, Spain,*

INTRODUCTION: RNA interference is a promising method of gene silencing that can be used as a novel form for cancer treatment. The main barrier facing therapeutic RNAi is the successful delivery of the small interfering RNA (siRNA) molecules into cancer cells within the body[1]. This study aimed to overcome this barrier by using gold nanoparticles (AuNPs) delivering siRNA into bone cancer cells (MG63) in order to knockdown the c-Myc oncogene by RNAi. Thiolated siRNA against c-Myc was conjugated covalently to the AuNP, which was further functionalised with RGD (to enhance cell interaction) and biotin (for imaging purposes). Results indicated successful delivery and knockdown, which was dependent on the cell accessibility to the siRNA on the nanoparticle.

METHODS: Nanoparticle toxicity was assessed by MTT assay; cellular uptake was visualized by TEM and quantified *via* ICP-MS, whilst c-Myc knockdown was assessed by In-Cell Westerns, BrdU and flow cytometry.

In-Cell Westerns. Cells seeded for 24 hours at $1x10^4$ cells/ml in DMEM/10% FBS (2% Penicillin, Streptomycin and L-glutamine). After 24 hours, AuNPs were added or siRNA with Lipofectamine (Invitrogen, UK). Following a further 24 and 48 hours, cells were fixed and permeabilised before treatment with 1% Milk protein-PBS at 37°C for 10 minutes. The primary antibody c-Myc (Abcam,UK) and GAPDH (Epitomics, USA) were diluted in 1% Milk protein-PBS and added for 1 hour at 37°C Samples were PBS-tween washed [0.5%V/V] and co-incubated with secondary antibodies Donkey anti-mouse IR680RD and Donkey anti-rabbit IR800CW (Licor, UK) in 1% Milk protein-PBS [0.2%V/V] Tween at 37 ◦C for 1 hour. The plates were scanned by an Odyssey SA.

RESULTS: All AuNPs were non-toxic, and uptaken into the MG63 cells. Increasing the siRNA concentration from 2nM to 15nM had a dose dependent effect on c-Myc knockdown, whilst reducing the amount of PEG coverage on the AuNP from 40% to 25% dramatically increased knockdown (fig 1).

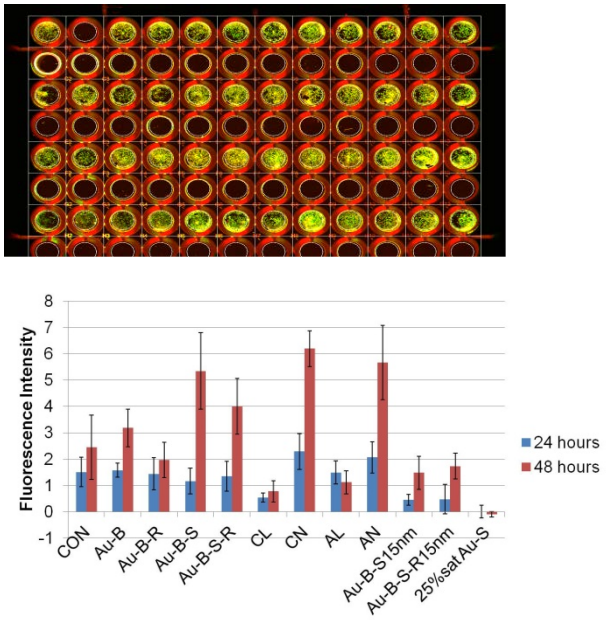

Fig. 1: ICW dat;,(top) visual image of the red green overlay of c-Myc and Gapdh intensities, (bottom)Graph comparing the levels of c-Myc protein in MG63s normalised to Gapdh . Cells were treated for 24 and 48 hours. The treatments included 4basic AuNPs @ 40% PEG coverage & 2nM (B=Biotin, R=RGD peptide, S=siRNA, SR=siRNA with RGD); c-Myc with Lipofectamine (CL), Allstar nonsense siRNA with Lipofectamine (AL), c-Myc alone (CN) and Allstar alone (AN). The two penultimate bars indicate the higher 15nM concentration (S15nM & SR15nM) with the final bar indicating the reduced PEG coverage (25% as compared to 40%, at 2nM). Error bars= St.dev N=6

DISCUSSION & CONCLUSIONS: This study demonstrates the importance of nanoparticle design. The siRNA needs to be cleaved by glutathione in the cytoplasm to allow interaction with the RISC complex and subsequent knockdown. Both a higher concentration of siRNA and a reduced PEG density on the particle surface greatly enhanced knockdown, highlighting the importance of considering the effect of steric hindrance when designing AuNPs to deliver small molecules.

REFERENCES: *[1] R.Lévy(2010) Gold nanoparticles delivery in mammalian live cells: a critical review, Nano Reviews 1, 1-18.*

Osteogenic micro-nanopatterned titania for orthopaedic applications

LE McNamara[1], T Sjöström[4], P Herzyk[2] RMD Meek[3], B Su[4], MJ Dalby[1]

[1] Centre for Cell Engineering, [2]Polyomics Facility, University of Glasgow [3]Southern General Hospital, Glasgow, UK. [4]School of Oral and Dental Science, University of Bristol, Bristol, UK.

INTRODUCTION: Titanium (Ti) has excellent load bearing properties for orthopaedic applications, but is bioinert, which can result in suboptimal implant fixation. Topographical patterning of implant surfaces has great potential to improve osseointegration, and we previously demonstrated that 15 nm high titania pillar-like features were more osteogenic than taller (55 nm, 90 nm high) [1, 2] and smaller pillars (8 nm high) [3]. In this study, the 15 nm high pillars were combined with micron scale pits with the aim of enhancing the osteogenic effect. Human mesenchymal stem cells (MSCs) were used to investigate the osteoinductive capacity of the resulting micro-nanofeatured surfaces.

METHODS: Nanofeatures were prepared on Ti surfaces by a block copolymer mask technique, and micropits were generated by micromachining. Human MSCs were cultured on these micro-nanopatterned surfaces and planar controls for 3 days to examine focal adhesions (FAs) and 21 days to study the abundance of the bone marker osteocalcin. Microarrays (HuGene 1.0 ST arrays, Affymetrix) were used to examine gene expression, including small regulatory RNA expression, in MSCs cultured for 11 days on micro-nano patterned Ti versus planar controls. Interactions between differentially expressed genes were investigated using Ingenuity Pathways Analysis (IPA).

RESULTS: MSCs on the micro-nanopatterned surfaces had a differentiating phenotype, with modulated FAs (Fig 1A), enhanced cell clustering around micropits, and increased production of bone markers. Cells upregulated expression of various osteogenic genes, including genes encoding bone morphogenic proteins (BMPs) and miRNAs (microRNAs) associated with BMP signalling. Fourteen small regulatory RNAs involved in editing of RNA transcripts were also increased in abundance. IPA highlighted relevant canonical pathways for stem cell functions and osteoblastic processes, and interaction networks featuring molecular hubs such as ERK (extracellular signal-regulated kinase) (Fig 1B).

DISCUSSION & CONCLUSIONS: The

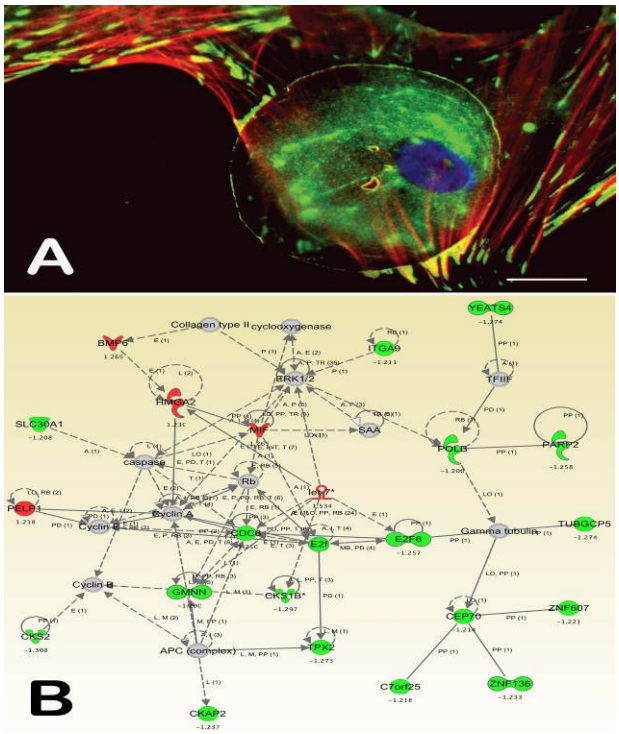

Fig. 1: A - MSC interacting with a micropit on the micro-nanopatterned Ti surface, stained for FAs (green), actin (red), and DNA (blue). Note the localisation of the nucleus to the interior of the pit. B – A high-scoring IPA-generated network of some genes upregulated (red) - including a BMP and a miRNA - or downregulated (green) in MSCs cultured on the micro-nanostructured surface.

combination of osteogenic micro- and nanofeatures in Ti promoted osteogenesis, including enhanced expression of osteogenic genes, small regulatory RNAs, and increased deposition of bone markers. The combined surface has promise for use in orthopaedic applications.

REFERENCES: [1] L.E. McNamara, T. Sjöström, Karl E.V. Burgess et al (2011) *Biomaterials* [2] L.E. McNamara, T. Sjöström, R.M.D. Meek et al (2012) *J. R. Soc. Interface* [3]T. Sjöström, L.E. McNamara, R.M.D. Meek et al (2013) *Adv. Healthcare Mater.*

ACKNOWLEDGEMENTS: The authors thank Carol-Anne Smith and Dr. Jing Wang for assistance and all in CCE for helpful discussion. The research was funded by EPSRC.

Human derived feeder fibroblasts for the culture of epithelial cells for clinical use in 2D and 3D models

A R O'Callaghan[1], J T Daniels[1], and M P Lewis[2].

[1] Department of Ocular Biology and Therapeutics, UCL Institute of Ophthalmology, University College London, London EC1V 9EL. [2] Musculoskeletal Biology Research Group, School of Sport, Exercise and Health Sciences, Loughborough University, Leicestershire, LE11 3TU.

INTRODUCTION: Limbal epithelial stem cells (LESCs) reside in the limbus and are responsible for the repair and maintenance of the corneal surface. A deficiency of these cells due to injury or disease can cause the vision affecting condition limbal epithelial stem cell deficiency (LSCD). LSCD can be treated using cultured LESC therapy (CLET) or cultivated oral mucosal epithelial transplantation (COMET). The current gold standard method for culturing LESCs uses an initial expansion step with a murine 3T3 feeder layer. Cell therapies should ideally be animal product free and murine 3T3s therefore ideally eliminated from the culture system. The aims of this study were 1) to investigate whether human oral mucosal fibroblasts (HOMFs) or human limbal fibroblasts (HLFs) could be used as alternative feeder layers to support the culture of LESCs and 2) how these cells would behave in 3D collagen constructs which could potentially be used as an alternative to the biologically variable amnion currently used for transplantation.

METHODS: Human oral mucosal epithelial cells (HOMEs) were isolated from buccal oral mucosal biopsies using Dispase and initially expanded on a growth arrested 3T3 feeder layer. Explant culture was then used to generate HOMFs. Human limbal epithelial cells (HLEs) were isolated from limbal rims using Dispase and initially expanded on a growth arrested 3T3 feeder layer. Explants were set up to generate HLFs. Following initial expansion, epithelial cells were split equally onto Mitomycin C growth arrested 3T3, HLF, and HOMF feeder layers and cultured until they stopped proliferating. The number of population doublings was calculated using colony forming efficiency at each passage, and epithelial cells were analysed by PCR and Western blot for their ability to express the corneal markers CK12, Pax6, and Mucin 16 as well as the putative stem cell markers CK15 and p63alpha. 3D organotypic models were set up using compressed collagen gels containing 3T3s, HLFs or HOMFs with epithelial cells (HLEs or HOMEs) on top. Following submerged culture, the gels were airlifted to induce stratification.

RESULTS: HOMFs were equivalent to 3T3s for supporting epithelial cell culture (both HLE and HOME) in 2D in terms of total passage number, the number of population doublings and maintenance of the stem cell markers CK15 and p63alpha. There was no significant difference in Pax6 and Mucin 16 protein expression for HLEs cultured on 3T3s, HLFs, and HOMFs. The number of passages and population doublings was significantly less for HLEs and HOMEs cultured on HLFs compared to 3T3s and HOMFs in 2D ($P<0.05$). When cultured in the 3D models, differences in the number of epithelial cell layers (more cell layers in models containing HOMFs than those with HLFs and 3T3s) and transparency (important for use in the cornea) of these constructs were observed with the different epithelial-fibroblast combinations.

DISCUSSION & CONCLUSIONS: Results from this study suggest that HOMFs could be used as a feeder layer instead of murine 3T3s for the culture of HLEs and HOMEs for use in CLET or COMET for the treatment of LSCD. This system could improve the safety of these procedures, by utilising an autologous source of feeder cells. 3D models provided additional insight into how these cells might behave once transplanted onto the eye and suggested that cell populated collagen constructs may be useful for the treatment of LSCD.

ACKNOWLEDGEMENTS: This work was supported by Fight for Sight, the Special Trustees of Moorfields Eye Hospital and NIHR Moorfields Biomedical Research Centre.

Microfabrication of Artificial Limbal Stem Cell Microenvironments

I. Ortega [1], A. J. Ryan [2], S. MacNeil [1] and F. Claeyssens [1]

[1] *Biomaterials and Tissue Engineering Group, Department of Materials Science and Engineering, Kroto Research Institute, University of Sheffield, Sheffield, United Kingdom.* [2] *Department of Chemistry, University of Sheffield, Sheffield, United Kingdom*

INTRODUCTION: Corneal blindness occurs as a result of limbal epithelial cells (LEC) deficiency due to causes such as chemical burns or Aniridia. LEC are located in the limbus in specific microenvironments or stem cell niches[1]. In some cases of corneal disease limbus and niches are destroyed and cells from the conjunctiva migrate to the cornea producing scar tissue which reduces vision[2]. Our aim is to develop models of the limbus in which to study LEC activity. We have designed two types of microfabricated corneal rings (one biodegradable and other non-biodegradable; fig.1a, 1d) containing micropockets to simulate LEC microenvironments. .

METHODS: Non-biodegradable rings were made using microstereolithography[3]. Biodegradable rings were made of poly (lactic-co-glycolic acid) 50:50 using a technique combination of microstereolithography and electrospinning[4]. Preliminary work on the evaluation of the constructs was performed using rabbit limbal explants and limbal epithelial cells. The potential use of the rings as cell delivery devices was evaluated using a 3D rabbit cornea model. Cells were characterized using CK3 (differentiation marker) and P63 (stem cell marker).

RESULTS: In both cases we demonstrated that cells attach and proliferate on the constructs (fig. 1b, 1c, 1e). We specifically located cells in the artificial microenvironments and for both approaches we obtained promising results regarding epithelial cell transfer, explant outgrowth and re-epithalisation of damaged corneas using an *ex vivo* 3D rabbit model. Preliminary data suggests that the presence of the microfeatures encourage cell migration from the outer ring to the central cornea.

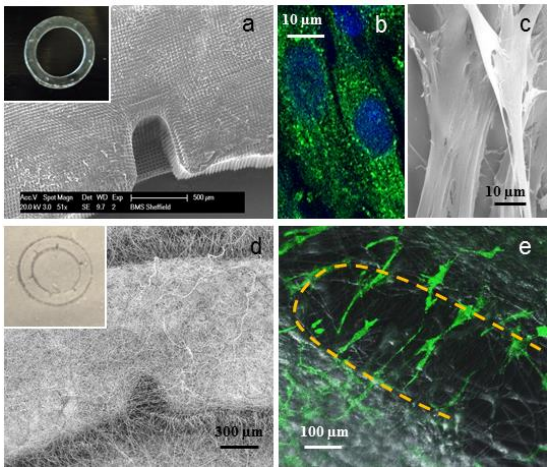

Fig1. SEM images of PEGDA and PLGA microfeatured outer rings (a, d). SEM and fluorescence images of Rabbit limbal cells on PEGDA constructs (b, c; green:vinculin) and on PLGA scaffolds (e; green: phalloidin-FITC).

DISCUSSION & CONCLUSIONS: This work provides a technique for producing artificial microenvironments for studying epithelial behaviour using *in vitro* and *ex vivo* models. Both types of constructs could be potentially used as stem cell carriers for the treatment of corneal disease.

REFERENCES: [1]Dua H S. et al, Br J Ophthalmol (2005), 89:529-532; [2]Huang A J. et al, Invest Ophthalmol Vis Sci (1991), 32:96-105; [3]Ortega I. et al, Biofabrication (2013), 5:025008; [4]Ortega I. et al, Acta Biomaterialia (2013), 9:5511-5520.

ACKNOWLEDGEMENTS: We thank the Wellcome Trust Foundation and the EPSRC Landscape Fellowship scheme for supporting this work.

Selective laser melted titanium attachment points for tissue-engineered sinew formation

JZ Paxton[1], TB Sercombe[2], LM Grover[1]

[1] School of Chemical Engineering, University of Birmingham, UK. [2] School of Mechanical and Chemical Engineering The University of Western Australia, Perth, Australia.

INTRODUCTION: Musculoskeletal tissue engineering seeks to engineer replacement orthopedic tissues *in vitro* to replace diseased or damaged tissue. In particular, as tendons and ligaments have a poor capacity for repair, there is great interest in developing replacement sinews to be implanted following injury. Many groups have attempted to engineer sinews *in vitro*, but the method of graft fixation on implantation has not been addressed. Indeed, the method of graft fixation will be of paramount importance to the success of the implant, so it is a significant consideration when designing replacement musculoskeletal tissues. We have previously reported the development of an engineered bone-to-bone ligament replacement manufactured from a cell-seeded fibrin gel and brushite cement anchors[1]. While the engineered sinews have a composition similar to native tissue, the sinew-cement interface can only withstand low loads under tension (~0.05N)[2]. In this study, we investigate the suitability of titanium (Ti) anchors manufactured by Selective Laser Melting (SLM) for use as anchors during formation of tissue-engineered ligaments, and therefore as a potential material to produce a full construct for easy fixation on implantation following ligament/tendon injury.

METHODS: *Manufacture of Ti anchors* – Solid blocks of Ti-6Al-4V were manufactured using a Realizer 100 SLM machine. directly from CAD designs. *Sinew formation* – 2 Ti anchors were pinned to the surface of a Sylgard-coated 35mm Petri dish and sterilised with 70% ethanol. The dish was coated with a solution of DMEM supplemented with 50U/ml thrombin, 400 µM Aminohexanoic acid and 20mg/ml aprotinin. 20mg/ml of fibrinogen solution was added dropwise and the fibrin gel was left to polymerise at 37ºC for 1hr. Chick tendon fibroblasts were seeded on top of the gel (100K/ml) and incubated at 37°C. Constructs were fed every 2-3days with supplemented DMEM with 250µM ascorbic acid (AA) and 50µM proline (P) for the duration of the experiment (42 days). *Interface longevity* – Qualitative assessment of the Ti-tissue interface was conducted by picking up the Ti anchor every 3 days and observing if the tissue remained attached. *Mechanical analysis* – The strength of the Ti-tissue interface in teardrop shaped anchors was measured using tensile testing in an Instron microtester equipped with a 10N load cell. Sinews were submerged in PBS at 37°C for the duration of testing and subjected to a tensile load (strain rate of 0.4mm/min) until failure at the interface occurred. (n=6)

RESULTS: SLM'ed Ti anchors provided a suitable anchor point for ligament formation (Figure 1), with sinew constructs successfully manufactured from two different shapes of Ti anchor.

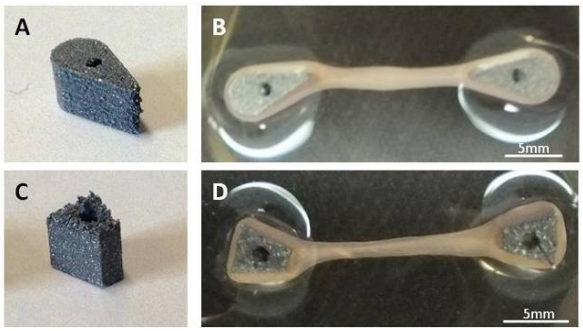

Fig. 1: Ti anchors (A,C) and sinew constructs after 4weeks in culture (B,D).

The Ti-interface remained intact for the duration of the study in both anchor shapes tested (42 days). The teardrop Ti anchor –tissue interface strength was reported to be 0.3 ± 0.06 N, a 6-fold increase on the interface strength reported previously in this system for brushite cements[2].

DISCUSSION & CONCLUSIONS: This preliminary study has validated the use of rapid prototyping to produce Ti anchors suitable for *in vitro* sinew formation. Our current work is focussed on modifying the shape of Ti anchor points, evaluating the use of a new biomedical alloy of Ti and the introduction of porosity into the anchors to augment tissue adhesion strength.

REFERENCES: [1] Paxton JZ. et al., Tissue Eng. (2010) 16: 3515-25. [2] Paxton JZ et al., ABME 38(6):2155-66

ACKNOWLEDGEMENTS: We would like to thank ORUK for funding. The purchase of the SLM equipment was supported through an *Australian Research Council's* LIEF grant (LE110100094).

Towards engineering a human neuromuscular junction *in vitro*

DJ Player[1], NRW Martin1, RA Ferguson[1], EJ Hill[2], V Mudera[3], MP Lewis[1,3]

[1] [1]*School of Sport, Exercise and Health Sciences, Loughborough University, Loughborough, UK.* [2]*School of Life and Health Sciences, Aston University, Birmingham, UK.* [3]*School of Life and Medical Sciences, UCL, London, UK.*

INTRODUCTION: Investigating the cellular and molecular mechanisms that regulate the development and physiology of the vertebrate neuromuscular junction (NMJ), is of great scientific interest. Indeed, understanding such mechanisms will provide evidence for the pathophysiology of neuromuscular diseases. To date, many models of NMJ formation have taken the form of *in vivo* models or basic monolayer cultures, with limited data surrounding NMJ development in bio-mimetic engineered models. Furthermore, such models have used tissue or cells isolated from animal sources due, limiting the translation of findings to human physiology, whilst also posing ethical and experimental limitations. Developing a human-based model of a NMJ would combat many of these issues, while also providing a pre-clinical model for use in trials of potential pharmacological, nutritional and exercise therapies for neuromuscular disease.

METHODS: Human primary muscle derived cells (MDC's) were isolated through explant culture of *Vastus Lateralis* biopsies from consenting individuals. Human SkM constructs were engineered as previously described[1,2] and at 21 days, constructs were sampled for immuno-histochemical (IHC) analysis. Neurons were generated from neuron-committed human teratocarcinoma (NT2) cells and were differentiated as described[1]. NT2's were plated to form neurospheres with the addition of retinoic acid for differentiation. Experiments were also conducted to ascertain the compatibility of culturing MDC's in NT2 media.

RESULTS: MDC's displayed the ability to differentiate into multinucleate myotubes in 3-dimensions (3-D, Fig. 1, right). Data also revealed no significant difference in the number of myotubes present in either monolayer or 3-D cultures in the presence of neuronal media, compared to standard MDC differentiation media ($p > 0.05$, ANOVA). NT2 cells were successfully differentiated into structures with extending neurites (Fig. 1, left). There was also evidence for the development of neuronal networks, whereby neurites extended to signal to other neuronal clusters.

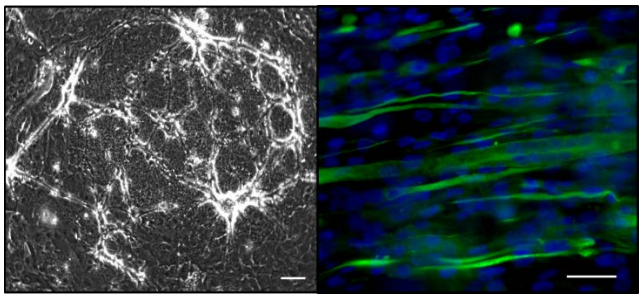

Fig. 1: Ntera-2 (NT2) precursors can be differentiated into neurons with extensive neurite outgrowth (left, bar = 100 μm). Isolated MDC's differentiate into aligned multinucleate myotubes in 3-dimensions (right, bar = 50 μm).

DISCUSSION & CONCLUSIONS: Data presented here, characterises the initial steps towards the analysis of co-cultures of MDC's and NT2 neurons. The ability of MDC's to differentiate to the same extent in the presence of neuronal media, allows for the early addition of neurons to the culture system. This will allow for greater interaction of seeded cell types through both mechanical and biochemical means, permitting enhanced patterning of key cellular and molecular process required for NMJ formation e.g. acetyl-choline receptor (AChR) clustering. The differentiation of NT2 cells to neurons now permits future co-culture experiments to investigate neural cell integration and interaction with MDC's. Future experiments will seek to investigate whether co-cultures contribute to the development of functional NMJ's.

REFERENCES: [1]Khodabukus and Baar, (2012), *Tissue Engineering: Part C*, Vol. 18, 5. [2]Podrygajlo et al. (2009), *Cell Tissue Res*. Vo. 336, 439-452.

ACKNOWLEDGEMENTS: This research was funded by NC3R's. Grant # NC/K00087X/1.

Cyclic hydrostatic pressure stimulates osteochondral differentiation of hMSCs seeded in 3D collagen hydrogels.

J Price[1], JR Henstock[1], Y Reinwald[1], AJ El Haj[1]
Institute of Science and Technology in Medicine, Keele University, UK

INTRODUCTION: Mechanical stimulation of tissue engineered constructs using bioreactors may prove useful for conditioning them to physiological environments prior to clinical implementation, as both mechanotransduction and biochemical factors play important roles in regulating tissue formation[1]. The aim of this study was to understand the effect of cyclic hydrostatic pressure (HP) as a mechanotransduction stimulus on hMSCs seeded in collagen hydrogels using a physiologically relevant pressure range similar to that experienced by osteocytes *in vivo* (0-280kPa).

METHODS: Collagen hydrogels with either low (0.5 mg/ml) or high (5.0 mg/ml) collagen concentration were seeded with hMSCs and cultured for four weeks in osteogenic media. A custom bioreactor (developed by Keele & TGT Ltd) was used to stimulate gels with 0 - 280kPa cyclic pressure at 1Hz, one hour per day for 28 days. µCT, fluorescent microscopy and histology were performed after 28 days culture.

RESULTS: Fluorescent microscopy revealed increased collagen autofluorescence in stimulated samples, indicating enhanced birefringence due to ECM remodelling causing collagen fibril alignment (*fig. 1 a,b*). µCT analysis showed increased mineralisation of nodules in the hydrogel in the pressure-stimulated samples over controls (*fig. 1 c, d*). Histological staining for calcium (alizarin red) showed increased mineralisation in stimulated hydrogels over controls (*fig. 1 e. f*).

DISCUSSION & CONCLUSIONS: Cyclic hydrostatic pressure results in enhanced mineralisation in hMSC-seeded collagen hydrogels at both low and high collagen concentrations. This was determined by µCT analysis and histology which revealed that the increase in density is due to calcification of the hydrogel. Evidence of collagen remodelling was also observed, suggesting that hydrostatic pressure stimulates cell-mediated remodelling of the extracellular matrix. Further work will focus on defining the parameters of force required to achieve the osteogenic effects and determining the mechanisms involved.

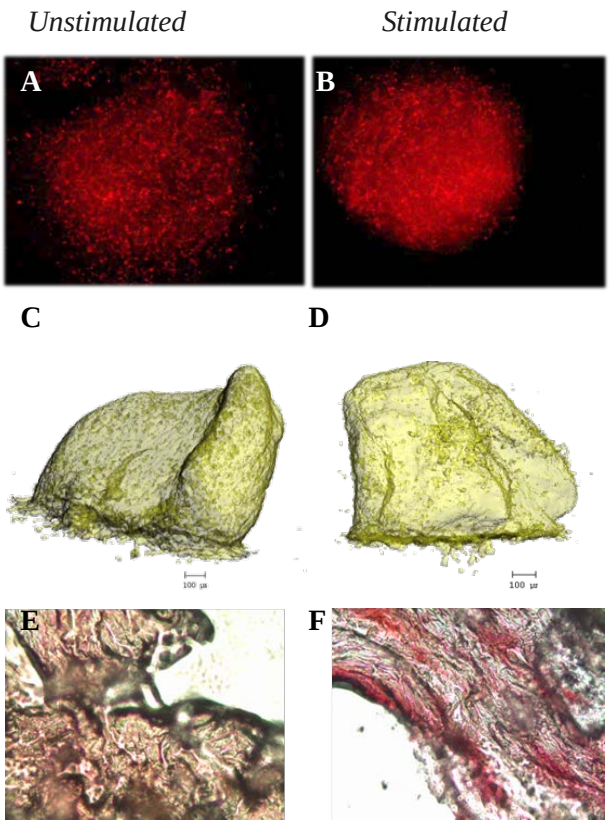

Fig. 1. Fluorescent microscopy of cell-seeded 0.5 mg/ml collagen hydrogels shows the distribution of cells (labelled with PKH26) and increased collagen autofluorescence in hydrostatically stimulated samples compared to unstimulated controls (a & b). µCT reconstrictions of the hydrogels illustrates the mineralising regions (c & d). The high density regions stained positively for calcium (alizarin red) with greater staining in hydrostatically stimulated samples (e & f).

REFERENCES: [1]Henstock JR, Rotherham M, Rose JB, El Haj AJ (2013) Cyclic hydrostatic pressure stimulates enhanced bone development in the foetal chick femur in vitro. Bone 53: 468-7

Growth factor-loaded biodegradable microparticles for bone tissue engineering

H Rashidi[1], H Cox[1], L White[1], O Qutachi[1], FRAJ Rose[1], ROC Oreffo[2], KM Shakesheff[1]

[1] *Centre of Biomolecular Sciences, School of Pharmacy, The University of Nottingham, UK*

[2] *Bone and Joint Research Group, Institute of Developmental Science, University of Southampton, UK*

INTRODUCTION: Critical sized defects in bone resulting from trauma and primary tumor resections have presented obstacles to the current treatment for bone repair. The identification of growth factors which play key roles in tissue regeneration have attracted great deal of attention in the past decade, however, the outcome from several clinical trials has been largely disappointing. The results from previous studies have suggested that spatio-temporal control is crucial to achieve optimal therapeutic effects of growth factors. Therefore, sophisticated scaffolds that can regulate the release of growth factors represent an attractive therapeutic path for bone tissue engineering.

In the current study, the effect of different growth factors on osteogenesis was studied in organotypic culture of the chick femur. Different protocols were developed to produce various formulations and sizes of microparticles containing selected growth factors using single and double emulsion techniques. Assessment of *in vitro* release kinetics showed that tailored release of growth factors was achieved by the inclusion of a triblock co-polymer in the microparticle formulations. Finally, the microparticles were transplanted into the chick femur and cultured for 10 days. The initial data suggested that controlled spatio-temporal release of bioactive growth factors can induce chondrogenesis and/or osteogenesis in the chick femur.

METHODS: Microparticles were prepared using double emulsion technique. Alteration of different factors such as viscosity and stirring speed enabled production of various sizes of microparticles from 2 to 100 microns. Microparticles were transplanted into 11 days old chick femur using glass needle and cultured for 10 days.

RESULTS: 11 days old chick was chosen as model system to integrate 3D culture conditions that combine foetal cells, scaffolds and niche signals to replicate the endochondral ossification process of human development *ex vivo* (Figure 1).

Following transplantation of growth factor-loaded microparticles, morphological changes was observed in host cells, while no difference was observed in bones transplanted by blank microparticles. In addition, up-regulation of early markers of differentiation in chondrocytes located in proliferative zone of the chick femur following injection of growth factor-loaded microparticles was observed (Figure 2).

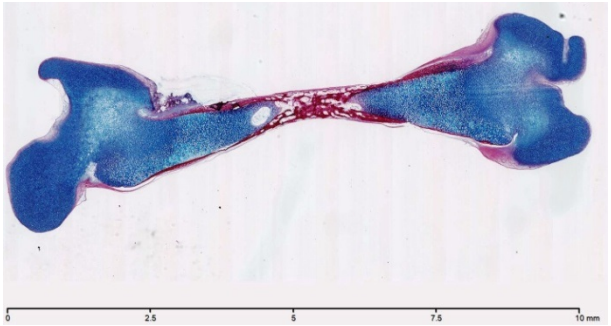

Fig. 1: Alcian Blue/Sirius Red staining of 11 days old chick femur.

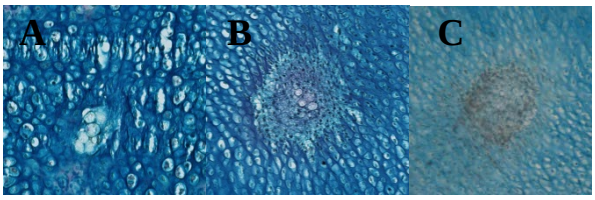

Fig. 2: Injected blank microparticles showed no effect on surrounding chondrocytes (A), while cells surrounding growth factor-loaded microparticles clearly showed morphological changes (B). Significant up-regulation of collagen II in cells around growth factor-loaded microparticles (C).

DISCUSSION & CONCLUSIONS:

Partial control on release of loaded growth factor/s can be achieved by modification of polymer formulation and size. Despite few disadvantages including limited period of culture to 10 days, organotypic culture of chick femur can be used as an *ex vivo* model to replicate endochondral ossification. Morphological changes and up-regulation of early markers of differentiation in chondrocytes located in proliferative zone of the chick femur following injection of growth factor-loaded microparticles indicated effectiveness of this strategy to direct cells toward certain differentiation pathways.

ACKNOWLEDGEMENTS: Presented research is part of LoLa project funded by the BBSRC.

Evaluation of electrospun gelatin/ polycaprolactone blends as a substrate suitable for use in corneal regeneration

JB Rose[1], A El Haj[3], HS Dua[2], A Hopkinson[2], FRAJ Rose[1]

[1]School of Pharmacy, Uni. of Nottingham, [2]School of Clinical Sciences, Uni. of Nottingham, [3] ISTM, Keele University

INTRODUCTION: The advent of new surgical techniques in corneal surgery has seen a paradigm shift in the way corneal blindness is treated[1]. These changes have called for a different approach to corneal tissue engineering. One such approach is developing component tissues of the cornea, such as partial thickness corneal stroma for use as a cellularised bandage. In this work the authors evaluate *in vitro*, the suitability of electrospun gelatin/ polycaprolactone scaffolds seeded with human corneal stromal cells (HCSC) as a potential candidate for preclinical development.

METHODS: Scaffolds were electrospun from blends of gelatin and polycaprolcatone (PCL) at various ratios (100:0, 50:50, 25:75, 0:100 – Gelatin: PCL). Scaffolds were characterised by scanning electron microscopy (SEM), Infra-red spectroscopy, water contact angle, and histology. After seeding HCSCs on selected scaffolds, quantitative assessments of adhesion and proliferation were carried out on each of the scaffolds through the AlamarBlue© assay. In addition assessments of transparency and cell infiltration of the scaffold was also investigated

RESULTS: The four blends of gelatin: PCL were electrospun successfully. All scaffolds facilitated some level of adhesion of HCSCs, however a significant difference between cell number adhered to the gelatin and PCL scaffolds was observed. Over 12 days there were no significant differences in the proliferation of HCSCs on any of the scaffolds. Assessment of the scaffolds after 12 days of cell culture showed that gelatin scaffolds were significantly more transparent than all others, and that HCSCs could successfully infiltrate the 100% gelatin scaffold.

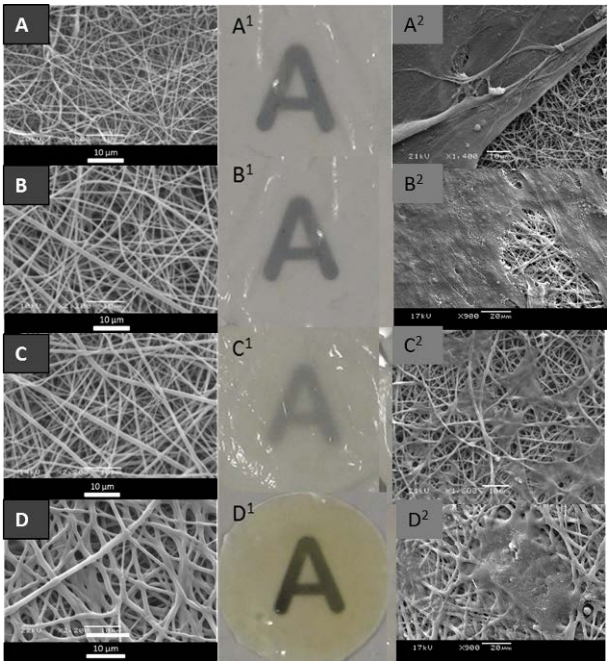

Fig. 1: SEM images of 4 chemically different electrospun matrices 100% gelatin (A); 50% gelatin: 50% PCL (B); 25% gelatin: 75% PCL (C) and 100% PCL (D). Macroscopic images demonstrating differences in the transparency of cellularised scaffolds over written letter A (1); SEM images of cell morphology of HCSCs on scaffold (2)

DISCUSSION & CONCLUSIONS: This work demonstrates that gelatin: PCL blends can be electrospun with modest control and that the electrospun sheets possess good cell compatibility with HCSCs. The relatively transparent gelatin scaffolds allow cellular infiltration and represent a suitable candidate for further development.

REFERENCES: [1]Keenan, T D L et al (2011). *Br. Journal Opth, 95*(4), 468–72..

Ex vivo and *in vitro* testing of a novel modified suture technique to incorporate a cell seeded tissue engineered tendon construct *in vivo*

P Sawadkar [1], S Alexander[1], L Bozec[2] and V Mudera[1]

[1] *Tissue Repair and Engineering Centre, UCL Division of surgery and interventional sciences, London.* [2] *Division of biomaterial and tissue engineering UCL Eastman Dental Institute, London*

INTRODUCTION: Surgically tendon repair is challenging as they are always under intrinsic tension which makes them more prone to injuries. When tendon rupture takes place due to trauma then the ruptured end releases tension and contracts proximally and distally to create a gap. When a gap is too large to be sutured under tension tendon grafts are used to bridge this gap**.** We have developed a highly reproducible technique to manufacture compressed cell seeded type I collagen constructs to replace tendon autografts. Previously we have tested these constructs *in vivo* in intercostal spaces of a lapine model to prove immunocompatibility [1] but, material properties of the engineered constructs are currently unsuitable to withstand complete load bearing *in vivo*. A modified suture technique has been developed to withstand physiological loading and off load the artificial construct whilst integration occurs.

METHODS: Lapine tendons (n= 56) were used to test mechanical strength of repairs and in situ break strength and a FEA stress model was built with COMSOL 3.5 software.

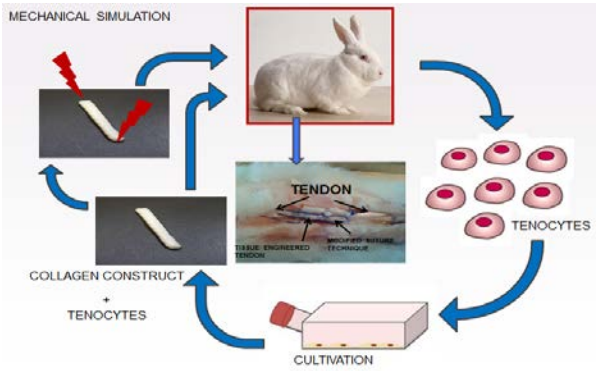

Fig.1: Fabrication of tissue engineered cell seeded tendon graft and load bearing suture technique.

To test the effect of the partial load on tenocytes mechanobiology was studied under static and 10% cyclic loads using custom designed force monitors with immunohistology and matrix remodling gene expression quantifiable outcomes.

RESULTS: The break point for modified suture technique with tissue engineered collagen construct in situ was significantly higher 50.62N compared to standard modified Kessler suture [12.49N ($p<0.05$)]. Mechanobiology studies showed that endogenous matrix tension was

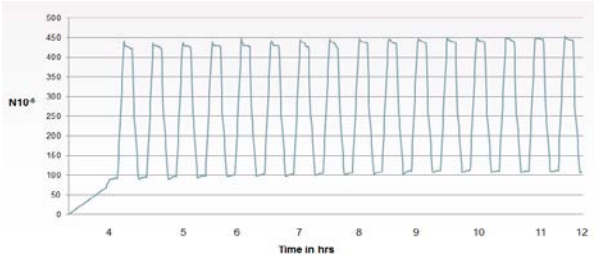

Fig. 2: Net force generated by tenocytes and homeostasis mechanism under 10% cyclic load.

maintained by tensional homeostasis and also showed significant upregulation of matrix remodelling genes COL1 (RQ 7.2), COL3 (RQ 0.8), Tenomodulin (RQ 2.3) and TGF-b (RQ 4.8) [$p<0.05$]

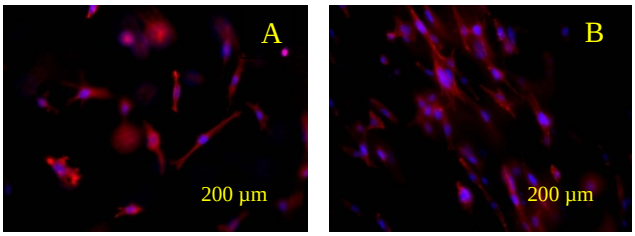

Fig. 3: Effect on tenocytes under (A) static and (B) cyclic loading.

Immunofluorescence microscopy images at 24 hours showed that on static load all cells were attached but had non-aligned morphology whereas in the cyclic load all cells were aligned in the direction of the force.

DISCUSSION & CONCLUSIONS: We are in the process of testing the cell-seeded tissue engineered tendon in a lapine model in the Achilles tendon using the modified suture technique developed for integration and function. We hypothesize that the 3D cell seeded construct will render a microenvironment for tenocytes and speed up neo-tendon formation and matrix synthesis *in vivo*.

REFERENCE:1) Mudera V,Morgan M, Cheema U, Nazhat S, Brown R. Ultra rapid engineered collagen constructs tested in an in vivo nursery site J Tissue Eng Regen M 2007;1(3):192-8.

A 3D *in vitro* mineralised culture system to investigate osteocyte biology and function

NEE Scully[1, 4], SL Evans[2, 4], DJ Mason[3, 4], BAJ Evans[1, 4]

[1] Institute of Molecular and Experimental Medicine, School of Medicine, [2] School of Engineering, [3] Division of Pathophysiology and Repair, School of Biosciences, [4] Arthritis Research UK Biomechanics and Bioengineering Centre, Cardiff University, Wales.

INTRODUCTION: Osteocytes make up >90% of bone cells, are embedded in mineralised matrix where they form a communication network. Osteocytes differentiate from osteoblasts, and are mechano-sensitive. They are very difficult to isolate with currently a dependence on cell lines (*e.g.* MLO-Y4, IDG-SW3) for *in vitro* studies of osteocyte biology.[(1, 2)] Recent publications have indicated that osteoblasts maintained in *in vitro* 3D collagen gels may differentiate to osteocytes.[(3-6)] We have further investigated these findings and developed a novel, 3D, mineralised culture system enabling the differentiation of osteoblasts to osteocytes, which can then be applied to the study of osteocyte biology and function.

METHODS: We maintained MC-3T3 and human primary (hOB) osteoblasts in 3D type I collagen gels (250 µl; 48-well plates; 15 days) in either α-MEM (basal medium) or mineralising medium (basal medium, dexamethasone, ascorbate-2-phosphate, β-glycerophosphate). Cell number, viability and phenotype (IHC, qRTPCR, confocal microscopy), gel stiffness (Losenhausen materials testing machine), and VEGF and IL-6 secretion (both putatively involved in mechano-regulation; ELISAs) were quantified. For some experiments, the effects of adding IGF-1 (50 ng/ml) to the basal medium were analysed. Methods of applying mechanical load to these gels are currently being optimised.

RESULTS: MC-3T3 and hOB cells appeared more dendritic over time and formed connecting cellular networks (H&E, phalloidin). Cell viability was similar in both media (>85% MC-3T3s; >95% hOBs), but cell numbers were significantly higher ($p<0.001$) in mineralising conditions. Mineralisation was confirmed from day 7 (calcein). DMP-1 was not expressed (IHC) at day 3 but then appeared to gradually increase from days 7–14. E11 was low at day 3 (IHC, qRTPCR), peaked at day 10 ($p<0.001$), and returned to lower levels by day 14. Gel stiffness significantly increased over 11 days ($p<0.01$) and the mineralised gels were stiffer than those in basal medium ($p<0.01$). VEGF and IL-6 secretion also changed significantly with time and culture conditions. Cell viability remained high when cells in gels were treated with IGF-1 (>85% MC-3T3s; >90% hOBs). From day 11 onwards, the expression of DMP-1, Cx43, RANKL ($p<0.01$) and FGF-23 ($p<0.001$) were significantly increased in MC-3T3s with IGF-1, compared to untreated. This increase in FGF-23 confirms differentiation to osteocytes.

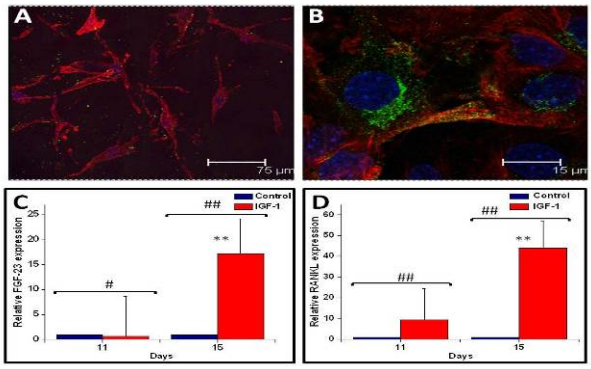

*Fig 1: A, B Confocal microscopy of A) hOBs (day 15) for actin (red), mineral (green), nuclei (blue) and B) MC-3T3s (day 21) for actin (red), Cx43 (green), nuclei (blue). C, D The effect of IGF-1 (50 ng/ml) on C) FGF-23 and D) RANKL expression (qRT-PCR). **, $P < 0.01$ compared to day 11 control, #, ##, $P < 0.05$, 0.01 compared to treatment on same day.*

DISCUSSION & CONCLUSIONS

Osteoblasts maintained in 3D gels differentiate along the osteocytic pathway. It is possible to mineralise these cultures thus mimicking further their *in vivo* environment. FGF-23 production with IGF-1 treatment highlights the possible role of IGF-1 in osteocyte differentiation and function. This work provides a novel model to study osteocyte differentiation and function, and has provided novel insights in to the role of IGF-1 in this process.

REFERENCES: [1]Kato Y *et al.* 1997, *J Bone Miner Res.;* 12: 2014-23. [2] Woo SM *et al.* 2011, *Bone;* 30: 718-25. *J Bone Miner Res.;* 26(11):2634–2646. [3]Ferrera D *et al.* 2002, *Bone;* 30: 718-25. [4]Murshid SA *et al.* 2007, *J. Bone Miner Metab.;* 25: 151-8. [5]Barron MJ *et al.* 2010, *J Biomech Eng.*; 132(4): 041005. [6]Boukhechba F *et al.* 2009, *J Bone Miner Res.;* 24(11):1927-35.

ACKNOWLEDGEMENTS: We thank Carole Elford, Kath Alsop and Tony Hayes for their contribution. The work was funded by Cardiff University and Arthritis Research UK.

Fibronectin fragments modulate ROCK activity to enhance osteogenic differentiation of bone marrow stromal cells

RI Sharma[1,2], JG Snedeker[1]

[1]*Department of Orthopaedics and Department of Mechanical Engineering, University and ETH Zurich, Switzerland,* [2]*Department of Chemical Engineering, University of Bath, United Kingdom*

INTRODUCTION: Formation of new bone relies upon osteoblasts originating from bone marrow stromal cells (BMSCs). Clinical scenarios exist for which inherent bone healing capacity is inadequate. Substrate based approaches can direct differentiation by relying on cell-matrix interactions from biochemical and mechanical cues which regulate cell signalling and differentiation [1]. In this study, we hypothesised that stiffer substrates and peptide fragments presenting cell-binding epitopes would result in differential cell contractility, and that this would promote cell spreading, ROCK activity, and lead to upregulated gene expression of osteogenic markers.

METHODS: Polyacrylamide substrates with three different elastic moduli ranges (10-30, 30-50, and 70-90 kPa) were functionalised with either whole length fibronectin or RGD, a tripeptide in the cell-binding region of fibronectin [2]. Human BMSCs were seeded for cell attachment studies, which were assayed by normalising cell counts to the initial seeding density. We quantified the expression of focal adhesion elements (paxillin, vinculin, focal adhesion kinase) with RT-PCR. Cell morphology was examined by staining the cytoskeleton with FITC-phalloidin. Phosphorylated ROCK activity was assessed with a colourimetric ELISA. After 14 days of culture, osteogenic differentiation was examined by staining for mineralised deposits with Alizarin Red, and RT-PCR confirmed the expression of osteo-relevant genes (Runx2, alkaline phosphatase, collagen I, and osteocalcin). Finally traction force microscopy was implemented to gain insights on cell contractility.

RESULTS: The RGD peptide substrates promoted a higher degree of cell attachment and expression of focal adhesion elements. This early expression translated to enhanced cell spreading and increased ROCK activity (Fig. 1). We observed increased BMSC osteogenic differentiation on RGD-functionalised substrates compared to fibronectin (Fig. 2A-D), with more nodules as the elastic modulus increased. Traction forces increased from intermediate to stiff RGD substrates but unexpectedly dropped on analogous fibronectin substrates (Fig. 2E).

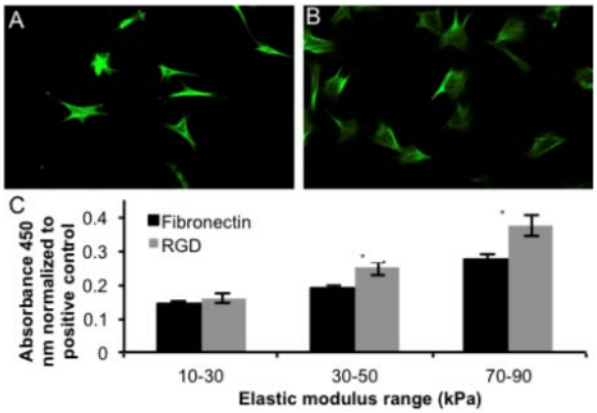

Fig. 1: Cells on (A) fibronectin 70-90 kPa were contracted compared to those on (B) analogous RGD substrates. (C) ROCK activity increased with elastic modulus and higher on RGD substrates.

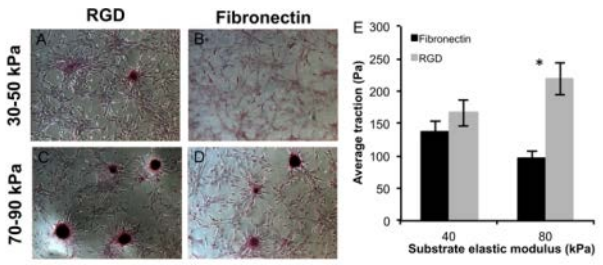

Fig. 2: (A-D) More calcium nodules were seen on RGD substrates, with an increase from stiffer substrates. (E) Traction force studies show an increase in force on RGD substrates.

DISCUSSION & CONCLUSIONS: A critical balance of spatial, biochemical, and mechanical cues are essential for osteogenic differentiation. Our findings demonstrate the relative importance of specific binding epitopes in mediating osteogenic cell response. It appears that integrin signalling and ROCK activity were at least partly decoupled from force-mediated activity. This study highlights the mechano-chemical nature of a biomaterial as a potent design element in the conception bone tissue engineering solutions.

REFERENCES: [1] R.I. Sharma and J.G. Snedeker (2012) *Plos One* 7(2):e31504. [2]K. von der Mark, et al (2010) *Cell Tissue Res* 339(1):131-53.

ACKNOWLEDGEMENTS: This work was funded by the Bonizzi-Theler Stiftung.

Control of cell fate and oxygen gradients in collagen constructs for tissue engineering applications

RJ Shipley[1], A Ardakani[2], K Stamati[2], U Cheema[2], R Brown[2]

[1] Department of Mechanical Engineering, University College London. [2] Tissue Repair and Engineering Centre, Institute of Orthopaedics and Musculoskeletal Sciences, University College London

INTRODUCTION: A key requirement of any scaffold is the ability to promote cellular function – the material must support cells within a 3D environment that mimics the architecture, biomechanical and biochemical environment of *in vivo* tissue. One option is to seed cells in a collagen gel – plastic compression increases the collagen density (and hence mechanical integrity) to representative *in vivo* values. This approach has been shown to sustain oxygen concentrations at physiological values throughout a construct.

An oxygen gradient is established radially through the construct, as a consequence of consumption by the cell population. This results in heterogeneity in cellular proliferation and death rates, as well as chemotactic migration. The current study quantifies these features through experimental data. These data parameterise a mathematical model that identifies design criteria that link cell seeding densities and construct size to hypoxia and spatial cell density distribution.

METHODS: Cell-seeded collagen spirals were fabricated using plastic compression[1], resulting in scaffold densities of 11.6% with $23.2x10^6$ human neonatal dermal fibroblasts cells/ml. Spirals were cultured for up to 10 days at which point three segments of compressed collagen matrix (outer, middle and core, in order of higher to lower oxygen exposure) were analysed by quantifying cell death and proliferation, using both live/ dead and proliferation assays. Real-time oxygen measurement data for the same setup was achieved using fibre-optic oxygen probes (Oxford Optronix, UK)[2].

A mathematical model was developed based on mixture theory, to track the concentration of oxygen, and density of cell, fluid and collagen throughout the construct. Constitutive laws were proposed to describe the stresses within each phase (cells, fluid or collagen), interactions between phases (e.g. drag between the cells and scaffold), and cell processes (e.g. cellular aggregation, contact inhibition and chemotaxis). The models were parameterised by data fitting against the experimental data described above.

RESULTS: An oxygen gradient of approximately 110 mmHg is measured from the outer surface to the construct core. Consequently, the outer segment showed an increase in both proliferative cell number (37% $p<0.01$) and viability (3.8% $p<0.01$) when compared to the middle and core segments. Cell viability decreased in the core (7% $p<0.01$) and middle (3.7% $p<0.01$) segments, but proliferative cell number increased in these segments (9.0, 9.7% respectively $p<0.01$).

The mathematical model took these data as inputs to predict the spatial distribution of cells and oxygen throughout the construct. Model predictions identified the dependence of minimum oxygen partial pressure upon both seeded cell density and construct radius (see Fig. 1).

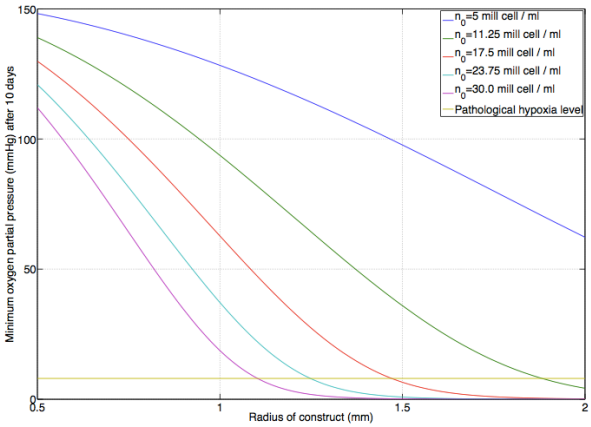

Fig. 1 Model predictions of the dependence of minimum oxygen partial pressure at the construct core, on construct radius and seeded cell density.

DISCUSSION & CONCLUSIONS: A combination of experimental data and mathematical modelling have quantified the link between spatial gradients in oxygen and cell density in collagen-based constructs. Design criteria have been identified that enable oxygen gradients to be controlled through construct size and cell seeding.

REFERENCES: [1] R.A. Brown, et al (2005) *Adv Funct Mater* **15**L 1762-70 [2] I. Streeter & U. Cheema (2011). *Analyst* **136**: 4013-4019.

Engineering capillary networks in 3D *in vitro*

K Stamati[1], J.V Priestley[2], V Mudera[1] and U Cheema[1]

[1] UCL, Tissue Repair and Engineering Centre, Institute of Orthopaedics and Musculoskeletal Science HA7 4LP Middlesex, London [2]Centre for Neuroscience & Trauma, Blizard Institute of Cell and Molecular Science Barts and The London School of Medicine and Dentistry, 4 Newark Street Whitechapel London E1 2AT

INTRODUCTION: Engineering a capillary network that can be integrated into tissue engineered constructs will increase both short term and long-term success of *in vivo* implants. The aim of our study was to test parameters that result in optimal endothelial cell network aggregation, such as supporting cell types and oxygen concentration levels. We tested endothelial cell (EC) aggregation in networks in co-cultures with human bone marrow stem cells (HBMSCs) or human dermal fibroblasts (HDFs) under different O_2 levels.

METHODS: HDFs or HBMSCs were co-cultured with human umbilical vein endothelial cells (HUVECs) in 3D collagen hydrogels with laminin. The constructs were cultured under normoxia (20% O_2) or hypoxia (5% O_2) for a week and then stained for CD31 to test cell morphology and aggregation. The length and number of network aggregates was counted and comparisons were made between the different conditions. Growth factor levels were tested using ELISAs for VEGF, Angiopoietin-1 and TGFβ.

RESULTS: ECs showed significantly different aggregation patterns depending on the supplementary cell type and oxygen levels in which they were cultured. ECs optimally aggregated in networks in co-cultures with HBMSCs in normoxia whereas in co-cultures with HDFs aggregated in networks only in hypoxia co-cultures. Network aggregates in HBMSC co-cultures were of an average length of 98μm and in HDF co-cultures 93μm. Cell aggregation patterns were associated with differences in growth factor levels. In HDF hypoxia co-cultures there were significantly higher levels of VEGF (~400pg/ml), compared to normoxia (~16pg/ml) and also higher levels of angiopoietin-1 in hypoxia (~190pg/ml) compared to normoxia (~30pg/ml). In HBMSC co-cultures VEGF levels were significantly higher in co-cultures in hypoxia (~1600pg/ml) compared to normoxia (~800pg/ml).

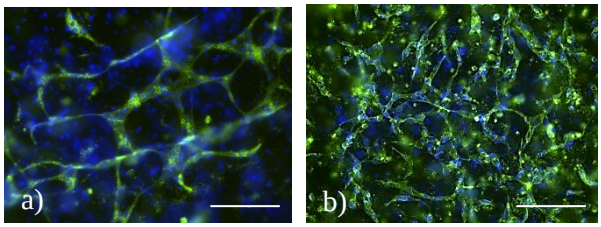

Figure 1: a) Endothelial cell networks in collagen-laminin hydrogels with HDFs in hypoxic conditions and b) Endothelial cell networks in co-cultures with HBMSCs in normoxia. CD31 in green, DAPI in blue. Scale bar 100μm

DISCUSSION & CONCLUSIONS: HBMSCs induced EC network aggregation in normoxic conditions, while networks only formed in hypoxic conditions with HDFs. Our findings show that interactions between ECs and supporting cell types are significantly affected by oxygen concentration levels. The release of some growth factors is influenced by oxygen conditions, which in turn guide cell response and aggregation. These findings can be used to drive specific EC aggregation patterns for use both in *in vitro* and *in vivo* testing.

REFERENCES: [1]U.Cheema, R.A.Brown, B.Alp, A.J.MacRobert (2008) Spatially defined oxygen gradients and vascular endothelial growth factor expression in an engineered 3D cell model. *Cell Mol.Life* Sci. **65**, 177-186.

ACKNOWLEDGEMENTS: Katerina Stamati is funded by UCL IMPACT and Oxford Optronix and Umber Cheema is a BBSRC David Philips fellow.

Tuneable peptide scaffolds for chondrocyte culture and recovery.

L.Szkolar[1,2], A. Miller [2], J.E.Gough[1], A.Saiani[1]

[1] *Materials Science Centre , School of Materials, The University of Manchester, UK.*

[2] *Manchester Institute of Biotechnology , School of Chemical Engineering, The University of Manchester, UK.*

INTRODUCTION: Degenerative diseases of cartilage affect a high proportion of the population. The focus of current research is to produce ways of culturing chondrocytes on a large scale [1] or producing replacement cartilage [2].

Self-assembly has emerged as a powerful tool for materials fabrication. It has been shown that peptide materials can allow for the culture and proliferation of chondrocytes [3,4], where cartilage-like ECM was produced.

This work looked at the effect of peptide sequence and mechanical properties on the culture of primary bovine chondrocytes. The peptide FEFKFEFK (F-8) has been shown to be suitable for cell culture. The natural ECM exhibits a net positive charge due to the attraction of sodium ions by proteoglycans. For this reason a nonapeptide analog to F-8 comprising an additional positive charge (F-9) was chosen for comparison.

METHODS: Cells were extracted [5] and cultured in 5 % CO_2 at 37 °C. BC's were maintained in DMEM supplemented with 10 % FBS 1 % antibiotic and 50µg/mL of ascorbic acid. Peptide solutions were prepared at concentrations of 10-30 mg mL^{-1} and adjusted to pH 7.5 with 1M NaOH. Cells were suspended in media at $5x10^5$ cells per 300µL and cultured in 3D. Cell counts were performed in triplicate by dissolving the gel in excess media and then counting using a haemocytometer. Antibody staining was performed to observe Col I and Col II.

RESULTS:

Fig. 1: Antibody staining of bc's cultured on a)F-8 and b)F-9 day 14. i)ColI ii)ColII.

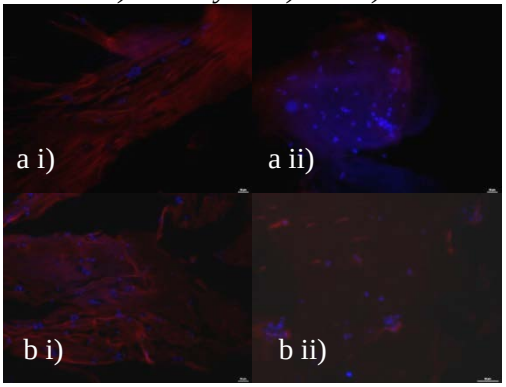

Fig. 2) Cell numbers,21 days on F-8[red] and F-9[pink]. Hydrogels had a G' of 10,000 Pa

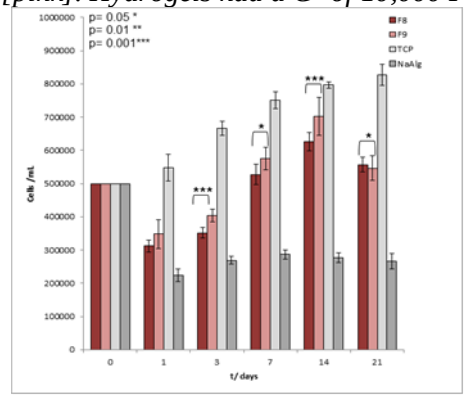

DISCUSSION & CONCLUSIONS: Peptide gels with different net charges at pH 7.5 were produced with equivalent strengths. Bovine chondrocytes were cultured for 21 days. After initial declines on both gels due to environmental change, numbers increased on both gels at day 3, with F-9 exhibiting a statistically significant increase in proliferation when compared to F-8. Both systems continued to increase until day 21, when numbers began to decline due to gel degradation.

An increase in the G' of both systems was seen after 7 days of culture suggesting the cells are laying down matrix (data not shown). Antibody staining was used to visually observe Col I and Col II production. Both systems exhibited Col I and some Col II at day 14.

REFERENCES: [1] Tae-Jin Lee et al (2011) *Biotechnol Lett* 33:829–836. [2] Benjamin D. Elder et al (2010) *Neurosurgery* 12:722-727, 201. [3] Holmes TC et al (2000) *proceedings Nat acad sci* 97:6728-6733. [4] J. Kisiday (2002) *Proceedings Nat acad sci* 15: 9996-10001 5 JJABarry (2004) *Biomat* 25:3559-3568

ACKNOWLEDGEMENTS:

Peptisyntha (a member of the Solvay Group), Belgium (http://www.peptisyntha.com)

Assessing nanoparticles in an engineered 3D *in vitro* model tissue system

NS Tan[1], X Yang[2], D Ossipov[2], J Hilborn[2] and RA Brown[1]

[1] *University College London, Tissue Repair & Engineering Centre, Institute of Orthopaedics & Musculoskeletal Science, Stanmore Campus, London, HA7 4LP, United Kingdom.* [2] *Department of Chemistry-Angstrom, Angstrom Laboratory, Uppsala University, , Lägerhyddsvägen 1, Box 538, SE-751 21, Uppsala, Sweden.*

INTRODUCTION: Nanoparticulate delivery systems are normally tested on 2-dimensional (2D) cell cultures, but oftentimes positive results do not translate well in vivo, leaving a need to develop more physiological 3-dimensional (3D) tissue models [1,2]. Here we present results of a novel 3D model, using plastic compression (PC) of collagen to form depots of hyaluronan nanoparticle (HA-NP) which can be used to determine their tissue fate.

METHODS: Collagen gels were prepared as previously described, with the exception of the inclusion of HA-NP (FITC-tagged; 500 nm diameter) in the collagen mixture [3]. The neutralised collagen was aliquoted into wells of 1.6 mm diameter, and allowed to set. Absorbent plungers were then placed on top of the gels to initiate plastic compression. A vast amount of fluid within the gel is removed, and with it, HA-NP. Thus, the retention rate of the NPs was measured, and improved upon by the addition of a second collagen layer to increase the number of collagen fibres to trap the NPs within the construct. Measurements were done by fluorometry following collagenase digestion of the loaded scaffolds and fluorescence microscopy of DAPI-stained sections to identify the spatial distribution of the HA-NP within compressed scaffolds plus the effects of cell density and release of HA-NP from the scaffolds over time.

RESULTS: The addition of a second collagen layer increased the retention of the mobile HA-NP in the constructs, and the retention increased with increasing volume of this second layer. In 1.0 ml constructs, a HA-NP depot was formed at the top, fluid leaving surface (FLS), whilst for 1.5/2.0 ml constructs, HA-NP accumulated at both the top and bottom surfaces, consistent with predicted non-linear fluid flow during the compression period. This effect was enhanced when a 2nd collagen layer was added on top of the PC-NP layer and co-compressed. Addition of cells with the collagen further complicated the fluid outflow, limiting the cell density used, but still enabling fabrication of dermal fibroblast tissue equivalents containing the HA-NP biomaterial.

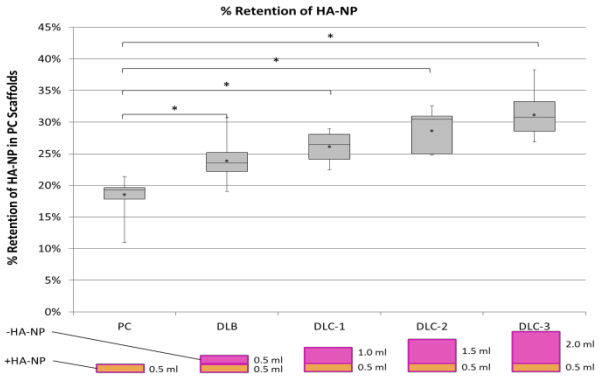

Fig. 1: Retention of HA-NP in collagen scaffolds following plastic compression.

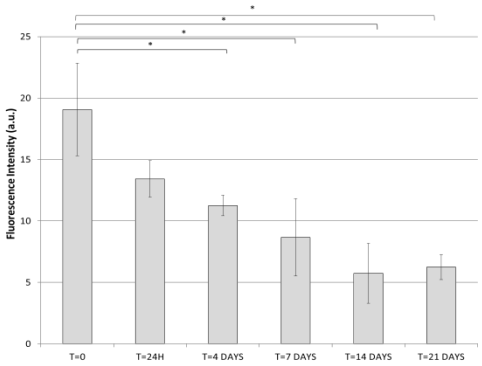

Fig. 2: HA-NP release from compressed collagen due to cellular remodelling of the scaffolds.

DISCUSSION & CONCLUSIONS: This system provides a controllable form of NP depot within a tissue equivalent, for the study of NP fate in 3D.

REFERENCES: [1] E.C. Cho, Q. Zhang & Y. Xia (2011) *Nature Nanotech. 6, 385–391*, McGraw-Hill, Inc. [2] D.N. Karunaratne, P.S. Silverstein, V. Vasadani, A.M. Young, E. Rytting, B. Yops, K.L. Audus (2005) Cell culture models for drug transport studies *in Drug Delivery: Principles and Applications*, (eds B. Wang, T. Siahaan, R. Soltero) John Wiley & Sons, pp. 103–124. [3] R.A. Brown, M. Wiseman, C.-B. Chuo, U. Cheema and S. N. Nazhat (2005) *Adv. Func. Mater. 15, 1762-1770.*

ACKNOWLEDGEMENTS: Biodesign, EU Commision Framework 7.

Cytokine stimulated decellularised matrices: Exploring matrix remodelling and cell-matrix interactions

AJ Taylor[1], BD Ratner[2], MR Alexander[1], LDK Buttery[1]

[1] School of Pharmacy, University of Nottingham, Nottingham, UK. [2] NESAC/BIO, Dept. of Bioengineering, University of Washington, Seattle, WA, USA.

INTRODUCTION: *In vitro* cell secreted decellularised matrices[1] provide a useful model system to understand how cell types produce, remodel & interact with their extracellular environs as they allow control of matrix expression with soluble factors such as cytokines & growth factors.

We describe the production of decellularised matrices stimulated with pro-inflammatory cytokines during matrix expression; characterise changes in matrix composition by ToF-SIMS; and assess behaviour of reseeded mPC and mES cells.

METHODS: Mouse primary calvarial (mPC) cells are grown in osteogenic conditions (BGP, Ascorbate, Dexamethasone) on tissue culture polystyrene multi-well plates or Thermanox PET coverslips. At day 7 or day 12, cultures are stimulated with pro-inflammatory cytokines (IFN-γ, TNF-α, IL-1β) for 48 hours. After 14 days, cells are removed by treatment with 20 mM ammonium hydroxide, followed by 50 U/ml DNase I, leaving an intact decellularised matrix.

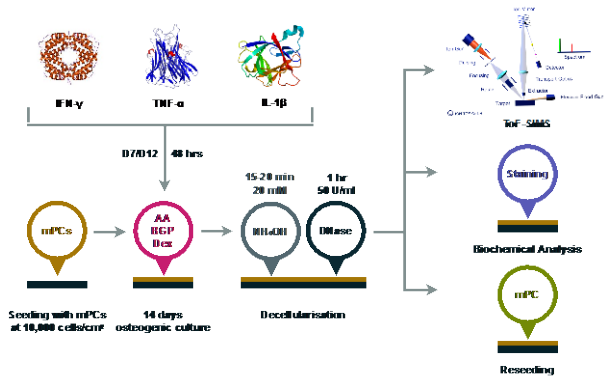

Fig. 1: Schematic showing the production, characterisation, and reseeding of cytokine stimulated decellularised matrices.

Composition of cytokine stimulated decellularised matrices are analysed by time-of-flight secondary ion mass spectrometry (ToF-SIMS)[2] alongside histological & immunohistochemical staining. mPC and post-EB mES cells are reseeded on their matrices. Their adhesion, morphology, and differentiation are assessed.

RESULTS: Matrices are demonstrated to be cell free and retain relevant ECM proteins. Principle component analysis of ToF-SIMS data allows separation of stimulated and unstimulated matrices from one another & Collagen I/Fibronectin protein coats. Loadings of amino acid fragment peaks suggest a reduction in collagen content in stimulated matrices. This is confirmed by histological methods.

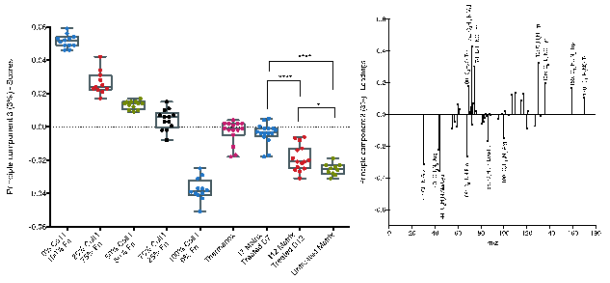

Fig. 2: PCA scores & loadings plots for ToF-SIMS analysis of cytokine stimulated decellularised matrices and adsorbed proteins.

Morphological and adhesion analysis of mPC cells reseeded on cytokine stimulated decellularised matrices reveal significant differences in cell behaviour compared to unstimulated matrices.

DISCUSSION & CONCLUSIONS: Using decellularised matrices and ToF-SIMS we have demonstrated the influence a pro-inflammatory environment on ECM composition and subsequent cell behaviour. This work highlights the value of surface analysis techniques and decellularised matrices in modeling disease states and understanding cell-matrix interactions in complex systems.

REFERENCES: [1] Decaris ML, Leach JK (2010) *Design of Experiments Approach to Engineer Cell-Secreted Matrices for Directing Osteogenic Differentiation.* Ann Biomed Eng 39(4): 1174–1185. [2] Brown BN *et al.* (2010) *Surface characterization of extracellular matrix scaffolds.* Biomaterials 31(3): 428–437.

ACKNOWLEDGEMENTS: AJ Taylor is funded by the EPSRC DTC in Regenerative Medicine. ToF-SIMS was performed at NESAC/BIO, University of Washington.

Polyurethane-Hydroxyapatite composite scaffolds for in vitro bone tissue engineering

G. Tetteh, I. Rehman, G. Reilly

Kroto Research Institute, University of Sheffield, Sheffield S3 7HQ

INTRODUCTION: Currently, both in vitro and in vivo testing of bone implants face several limitations. In-vitro tests are limited in their lack of a dynamic environment and the inability to investigate the mechanical properties between bone matrix and implant surface, while in-vivo experiments are limited by the difference in structure and cell behavior between animal and human bone.

Therefore, the long-term goal of this work is to develop a biomimetic tissue engineered bone construct that can be used in studying in vitro bone formation around implants. The first step towards this is to optimize a bioactive mechanically stable scaffold. In this study we investigated the ability of a medical grade flexible polyurethane to support bone cells and different methods of incorporation of hydroxyapatite to improve the material's ability to support matrix forming osteoblasts.

METHODS: Polyurethane (Z9A1 and Z3A1 from *Biomer*) polymer was dissolved in different solvent [Dimethylformamide (DMF) and Tetrahydrofuran(THF)] combinations and electrospun to attain scaffolds with random nano and micro-diameter fibers Polyurethane-Hydroxyapatite (PU_HA) composites were electrospun with 5%wt micro and nano-particle sized HA.

MTT cell viability assay using MLO-A5 osteoblastic mouse cells was used for biocompatibility studies of on the electrospun scaffolds. DAPI and Phalloidin stains were used to observe cell morphology on the polyurethane scaffolds whilst Sirus Red and Alazarin Red were used to stain for collagen and calcium on day 14 of cell culture.

RESULTS: SEM image analysis of electrospun plain polyurethane (Z3A1 & Z9A1) using ImageJ software showed differences in fibre morphology with changes in solvent combinations, whilst MTT assay showed that cells were viable on all scaffolds made from these different solvent combinations.

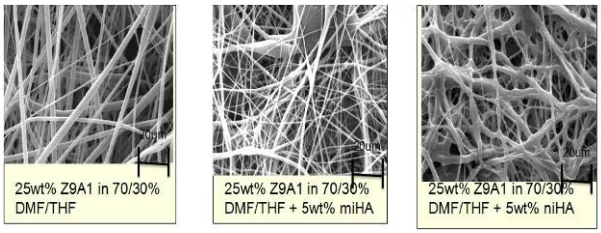

Fig. 1: SEM images of electrospun plain PU_HA scaffolds with 5% micro and nano HA.

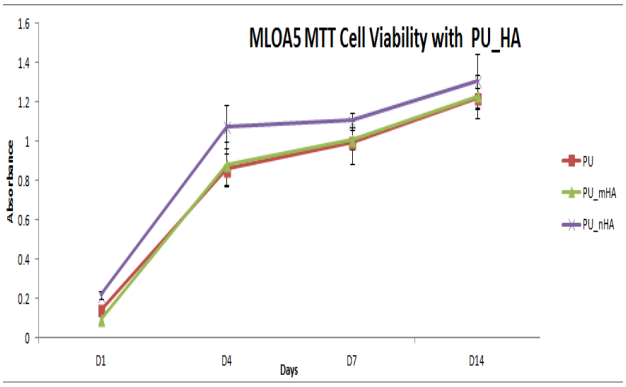

Fig. 2: MTT cell viability on electrospun composite polyurethane hydroxyapatite scaffolds

DISCUSSION & CONCLUSIONS: Electrospun plain polyurethane scaffolds support proliferation of MLOA-5 osteoblastic cells, but polyurethane scaffolds with nano-HA composites may possess better bioactive properties than polyurethane with micro HA composites. These scaffolds have potential to support bone matrix formation for in vitro testing.

REFERENCES: [1] Sittichockechaiwut, A., et al. *Bone*, 44.5 (2009): 822-829. [2] Khan, A. S., et al. *Acta Biomaterialia*, 4.5 (2008): 1275-1287.

ACKNOWLEDGEMENTS: R. Delaine-Smith, Kroto Research Institute, University of Sheffield, Sheffield, UK and the Ghana Education Trust Fund.

Can skeletal muscle grown *in vitro* be used to investigate insulin resistance?

MC Turner[1], **DJ Player**[1], **NRW Martin**[1] **, MP Lewis**[1]

[1]*Loughborough University, Loughborough, Leicestershire, United Kingdom*

INTRODUCTION: Hyperinsulinemia is a potent cause of insulin resistance (1), and thus impaired glucose uptake, which in turn can result in type II diabetes. Since skeletal muscle accounts for the majority of glucose uptake in the body (2), investigation in to the underlying mechanisms involved in the development of insulin resistance in this tissue is warranted. *In vitro* experimentation is an ideal methodology to help understand the development of insulin resistance on a cellular and molecular basis, and has already led to a degree of understanding of the aetiology of the disease (3,4). The purpose of the present experiments was to establish culture parameters that would drive insulin resistance in cultured skeletal muscle cells. These parameters would then form the basis of a system to develop "diabetic" tissue engineered skeletal muscle.

METHODS:
C_2C_{12} myoblast were grown until confluent, before being incubated with either a control (CON) differentiation media (DMEM + 2% HS), or an insulin treated (IT) media (DMEM + 2% HS and 100nM Insulin). The media was changed every 12 hours for 72 hours as previously described (3). Cells were then re-stimulated (ST) with insulin (100nM) or left un-stimulated (US). The subunit p85 of phosphoinositide 3-kinase (p85 PI-3 Kinase) and Akt, two proteins implicated in insulin signalling were measured by immunoblotting. Furthermore, mRNA expression of Hexokinase II and Peroxisome Proliferator-Activated Receptor (PPAR)-coactivator (PGC)-1α, two important genes involved in cellular metabolism were investigated by qRT-PCR. Statistical analysis was conducted using a one-way ANOVA or equivalent non-parametric test. The data is presented as mean ± SEM and were an accumulation of three independent experiments.

RESULTS:
There were no changes in total p85 PI-3 Kinase expression ($p > 0.05$). There was an increase in phosphorylation of Akt at residue serine 473 (Ser^{473}) in CON-ST vs. CON-US ($p < 0.01$), however this effect was blunted in the insulin treated condition ($p > 0.05$). There was a significant main effect for treatment on mRNA expression of Hexokinase II (HKII) ($p < 0.01$), with significant differences between CON-US and CON-ST conditions ($p < 0.01$), however, there were no differences between CON and IT groups. PGC-1α expression was significantly lower ($p < 0.01$) following IT-ST compared to CON-US and CON-ST, respectively.

DISCUSSION & CONCLUSIONS:
Exposure of skeletal muscle cells to a hyperinsulineamic environment reduces phosphorylation of Akt, a key regulator in insulin signalling. In addition, mRNA expression of genes implicated in both mitochondrial biogenesis and glucose metabolisms were also impaired. This cell culture model replicates a selection of the protein and transcriptional features of an *in vivo* diabetic skeletal muscle. In future experiments we hope to recreate these findings when skeletal muscle cells are cultured in a three-dimensional scaffold, in order to create a truly physiological model of insulin resistant skeletal muscle.

REFERENCES: (1) Gaster M, Petersen I, Hojlund K, Poulsen P, Beck-Nielsen H (2002). *Diabetes*; 51(4):921-927. (2) DeFronzo RA, Gunnarsson R, Bjorkman O, Olsson M, Wahren J. (1985). *J Clin Invest*; 76(1):149-155. (3) Kumar N, Dey CS. (2003) *Biochem Pharmacol* 15; 65(2):249-257. (4) Del Aguila L, Claffey K, Kirwan J. (1999). *Am J Physiol -Endocrinol Metab* 276(5):E849-E855.

ACKNOWLEDGEMENTS: The authors would like to acknowledge Dr Amarjit Saini for his support during the experiments.

Endothelial cell induction of osteogenesis using an *in vitro* organotypic culture.

B van Herwijnen[1], J M Kanczler[1], R O C Oreffo[1,]

[1] *Bone and Joint Research Group, Centre for Human Development, Stem Cells and Regeneration, Human Development and Health, Institute of Developmental Sciences, Southampton General Hospital, Southampton, England.*

INTRODUCTION: Elucidation of bone development and reparation is paramount in order to advance skeletal regenerative strategies. Endothelial cells (ECs) have been shown to induce osteogenesis when in direct contact with bone marrow stromal cells (MSCs). [(1)] This study used an organotypic embryonic femur culturing system to investigate how ECs modulate bone development**.**

METHODS: Segmental defects were created in the mid diaphysis of embryonic chick femurs of E11-E18. EC pellets and the bone ends were placed in juxtaposition or 2mm apart with or without the implantation of EC pellets (2 x 10^5) (n=6 respectively). These femurs were then organotypically cultured for 10 days in serum free basal medium. Histological and immunohistochemical analysis of femur samples included alcian blue/Sirius red (proteoglycan and collagen markers for cartilage and bone), von Willebrand factor (vWF) (EC markers) and STRO-1 expression (MSC marker).

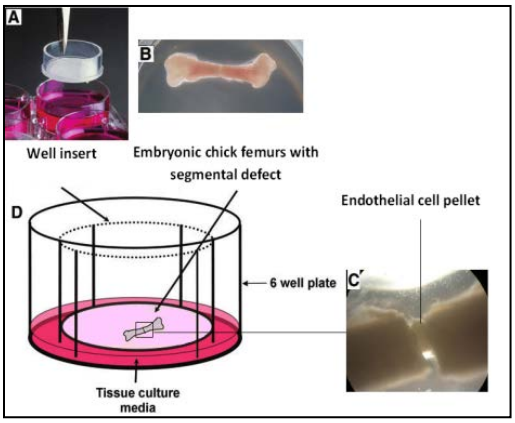

Fig. 1. The embryonic chick femur organotypic culture model. (A) *0.44 µm filter membrane inserts positioned in six-well plates.* ***(B)*** *Embryonic chick femur defects were created, and placed on the membrane.* ***(C)*** *EC pellets (2x 10^5 cells) were added and the bone ends placed in juxtaposition.* ***(D)*** *Culture media was then added to the six-well plates to create an air/liquid interface.*

RESULTS: In E11 EC pellet cultures bone healing was induced, which was not observed in controls. Furthermore an increase in STRO-1 expression in cells was observed indicating a phenotypic change towards MSCs. In E18 femur defects early cartilage changes were observed which may be the early stages of endochondral ossification ***(Fig. 2A)***. However, in the defect femurs with implanted EC differing structures in the bone were observed, with marrow like cavities forming and the onset of growth plate like regions ***(Fig. 2B)*** This occurs in conjunction with an increased change in cartilage cell phenotype (see circled cell population). Additionally a distinct change in cell staining was observed with enhanced STRO-1 expression over vWF suggesting an endothelial to mesenchymal transition.

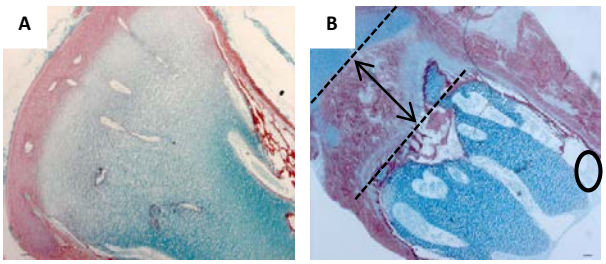

Control EC Pellet

Fig. 2. A/S staining showing the effects of human EC pellet implantation into segmental defects of E18 chick femurs at the epiphysis of E18 chick femurs following a 10 day organotypic culture. (A) *Epiphysis of control defect femurs* ***(B)*** *Epiphysis of defect femurs with implanted EC. (Scale bar 100 µm).*

DISCUSSION & CONCLUSIONS: The results demonstrate that ECs have an osteogenic effect and promote endochondral ossification when implanted into the embryonic femur defect. Thus ECs play an important role in endochondral ossification with significant therapeutic implications for future bone tissue engineering.

REFERENCES: [1] Kaigler D, Krebsbach PH, West ER, Horger K, Huang YC, Mooney DJ. Endothelial cell modulation of bone marrow stromal cell osteogenic potential. FASEB J. 2005;19(6):665-7.

ACKNOWLEDGEMENTS: BBSRC for funding.

Development and Characterisation of a 3 dimensional model to culture zebrafish (*Danio rerio*) muscle cells.

K.K.Vishnolia[123], E.Spikings[1] and M.P.Lewis[1234]

[1]*Institute of Biomedical and Environmental Science and Technology, University of Bedfordshire, Luton*

[2]*Musculoskeletal Biology Research Group, School of Sport, Exercise and Health Sciences, Loughborough University,*

[3]*Institute for Sport and Physical Activity Research, University of Bedfordshire,*

[4]*UCL School of Life and Medical Sciences*

INTRODUCTION: Over the past two decades Zebrafish have been used as a model organism to study human myopathies and dystrophies due to its unique quality of having 95% genetic homology with human beings. All the work done until now has been in-vivo due to the fact that we were not able to isolate and culture zebrafish muscle progenitor cells in-vitro repeatedly. However some work has been done in past to culture skeletal muscle cells from zebrafish using early embryonic stages and also from bigger fish such as Atlantic salmon and Rainbow trout. But previous work has been done in 2 dimensions (2D), which does not provide cells proper in- vivo physiologically relevant environment to grow.

In the present study a protocol has been developed to successfully isolate and culture zebrafish muscle progenitor cells in 2D.

METHODS: Zebrafish muscle cells were isolated and cultured on six well plates at 500K/cm2 for 2D experiments as control for immuno- staining and to perform the gene expression study.

Zebrafish muscle cells cultured at different plating densities in 3 dimensional tissue engineered collagen based model as previously described (Smith et al., 2012) to find the optimum plating densities for future experiments.

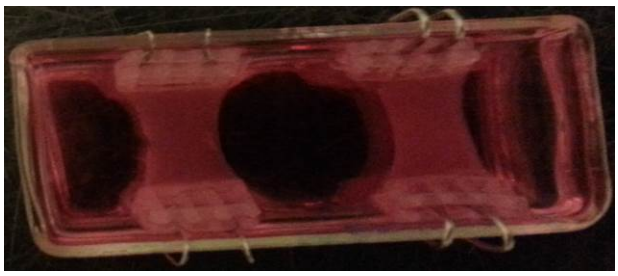

Fig 1: Picture of two tissue engineered collagen gels in a chamber slide embedded with zebrafish skeletal muscle cells.

RESULTS: Zebrafish muscle cells cultured in 2D and collagen gels were blocked and stained. Cells were stained for desmin protein (marker for muscle specific cells) with desmin anti- body and nuclei with dapi.

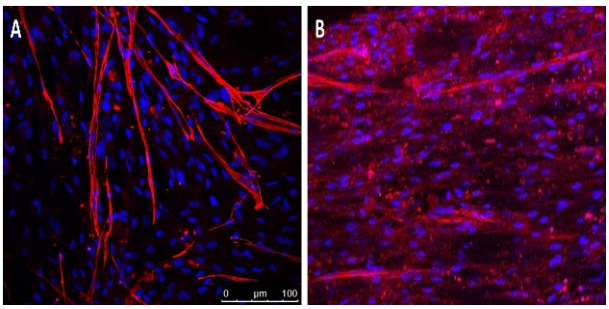

Fig 2: Pictures of zebrafish skeletal myotubes cultured in vitro A) Zebrafish muscle myotubes cultured in 2D, B) zebrafish muscle myotubes cultured in tissue engineered collagen gel.

DISCUSSION & CONCLUSIONS: Immunohistochemistry data was also supported with real time gene expression data for specific genes responsible and expressed specific time point. Data illustrated elevation in the expression level of MyoD when the cells are proliferating and committing to myogenic lineage but decrease after determination. IGF-1 increases through the time points as it's involved in proliferation, differentiation and hypertrophy. Despite the low level of relative expression slow myosin heavy chain exceeds the expression of fast myosin heavy chain which is in line with previous literature for in-vivo zebrafish muscle cells (Beermann et al., 2010). Direct comparison was also done between zebrafish muscle cells cultured in 2D and tissue engineered collagen gels.

REFERENCES *Beermann ML, Ardelt M, Girgenrath M, Miller JB* (2010) Prdm1 (Blimp-1) and the expression of fast and slow myosin heavy chain isoforms during avian myogenesis in vitro. Plos one Apr1:5(4).

Smith AS, Passey S, Greensmith L, Mudera V, Lewis MP (2012) Characterization and optimization of a simple, repeatable system for the long term in vitro culture of aligned myotubes in 3D. J Cell BioChem. 2012 Mar 113(3);1044-53.

Cell seeding in hollow fibre bioreactors

SM Acott[1], R Acione[2], MJ Ellis[1]

[1]*Department of Chemical Engineering & Centre for Regenerative Medicine, University of Bath, Bath, United Kingdom.* [2]*Bristol Royal Infirmary, Bristol, United Kingdom.*

INTRODUCTION: To grow a sufficient quantity of cells on a scaffold it is important to ensure a high initial cell attachment which is evenly distributed. This is however challenging on three-dimensional surfaces such as hollow fibre membranes. To this end a new dynamic method of cell attachment of MG63 human osteosarcoma cells onto hollow fibres of poly(lactic-co-glycolic) acid (PLGA) has been developed.

METHODS: PLGA hollow fibre membranes were fabricated using wet spinning phase inversion. A solution of 20% w/w PLGA in N-methyl-2-pyrrolidone (NMP) solvent was passed through a spinneret into deionised water, the fibres are left in the water, replaced twice a day, for three days to allow complete solvent removal[1].

The fibres were 1.3 mm in external diameter and were cut into lengths of 120 mm. They were sterilised in penicillin/streptomycin (P/S) solution for 6 hours at 4°C, washed with Dulbecco's Modified Eagle Medium (DMEM) and sorted into bundles of five fibres. These bundles are glued into an autoclaved cylindrical glass bioreactor module, which has been coated in Sigmacote to prevent cell attachment to the glass. The module was filled with 5ml complete MG63 medium and left to soak for 30 minutes. The media was removed and the cell suspension added at a density of 20,000 cells/cm^2, providing a total of 490,000 cells in 5ml of fresh medium.

Modules were attached to a Stuwart STR4 rotator drive at one of three different angles (0°, 45° and 90°) for 6 hours at 37°C and 5% CO_2. The RPM was set at one of three speeds (4, 6, 8 RPM). Cell seeding onto PLGA flat sheet membranes and tissue culture plastic was used as controls. The number of cells attached to the fibre surface, and that which remained in the media was determined by picogreen assay. The fibres were removed from the module and cut into fifths to allow cell distribution analysis, before lysing and counting.

RESULTS: It has been shown that a rotational velocity of (X m/s) and a reactor angled to (Y°) provides the greatest quantity of cell attachment of (Z %). Increasing the RPM showed a (positive) correlation with cell attachment. Decreasing the perpendicular angle of the reactor relative to the rotating drum also showed a (positive) correlation. Comparable static seeding showed that dynamic methods provided (X times) greater rates of cell attachment.

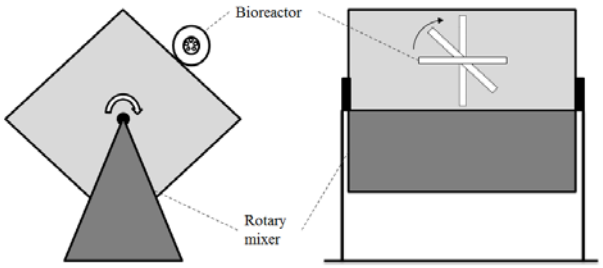

Fig. 1: A side and front facing view of a hollow fibre bioreactor attached to a Stuwart STR4 rotator drive.

Further analysis of the fibres indicated that a reactor angle of (X°) provided the greatest cell distribution along the length of the hollow fibres. The most uneven distribution occurred at (Y°).

DISCUSSION & CONCLUSIONS: Compared to static seeding on flat sheet membranes and hollow fibres, a dynamic method of seeding shows increased cell attachment and distribution. An optimum velocity and reactor angle arises due to there being a suitable middle ground between the gravity settling of the cells onto the fibres expected at lower velocities, and the higher degree of mixing at higher velocities. Steeper reactor angles provide an increased cell distribution due to the increase in cell movement as the bulk liquid moves between the two ends of the reactor with greater gravitational force.

REFERENCES:[1] Ellis, M.J. & Chaudhuri, J.B. (2007). Poly(lactic-co-glycolic acid) Hollow Fibre Membranes for use as a Tissue Engineering Scaffold. *Biotechnology and Bioengineering*. 96 (1), p177-187.

ACKNOWLEDGEMENTS: Funded by the University of Bath URS award.

A novel scaffold for soft tissue reconstruction

J Appelt[1, 2], Y Martin[1], AD Metcalfe[1, 2], G Phillips[1, 2]

[1] Blond McIndoe Research Foundation, East Grinstead, [2] School of Pharmacy and Biomolecular Sciences, University of Brighton

INTRODUCTION: The loss of subcutaneous adipose tissue due to burns, tumour resection or congenital abnormalities can affect the patient physically and emotionally. Current reconstructive strategies can yield unpredictable and often unsatisfactory results. Our group recently reported a novel macro-microporous scaffold for soft tissue reconstruction[1]. One of the key features of this scaffold is a well interconnected and porous structure. Here, we report the effect of pre-freezing and freeze-drying, using ice as porogen, on scaffold fabrication with the aim to increase the scaffold's micropore size range and mean pore size, to ensure sufficient interconnectivity.

METHOD: Gelatin (7%w/v) was cross-linked using glutaraldehyde (25%w/v) around 1g of preformed alginate beads in a 17.4x15.62mm mould. The beads were subsequently leached from the construct using sodium citrate (10%w/v) to produce macropores. Pre-freezing was carried out through freezing the scaffold overnight at -20˚C or -80˚C. Freeze drying was performed with a Christ Alpha Freeze-dryer. Images were acquired using a Field Emission Gun SEM (Zeiss Sigma FEG-SEM) with Smart SEM version 05.04 software.

RESULTS: Freeze-drying and pre-freezing resulted in an increase in micropore size. In the original scaffold, the micropore size ranged from 6-125µm, with a mean of 30µm (Fig 1A). Freeze-drying resulted in a mean micropore size of 44µm, ranging from 6-112µm (Fig 1B), pre-freezing at -20˚C in a mean size of 190µm, ranging from 93-287µm, and pre-freezing at -80˚C in a mean size of 887µm, ranging from 18-4700µm (Fig 1C). The micropores provide sufficient space for the passage of cells, nutrients and waste removal. Neither pre-freezing nor freeze-drying affected the size or structure of the macropores, which are designed to accommodate adipose-derived stem cells which will replace the missing tissue in time. Interconnectivity between micro and macropores was clearly visible in all conditions tested.

DISCUSSION & CONCLUSION: The microporous structure of the scaffold walls could be modified by pre-freezing and freeze-drying, resulting in larger mean pore size, while the macropores were not affected. The interconnectivity between micro and macropores is essential for passage of cells and nutrients and is clearly achieved using this fabrication method.

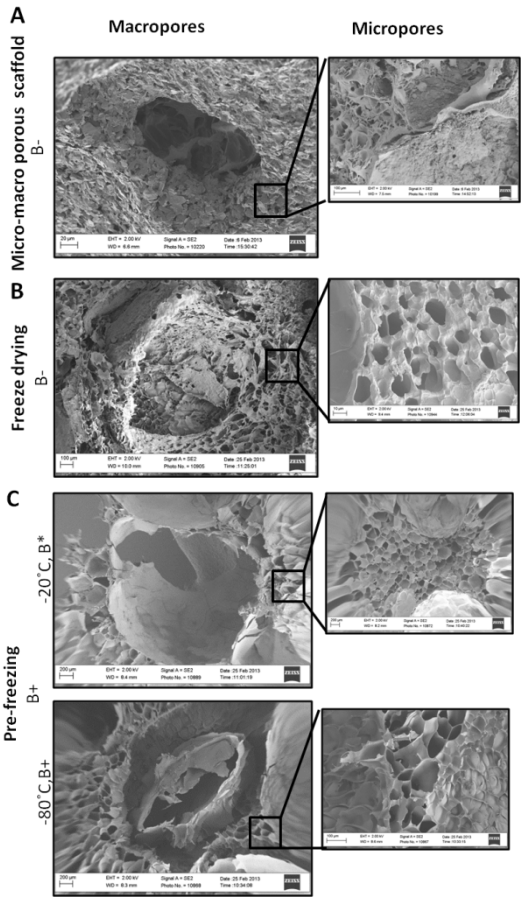

Fig.1.Scanning Electron Microscopy (SEM) shows A) the original macro-microporous structure, B) the effect of freeze-drying and C) the effect of pre-freezing at -20˚C/ -80˚C on the scaffold structure.

These findings are a step forward in the construction of a 3D structure which is suitable for soft tissue reconstruction in patients suffering from tissue contour loss.

REFERENCES: [1]Phull, et al. (2013) J Mater Sci Mater Med. 24(2): 461-7

ACKNOWLEDGEMENTS: This work was supported by charitable donations to the Blond McIndoe Research Foundation.

Attachment and migration of adult mesenchymal stromal cells used for cell therapy is dependent on functional Neuropilin 1

Owen Bain[1], Giulia Detela[1], Christopher Mason[1], Anthony Mathur[2], Ivan Wall [1,3]

1 - Advanced Centre of Biochemical Engineering, Torrington Place, University College London, UK
2 - Department of Clinical Pharmacology, William Harvey Institute, Charterhouse Square, London, UK
3 - WCU Department of Nanobiomedical Science, Dankook University, Cheonan, Korea

INTRODUCTION:

Mesenchymal Stromal Cells (MSCs) are a promising candidate for cell-based intervention for a number of clinical indications[1]. In order to optimise engraftment of delivered MSCs, the mechanisms by which they adhere and spatially organise themselves within the extraceullar matrix (ECM) need to be defined. Fibronectin is up regulated in the border zone of the infarction and MSCs are widely known to express the complimentary integrin α5β1. Neuropilin 1 (NRP1), a co-receptor for VEGF and PDGF receptors, is also known to interact with integrin α5β1[2]. In this study we aimed to identify the requirement for NRP1 during engraftment of MSCs

METHODS:

Bone marrow derived mesenchymal stromal cells were derived from healthy donor bone marrow aspirates and expand in culture. Passage 3 was used for all experiments. NRP1 was knocked down using Silencer® siRNA (Invitrogen) before use in the following assays to assess the impact on engraftment.

Static adhesion was analysed by plating MSCs onto fibronectin or bvine srum abumin for 5 and 20 minute s. Chemotaxis of MSCs towards PDGF-aa and SDF-1 was performed in transwells for 3 hours.

To characterise the angiogenic effect *in vitro*, MSCs were seeded onto a pre-existing endothelial network in matrigel and the impact upon the network over 72 hours was observed and quantified.

RESULTS: Knocking down NRP1 significantly decreases attachment of MSCs to fibronectin, but not other ECMs vitronectin and collagen type I (Figure 1). The functional capacity of MSCs to support a vascular network was accessed. Knocking down NRP1 decreased the capability of MSCs to support the HUVEC network (Figure 2)

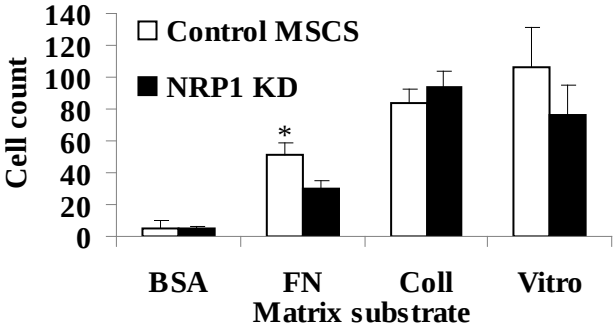

Figure 1 Average cell count of adhered cells per field view after 20 minutes to Bovine serum albumin (BSA), Fibronectin (FN), Collagen type I (Coll) and Vitronectin (VN)

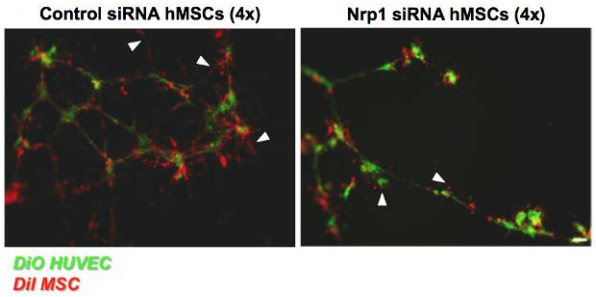

Figure 2 48 hours after MSCs (red) were seeded onto a HUVEC(green) network. White arrow represents co-localisation of MSCs and HUVECs.

DISCUSSION & CONCLUSIONS: These results indicate the importance of NRP1 adhesion of MSCs to fibronectin.

Also, NRP1 modulates the role of MSCs for neo-angiogenesis, both in tubule function and ability to support a pre-existing vascular network; highlighting the peri-vascular role of MSCS

REFERENCES:

1 - Clifford DM, et al. Stem cell treatment for acute myocardial infarction. Cochrane Database of Systematic Reviews 2012, Issue 2

2 –Valdembri D, et al. Neuropilin-1/GIPC1 Signaling Regulates α5β1 Integrin Traffic and Function in Endothelial Cells. PloS Biol. 7:e1000025

Capacitive electrical field stimulation for bone tissue engineering

R Balint[1], NJ Cassidy[2], S Gembali[1], SH Cartmell[1]

[1] *Materials Science Centre, University of Manchester, Grosvenor Street, Manchester, M13 9PL, UK*
[2] *School of Physical and Geographical Sciences, William Smith Building, Keele University, Staffordshire, ST5 5BG, UK*

INTRODUCTION: Electrical stimulation has been receiving increasing attention in the last few years in the discipline of bone tissue engineering. This interest is motivated by the observations that electrical stimulation can influence the behaviour of stem cells and various musculoskeletal lineages, enhancing proliferation and differentiation[1]. Furthermore it is currently used to help the healing of normal and non-union fractures, osteoporosis, osteoarthrosis, lumbar spine fusions and to better integrate implanted biomaterials. Our group was previously able to show the benefits of direct electrical stimulation for orthopaedic tissue engineering, but our work now focuses on developing the capacitive technique into a useful tool for regenerative medicine.

METHODS: An autoclaveable capacitive bioreactor system that allows the reliable delivery of electric field stimulation was custom designed. Simulations of the electric field inside the bioreactor were created in the FEM simulation environment COMSOL Multiphysics. Stimulation with two different parameter combinations (Regime 1 and Regime 2) was delivered to commercial bone marrow derived human Mesenchymal Stem Cells (hMSCs) and human osteoblasts (hOBs) for 1h/day for 7 days. Their effect was measured upon cell numbers using Picogreen, metabolic activity with Alamar Blue, ECM deposition using Alkaline Phosphatase assay.

RESULTS: Stimulation with Regime 1 has significantly lowered hMSC cell numbers. Both Regime 1 and Regime 2 enhanced the metabolic activity of hMSCs, but not of the hOBs. Regime 2 was found to significantly increase the alkaline phosphatase activity of the osteoblasts. Neither of the regimes was observed to have a significant effect on the alkaline phosphatase activity of hMSCs.

DISCUSSION & CONCLUSIONS: The developed bioreactor is easy to use and shows good biocompatibility. Our results show that cell number, metabolic activity and alkaline phosphatise activity can all be influenced using electrical stimulation, demonstrating the technique's usefulness for tissue engineering. The different maturation stages of the cells seem to have an effect on how the cells respond to the stimuli. Further optimisation of the parameter combinations is currently underway.

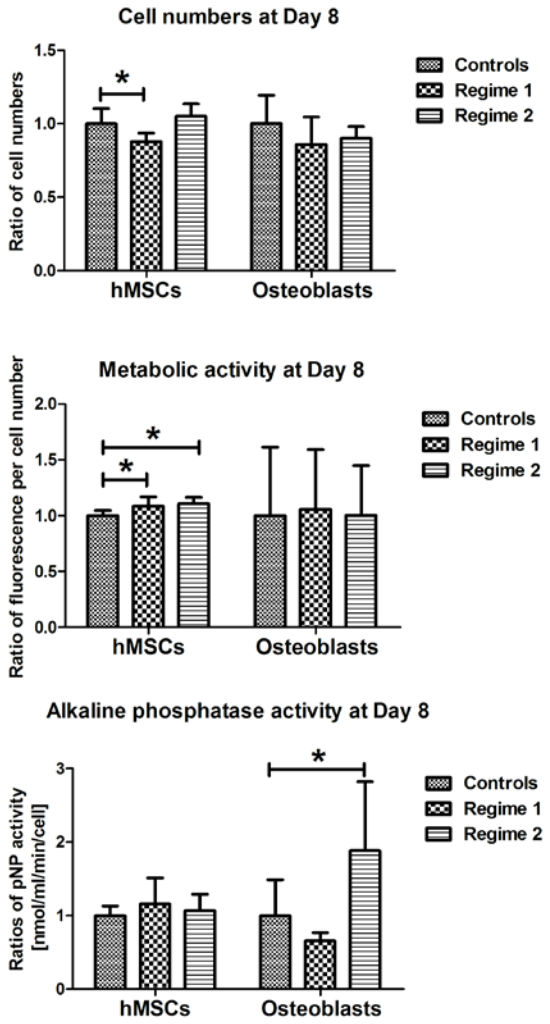

Fig. 1: The effect of Regime 1 and Regime 2 on hMSC and hOB cultures after 7 days of stimulation.

REFERENCES: [1] R Balint, NJ Cassidy, SH Cartmell (2012) *Tissue Eng Part B Rev*. **19**:48-57

ACKNOWLEDGEMENTS: We would like to thank the EPSRC "Bridging the gap" and DTA awards, and Orthopaedic Research UK for the financial support.

CFD-aided design of a fluidised bed bioreactor for bone tissue engineering

I Benzeval[1], IG Turner[2], MJ Ellis[1]

[1] *Chemical Engineering,* [2] *Mechanical Engineering, and Centre for Regenerative Medicine, University of Bath, Bath, UK*

INTRODUCTION: The aim of this project was to perform CFD analysis of liquid-solid fluidisation to inform the design and development of a fluidised bed bioreactor for the culture and growth of bone cells seeded into porous bioceramic particles. The need for artificial bone graft material, particularly for large defects which cannot be filled with autologous bone, is driving research into synthetic alternatives[1,2]. The project utilises calcium phosphate particles (4 – 10 mm diameter), with large (500 - 1500 μm diameter) interconnected pores. The fluidisation of the particles was modelled to inform the sizing of the bioreactor, to find a balance between quality of fluidisation and the volume of media required to be pumped.

METHODS: The liquid phase was modelled to represent phosphate-buffered saline at 37 ^{o}C. The solid phase was modelled as 4 mm glass spheres with a density of 2500 kgm^{-3}. The fluidisation was modelled in columns of 25, 35 and 80 mm diameter, all 400 mm long. A k-ε turbulence model was used to govern the flow of the liquid phase, a dense discrete phase model was used for the solid phase. The flow of liquid was incrementally increased from 0.01 ms^{-1} to 0.042, 0.06 and 0.10 ms^{-1} at 10, 30 and 50 s respectively. These velocities cover the range theoretically required to fluidise the particles.

RESULTS: The steady state depth of the bed increased for each column size when the flowrate was stepped from 0.06 to 0.10 ms^{-1}. Figure 1 shows the behaviour (volume fraction) of the solid phase as the velocity of the liquid is increased between these two values for the 25 and 35 mm columns. It can be seen that as the velocity increases, the bed of solid particles is temporarily pushed up the column as a slug before returning to a bed of greater depth than was present initially. The steady state depth of the bed in the 80 mm column increased by a similar amount, but no slugging behaviour occurred.

DISCUSSION AND CONCLUSIONS: The results of the simulations identified factors critical to the successful design of a fluidised bed bioreactor, i.e. the column diameter. A relatively narrow column can result in a significant slugging response that is not present in a larger column. This slugging effect would potentially have a negative effect on cells grown on the solid phase due to the increased shear stresses involved. It could be said that a wider column is preferable, however a balance must be found between the degree of fluidisation required, the dimensions of the column to house the bed and the cost of operation. As the diameter of the column is increased the amount of slugging decreases but the volume of media and size of pump required to maintain the same flowrate increase significantly.

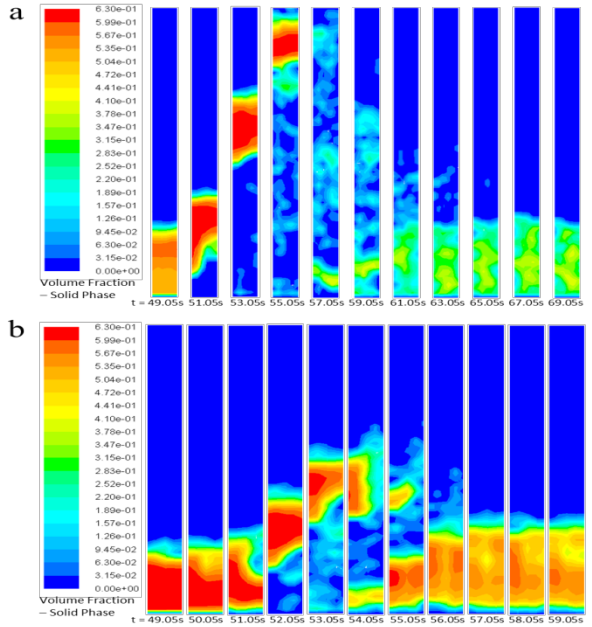

Fig 1: Volume fraction of the solid phase as the velocity is increased, at t = 50 s, from 0.06 to 0.10 ms^{-1}. Images represent a 2D plane through the middle of the reactor. a) 25 mm column, b) 35 mm column

These findings demonstrate the application of CFD modelling to enable the successful design and development of a fluidised bed bioreactor for the culture and growth of bone cells seeded on to porous bioceramic particles.

REFERENCES: [1] Boyan B. *et al*. 2003. Bone Graft Substitutes: ASTM International [2]Stevens MM. 2008. Biomaterials for bone tissue engineering. Materials Today 11(5):18-25.

ACKNOWLEDGEMENTS: This work was funded by EPSRC Grant EP/I015922/1.

Determining the Antibacterial Potential of Oral Mucosal Lamina Propria-Progenitor Cells

E. Board-Davies[1], A. Sloan[2], P. Stephens[1] and L. C. Davies[1]
[1]Wound Biology Group, [2]Mineralised Tissue Group, Cardiff Institute of Tissue Engineering and Repair, Tissue Engineering and Reparative Dentistry, School of Dentistry, Cardiff University

INTRODUCTION: Oral mucosal wound healing is characterized by rapid re-epithelialisation and remodeling potentially due to the presence of oral mucosal progenitor cells (OMLP-PCs). This study aims to investigate whether in addition to their potent immunomodulatory phenotype[1] OMLP-PCs possess antibacterial properties and in turn establish any such mechanism of action.

METHODS: Optimal growth conditions in tissue culture compatible media for Gram positive (*S.pyogenes* NCTC8198, *P.mirabilis* NCTC11938) and Gram negative (*P.aeruginosa* ATCC15692, *E.faecalis* NCTC775) bacteria were established by recording their growth profiles in RPMI media supplemented with 0-20% Brain Heart Infusion (BHI) broth and 10-20% FCS.

All bacteria were grown to midlog, centrifuged and the supernatant and bacterial pellet harvested. Bacterial protein was isolated using the QIAGEN Qproteome® Bacterial Protein Prep Kit.

OMLP-PCs (25-30 PDs; n=3) were seeded ($4x10^4$ cells/well) and incubated with bacterial protein (50µg/ml), bacterial supernatant (1:5) or live bacteria (150CFU/ml) and visualized for 12 hours using the Cell IQ™ system. Cell movement was tracked using the Cell IQ™ software.

RESULTS: Cell tracking data (Fig. 1) demonstrated that OMLP-PCs moved significantly slower when exposed to both live bacteria ($P \leq 0.05$) and bacterial supernatant ($P \leq 0.05$). This was not simply due to induction of cell death as the OMLP-PCs still appeared viable after 42 hours of exposure to the bacteria/supernatant. With respect to the bacterial protein from both Gram-positive and Gram-negative bacteria, although this did not significantly affect cell migration speed, OMLP-PCs demonstrated a reproducible interaction with this protein (Fig2).

DISCUSSION & CONCLUSIONS: Initial data indicate that OMLP-PCs directly respond to live bacteria as well as the presence of their soluble cellular proteins and secretome. This appears to be irrespective of Gram classification. Investigations are focused on determining whether OMLP-PCs can directly suppress bacterial growth in a bactericidal or static manner.

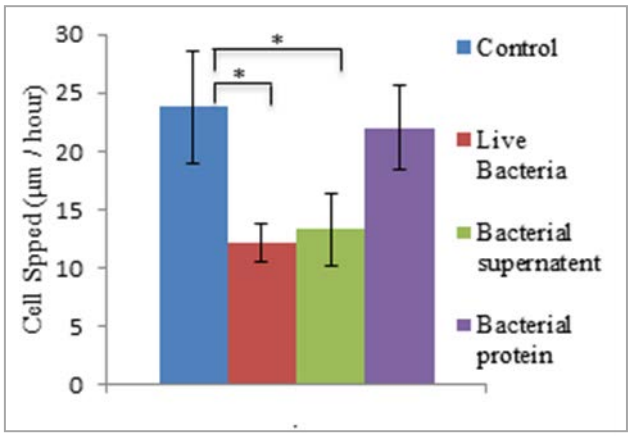

Fig 1: Graphical representation of the speed of OMLP-PC cell movement when exposed to live *E. faecalis* and its protein or supernatant. A significant decrease in the speed was noted when the cells were exposed to live bacteria and bacterial supernatant. $P \leq 0.05$

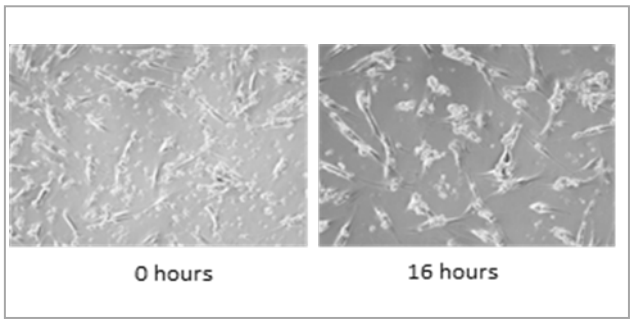

Fig 2: OMLP-PC interaction with soluble protein extracted from *E faecalis. These data are representative of all bacteria tested.*

REFERENCES: [1]Davies *et al.*, 2012, *Stem Cells and Development* 21(9): 1478-1487

ACKNOWLEDGEMENTS: The authors would like to acknowledge funding from Cardiff University. Elen Bray and Kevin McCormack from CM Technologies provided vital assistance in the use of the Cell IQ™ system and software.

Building a 3D model of airway smooth muscle to study asthma

JC Bridge[1], GE Morris[1], J Aylott[1], MP Lewis[2], FRAJ Rose[1]

[1] School of Pharmacy, University of Nottingham, England [2] School of Sport, Exercise and Health Sciences, Loughborough University, England

INTRODUCTION: Airway smooth muscle (ASM) is the key effector cell in regulating airway contraction. Previous *in vitro* studies into ASM contraction have largely been limited to two dimensional (2D) single cell cultures and collagen gel contraction studies. Recent developments in tissue engineering have generated novel technologies for developing three dimensional (3D) multicellular models that better mimic the natural extracellular matrix (ECM). One method for producing such matrices is electrospinning, where non-woven mats of polymer fibres (ranging from around 100nm to several µm in diameter) can be made by passing a polymer solution through a highly charged capillary. This is an attractive approach due to its simplicity, low cost and the wide range of both synthetic and natural polymers that are available to be electrospun.

The aim of this work was to assess a range of fully aligned electrospun polyethylene terephthalate (PET) scaffolds for providing the appropriate topographical properties for ASM cell alignment. The optimal scaffold can then be used as a platform to model the contraction of a fully aligned sheet of ASM to various bronchoconstrictors.

METHODS: Solutions of PET at varying concentrations (35%, 20% and 10% w/v) were electrospun onto a rotating mandrel to produce aligned fibrous mats with a range of fibre diameters. Fibre diameter and degree of alignment were measured from scanning electron microscope (SEM) images of the scaffolds (480 measurements from 24 images per aligned scaffold). Primary human ASM cells were seeded onto the scaffolds and cultured for a two week period. Cell viability was monitored periodically using the alamarBlue® assay. After 2 weeks cells were fixed and immunostained to assess the degree of cell alignment, elongation and confluency.

RESULTS: Highly aligned fibrous sheets were achieved using each PET concentration (>50% of fibre angle measurements within 10° of the mean angle) Individual fibre diameter increased with increasing PET concentration; 10% w/v (215nm±0.0027), 20% w/v (1.13µm±0.013) and 35% w/v (3.53µm±0.043). Cell alignment closely followed fibre orientation (>75% of cells aligning within 20° of the fibre angle). ASM cell morphology was altered when cultured on the scaffolds when compared to 2D controls.

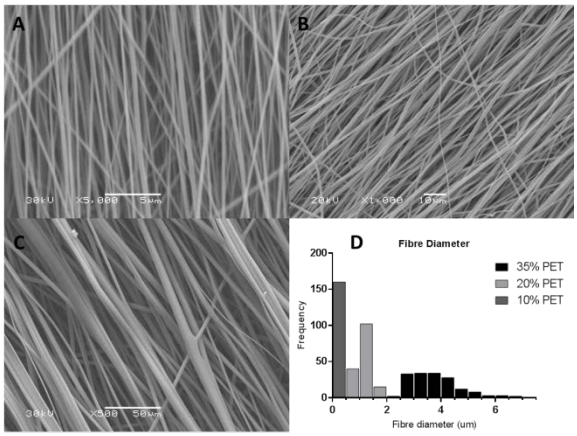

Fig.1: SEM Images of Aligned Acellular Scaffolds (A:10% PET, B:20% PET, C:35% PET) D shows the range of individual fibre diameter in each scaffold..

DISCUSSION & FUTURE WORK: Increasing the PET solution concentration produced, thicker fibres. However, with increased fibre diameter, the uniformity of the fibre size decreases. The ASM cells cultured were aligned on all scaffolds but were unable to form a confluent layer on the 35% PET scaffold.

In future, the 20% and 10% scaffolds will be used to culture confluent sheets of ASM which will be challenged using bronchoconstrictors.

The physical contraction of the sheets will be measured using a specifically tailored culture force monitor (CFM). This will provide novel insights into the regulation of ASM contraction in asthma and other diseases of the airways.

Mechanical properties of single cells in seeking tumour diagnostics and therapies

Y H Chim[1], N. Rath [2] M F Olson[2], H Yin[1]

[1] *Biomedical Engineering, University of Glasgow, Glasgow.* [2] *Beatson Institute for Cancer Research, Glasgow.*

INTRODUCTION: Rho associated kinase (ROCK) signaling has been extensively researched in cancer, particularly in relation to tumour cell motility and metastasis [1]. It has been shown, in previous work, that an increase in cellular tension has been linked with skin tumour formation [2], however, the contributions of individual elements to tissue stiffening and their physiological significance in tumour development remains unclear. Here, we utilized an established tissue model (with and without activated ROCK pathways) and present a study of the mechanical properties of single keratinocyte cells using atomic force microscope (AFM) force spectroscopy.

METHODS: Primary murine keratinocytes were extracted from the tail skin of a genetically modified mouse that expresses a ROCK-estrogen receptor fusion transgene, and cultured at 37°C, 5% CO_2 in keratinocyte growth medium for a period of 24 hours. The ROCK pathway was activated through the inclusion of an estrogen analogue in the growth medium.

Force spectroscopy measurements (*Fig. 1*) were performed at specific time points (for a duration of 1 day) using a sample size of 80 cells and applying five consecutive force-indentations for each. A Hertzian spherical model has been applied to the force spectroscopy data to deduce an elastic modulus of the cell structure [3] and comparisons have been made between the pathways.

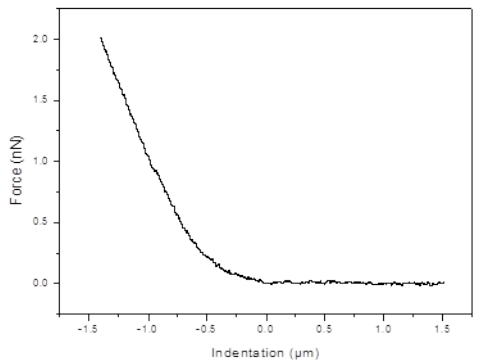

Fig. 1: A graph showing typical force-indentation measurement for a single ROCK activated keratinocyte cell using a spherical indenter of ~2.5µm.

RESULTS: The keratinocytes with activated and non-activated ROCK pathways showed stiffnesses of 2.0±0.6 kPa at the initial time point. At t = 1 day the non-activated ROCK pathway cells retained a stiffness of 2.0±0.6 kPa whereas the activated ROCK pathway keratinocytes exhibited an average stiffness of 0.9±0.3 kPa a reduction in stiffness of 55%. During consecutive force-indentation cycles a reproducible contact point was observed, indicating no plastic deformation of the sample or motion from the cell was observed within the duration of the measurements.

DISCUSSION & CONCLUSIONS: From previous studies it has been observed that cellular tension drove an increase in tissue stiffness [2]. The results presented here show an activated ROCK pathway leading to a decrease in cell stiffness. This is in close agreement with other studies that found cancerous cells to be more compliant than non-cancerous cells [4]. The results presented here support the theory that observed increases in stiffness within the skin following ROCK activation could be due to an increase in the stiffness from the extracellular matrix (ECM) upon which the cells adhere. Further work will include mechanical measurements upon fibroblasts and the ECM to gain further understanding of the mechanics of skin tumour formation.

REFERENCES: [1] N. Rath, M.F. Olson (2012) *EMBO reports* **13**:900-908. [2] M.S. Samuel, J.I. Lopez, J. McGhee, et al. (2011) *Cancer Cell* **19**:776:791. [3] M.J. Puttock, E. G. Thwaite (1969) *National Standards Laboratory Technical Paper* **25**:1-64. [4] M. Lekka, K. Pogoda, J. Gostek, et al. (2012) *Micro* **43**: 1259-1266.

ACKNOWLEDGEMENTS: We would like to thank the Engineering and Physical Sciences Research Council for funding the project.

Enhancing bone marrow cell engraftment and potency in hypoxia using ligands of the Notch signalling pathway *in vitro*.

Giulia Detela[1], Owen Bain[1], Prof. Anthony Mathur[2], Ivan Wall[1,3].
[1]Department of Biochemical Engineering, University College London, Torrington Place, London WC1E 7JE. [2]Department of Cardiology, London Chest Hospital, Queen Mary University of London, Barts and the London NHS Trust, Bonner Road, London E2 9JX, UK. [3]Department of Nanobiomedical Science & WCU Research Center, Dankook University Graduate School, Cheonan 330-714, Korea.

INTRODUCTION: Bone marrow-derived mesenchymal stromal cells (MSCs) have been explored as a therapy for myocardial infarction; yet clinical trial results reveal only modest improvements in cardiac function and minimal engraftment of delivered cells. Little evidence exists regarding the molecular mechanisms that are required for long-term cell retention within the heart. Indeed, the identification of cell delivery methods that achieve sustained engraftment remains one of the primary research goals for cardiac cell therapy[1]. Based on the central role of Notch in vascular development and in activation of adhesion receptors[2], we hypothesised that stimulation of Notch signalling would enhance engraftment capabilities of MSCs that might ultimately support vascular regeneration in ischemic myocardium. Our aim was to characterise the effect of soluble Notch ligands Jagged 1 (sJag1) and Delta-like 4 (sDll4) on engraftment responses of human MSCs.

METHODS: Human MSCs (Stro1+/Thy1+/ CD44+/CD146+/CD14-/CD19-) were expanded to passage 3 and functional characterisation of cell attachment and migration was assessed on fibronectin. Acute preconditioning of cells with sJag1 or sDll4 for 45 minutes was conducted prior to performing the assays and cell responses were characterised in presence or absence of these ligands. Additionaly, we assessed their impact on formation and maintenance of vessel-like networks in endothelial cell-MSC co-cultures on matrigel. A hypoxic air-tight container was fabricated[3] and all experiments were repeated in 2% oxygen tension to mimic the myocardial tissue post-injury.

RESULTS: Under normal oxygen tensions, human MSCs rapidly attached to fibronectin. sJag1 significantly enhanced this effect after 40 minutes ($p<0.05$). Moreover, both sJag1 and sDll4 significantly enhanced migration of MSCs across fibronectin ($p<0.05$). When tubule network formation over 18 hours was assessed, neither untreated human MSCs nor those pre-conditioned with Notch ligands impacted on branch formation in vessel-like structures. Neither did human MSCs impact on maintenance of those branch points after 72 hours. In hypoxia, sJag1 significantly enhanced MSC attachment on fibronectin as early as 20 minutes ($p<0.05$). sJag1 also enhanced cell migration on fibronectin in hypoxia ($p<0.05$). Endothelial/human MSC co-cultures were assayed under hypoxic conditions (*Figure 1*). Vessel branching was significantly increased when MSCs were pre-conditioned with sJag1 and sDll4 in hypoxic culture compared to normoxia ($p<0.05$). However, untreated MSCs were not capable of enhanced activity in hypoxia.

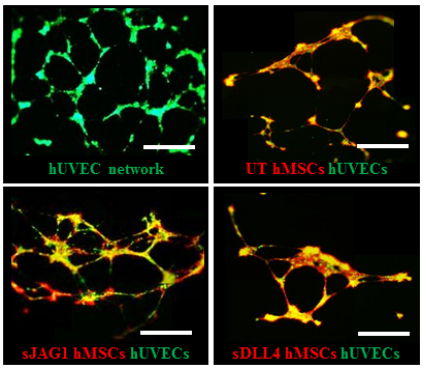

Figure 1. sJag1 and sDll4 preconditioning induces higher tubule formation in the co-culture setting.

DISCUSSION & CONCLUSIONS: In conclusion, our data supports the hypothesis that Notch ligands can enhance MSC engraftment potential and enhance functionality that supports vascular responses in a low-oxygen environment. Current studies in our lab aim to further understand the impact of preconditioning on improving cell function in vivo for the treatment of cardiovascular diseases.

REFERENCES: [1]D.M. Clifford et al (2012) *The Cochrane Library* **2**: 1-207. [2]A. Karsan (2008) *Sci Signal.* **1(2)**:pe2. [3]P. Mondragon-Teran et al., (2009) *Biotechnol. Prog.* **25(5)**:1480-8.

ACKNOWLEDGEMENTS: UCL Department of Biochemical Engineering.

The Use of Oral Mucosal Fibroblasts as a Novel Treatment for Increasing Transparency and Flap Strength in LASIK Wounded Sheep Cornea

EP Dooley[1], CS Kamma-Lorger[1], LC Davies[2], T Alhamad[1], SR Morgan[1], P Stephens[2], KM Meek[1]

[1] *Structual Biophysics Group Cardiff School of Optometry and Vision Sciences.*
[2] *Wound Biology Group, School of Dentistry, Cardiff University*

INTRODUCTION: Millions world-wide undergo the corneal refractive surgery LASIK (Laser-Assisted in Situ Keratomileusis) to correct for myopia and prespyopia. Although the procedure has a high success rate, the corneal flap created during surgery only superficially heals along the wound margin and can be easily displaced up to a decade later. Recent research has aimed to strengthen LASIK-type flaps using cell based treatments (using activated corneal fibroblasts) in an *in vitro* organ culture model. Results indicated that the cells increased the flap strength over the four-week culture period, however transparency was compromised through an increase in light scatter caused by a-sma activation.

We hypothesized that using a adult fibroblast, such as the oral mucosal fibroblasts, which does not express a-sma and is well documented to exhibit preferential (minimal scar) wound healing, would result in a decrease in light scattering whilst maintaining flap strength. In this study we investigated the ability of oral mucosal fibroblasts to increase corneal flap strength whilst maintaining transparency using the *in vitro* organ culture described above.

METHODS: Ovine corneas were cultured as established by Foreman et al (1996)[1]. Flaps were created using a Bausch and Lomb Hansatome Microkeratome. Half of the corneas were treated with oral mucosal fibroblasts (n=15) and the other half left as controls (n=15). Following the three-week culture period corneas were tested for flap strength (using a Lloyds Instrument extensometer), transparency (spectrophotometry) and for the presence of a-sma activation (immunohistochemistry).

RESULTS: The cell-treated corneas demonstrated greater transparency than the control samples at all three time points. By the three week time-point, the transparency of the cell-treated corneas was similar to that of the controls at one week. The immunohistochemistry (a-sma) and Hoechst staining indicated a marked increase in the number of cells present in the cell treated corneas compared to the controls at all three time points. The force required to detach the flap in the non-cell treated control group remained similar at the three time-points .03-.05 N. Student T-tests did not demonstrate any statistical differences between each of the control time-points. The mean detachment force for the oral mucosal fibroblasts increased with each time-point. At three weeks, the oral mucosal-treated flap strength increased, significantly to 0.12 N.

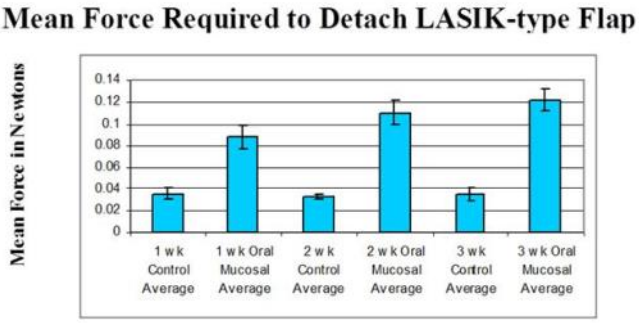

Fig. 1: Mean force required to detach LASIK-type flaps in cultured sheep corneas over three week time-points. There is a progressive and significant increase in required flap strength in the cell treated corneas. There is also a higher variation in standard error in the oral mucosal treated tissue.

DISCUSSION & CONCLUSIONS: The oral mucosal fibroblasts treated corneas demonstrated significant and reproducible increases in both the flap strength and transparency of LASIK-type wounds in an *in vitro* organ culture model. This preliminary study indicates that oral mucosal fibroblasts could be a potential source of autologous adult cells which could prove as an alternative to stem-cells in ocular wound repair.

REFERENCES: DM Foreman et al (1996) *A Simple Organ Culture Model for Assessing the Effects of Growth Factors on Corneal Re-epithelialization Experimental Eye Research* Volume 62, Issue 5, May 1996, Pages 555–564. SL Mi et al (2011) *Adhesion of laser in situ keratomileusis–like flaps in the cornea: Effects of crosslinking, stromal fibroblasts, and cytokine treatment Journal of Cataract & Refractive Surgery* Vol 37, Issue 1Pages 166–172

ACKNOWLEDGEMENTS: Professor Tim Wess' Research Group for use of extensometer and Dr. Sarah Youde for the cell passage.

The effect of cyclic mechanical strain on skeletal muscle myogenic differentiation of myoblasts and mesenchymal stem cells

J M Dugan[1], S H Cartmell[2], J E Gough[2]

[1] *Kroto Research Institute, University of Sheffield, Sheffield, UK.*

[2] *School of Materials, University of Manchester, Manchester, UK.*

INTRODUCTION: Tissue engineering skeletal muscle *in vitro* is of great importance for the production of tissue-like constructs for treating traumatic injury or congenital deformities. However, it is essential to find new sources of cells for muscle engineering as it is not possible to efficiently expand and culture primary myoblasts *in vitro*. Mesenchymal stem cells (MSCs) may be a promising source of myogenic progenitor cells. As skeletal muscle is a mechanically dynamic tissue, we have investigated the effect of cyclic mechanical strain on the myogenic differentiation of a co-culture system of murine C2C12 myoblasts and human adipose-derived MSCs.

METHODS: Monocultures and co-cultures of C2C12 myoblasts and human MSCs were subjected to cyclic strain during myogenic differentiation using a FlexCell system. Viability and proliferation were assessed and morphology was observed by confocal microscopy. Immunocytochemistry (ICC) and species-specific quantitative gene expression analysis were performed to assess differentiation.

RESULTS: In monoculture C2C12s differentiated to form multinucleated myotubes irrespective of cyclic strain although a greater degree of bulk orientation was observed in the strained cultures. Although MYH2 expression was unaffected by strain, TTN expression was reduced and ICC revealed less striation of myosin heavy chain indicating that strain may perturb sarcomeric assembly and maturation in this system. MSCs in monoculture were apparently unaffected by cyclic strain in terms of myogenic differentiation (none observed) and expression of RUNX2, PPARG and ALCAM indicating that they remained undifferentiated over the course of 7 days.

In co-culture, human MSCs fused with differentiating C2C12s to form heterokaryon myotubes which expressed human MYH2 and TTN. No expression of human MYOD1 or MYOG was observed, however, although localisation of murine MyoD at human nuclei was observed by ICC using a human-specific antibody for the nuclear envelope. Cyclic strain did not affect the degree of myogenic differentiation in the co-culture system. Interestingly, increased expression of human RUNX2 together with decreased PPARG was observed in the co-cultures indicating a small amount of differentiation toward the osteogenic lineage presumably in response to factors secreted by the myoblast cell line.

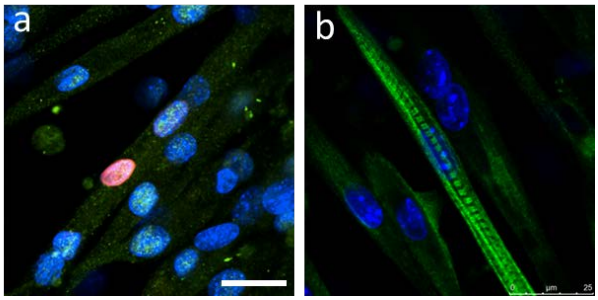

Fig. 1 (a) Heterokaryon myotube showing colocalisation of murine MyoD at a human nucleus originating from an MSC. (b) A striated C2C12 myotube formed under static conditions.

DISCUSSION & CONCLUSIONS: Contrary to some other reports[1], cyclic mechanical strain did not significantly affect the degree of myogenic differentiation of C2C12s or MSCs although myotube orientation and C2C12 proliferation was affected and sarcomeric development was perturbed. In the co-culture system, human MSCs appeared to take part in myogenesis and expression of human skeletal muscle proteins was observed. No expression of human myogenic regulatory factors was observed, however, leading us to tentatively conclude that the human skeletal muscle protein expression was switched on intracellularly after fusion. The nature of the fusion event between human MSCs and murine myoblasts is not well understood but points to a potential regenerative role for MSCs in the treatment of skeletal muscle disease and injury[2].

REFERENCES: [1]A. Kumar *et al.* (2004) *FASEB J.* 18:1524-1535. [2]A. Gentile *et al.* (2011) *Mol. Biol. Cell.* 22:581–592.

ACKNOWLEDGEMENTS: Funding was provided by EPSRC via a doctoral prize fellowship.

Three-dimensional articular cartilage tissue engineering using compressed collagen scaffolds

T Eriksson[1], N Mordan[1], V Salih[1]

[1] *Biomaterials and Tissue Engineering, UCL Eastman Dental Institute, London, UK*

INTRODUCTION: Articular cartilage lacks the ability to repair itself after damage, which makes injuries common, the need for a replacement prominent and tissue engineering of cartilage challenging. Articular cartilage is made up of collagen type II and chondrocytes embedded in calcified lacunae. Cells have been shown to respond differently to the stiffness of the matrix.[1] In the case of chondrocytes, rounded cells have been shown to be active, whereas those cultured for a long time become fibroblast-like and inactive [2]. Thus, the effects of compression on the chondrocytes embedded in a collagen matrix and their synthesis of collagen type II within a collagen type I matrix was analysed.

METHODS: Type I collagen gels were made under sterile conditions by solidifying liquid rat-tail collagen by adding 60µl of 5M NaOH and 150-200µl of 1M NaOH whilst gently mixing the solution. 100,000 chondrocytes per ml of collagen were then added prior to gel polymerisation. Plastic compression [3] was carried out on half of the gels. The cellularised collagen gels were incubated in normal DMEM (with 10% foetal bovine serum and 1% penicillin/streptomycin) or chondrogenic media (DMEM supplemented with 10ng/ml TGF-β1, 50nM ascorbate and 100nM dexamethasone) for 1, 7 and 14 days (37°C, 5% CO2, 90% humidity). Analysis of the gels was performed by histological staining: Safranin O for sulphated proteoglycans, Alcian blue for muco-polysaccharides and immunohistochemistry for collagen type II. Transmission electron microscopy examined the cellular ultrastructure and the collagen fibres [4].

RESULTS: The chondrocytes in both types of media appeared rounded inside the compressed collagen gels, indicating native-like activity. The results show that the compression of the collagen gel promotes collagen type II synthesis by the cells even when in a collagen type I matrix and independent of media type. Chondrocytes inside the compressed scaffolds were shown to be more active than those in the non-compressed ones, which had undergone apoptosis when viewed in the TEM. The collagen scaffold was also clearly visualised, with potential collagen fibres made by chondrocytes as shown by TEM images.

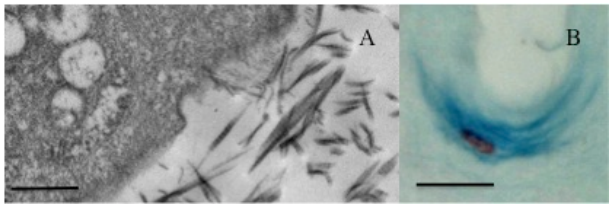

Fig. 1: A) Image of chondrocyte and collagen fibres as imaged through TEM. Potential collagen fibre extrusion through the cell membrane is visible. B) Alcian blue stain indicates increased mucopolysaccharide staining (blue) around the chondrocytes. Scale bars A: 500nm, B: 50µm.

DISCUSSION & CONCLUSIONS: The chondrocytes inside a compressed gel appeared more rounded and proliferated more, indicating that the compressed construct was an improved and more in vivo-like environment for these cells. The cellular production of collagen II without additional growth factors is significant, as it reduces the number of reagents used for a potential transplantable construct. Further experiments should however be carried out to further determine the proteins produced by the chondrocytes within the construct. Mechanical testing of the constructs could also be performed. Repeated compression to stimulate the effects of joint movement could further improve the properties of the chondrocyte-collagen scaffold. These results indicate that simple mechanical manipulation of the chondrocyte growth environment is enough to stimulate behaviour as seen in cells in native articular cartilage. This effect could be utilised in developing future articular cartilage constructs for therapy.

REFERENCES: [1] Discher DE (2005) *Science* **310:**1139-43. [2] Benya PD (1982) *Cell* **30:**215-24. [3] Brown RA (2005) *Advanced Functional Materials* **15:**1762-70. [4] Richardson N (2009) *International Endodontic Journal* **42**:908-21.

ACKNOWLEDGEMENTS: Prof JC Knowles UCL BTE; the Blizard Institute for Core Pathology at QMUL, London.

Finite element analysis of nanoindentation of chondrocytes

J Chen[1,2*], T Stewart [1]

[1] *School of Mechanical and System Engineering, Newcastle University, UK.*

[2] *Arthritis Research UK Tissue Engineering Centre, Newcastle University, UK*

*E-mail: Jinju.chen@ncl.ac.uk

INTRODUCTION: The viscoelastic properties of the living cells are important for quantifying the biomechanical effects of drug treatment [1], diseases [2] and aging [3]. Nanoindentation techniques have proven effective to characterize the viscoelastic properties of living cells [4-5]. However, the commonly used Hertz–Heaviside model does not represent real tests. Therefore, finite element analysis (FEA) was adopted to study viscoelastic responses of cells during nanoindentation tests, which adds value to the development of new mathematical models.

METHODS: A 2-dimensional symmetric FEA was used to model the indentation responses for a chondrocyte placed in a flat surface and inside a microfabricated well. Fig. 1 shows the FE meshes used in this study. Prony series models were used to describe the viscoelastic behaviour of chondrocytes [6].

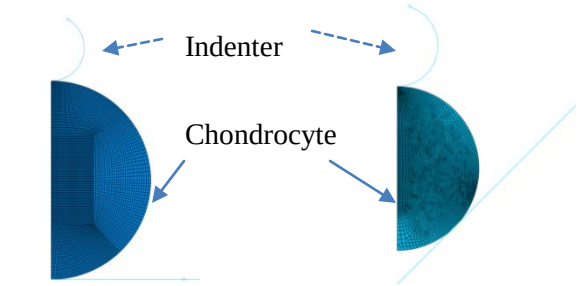

Fig. 1: Finite element meshes for indentation of cell placed on flat surface and inside a well.

RESULTS: The viscoelastic integral operator in combination with dimensional analysis was used to account for the realistic deformation rate and the dimensional effect. During the finite ramping period, we obtain the relation between force (P) and depth (δ),

$$P(t)=\frac{4}{3(1-\nu^2)}\sqrt{R}\delta^{\frac{3}{2}}(t)E_{t=0}\times\left[g_\infty+g_1\frac{\tau}{t}\left(1-e^{-t/\tau}\right)\right](1+\alpha\gamma) \quad (1)$$

Where R and t are effective tip radius and loading time, $E_{t=0}, g_\infty, g_i$, τ are viscoelastic parameters. $1+\alpha\gamma$ is the correction parameter. Fig. 2 displays the comparison of force–depth curves determined by FEA, Hertz–Heaviside model and new predictive model for a cell placed on a flat surface and within a well. Fig.3 depicts the viscoelastic responses of chondrocyte determined by experimental measurement and modeling.

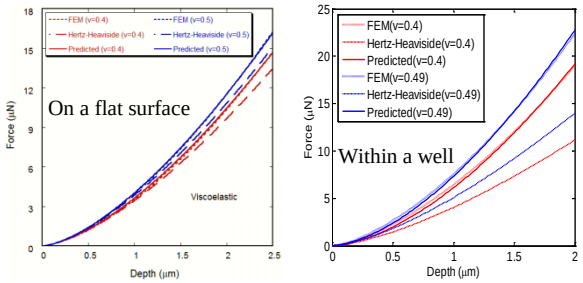

Fig. 2: Comparison of force-depth curves determined by FEA, Hertz–Heaviside model and predictive model presented in this study.

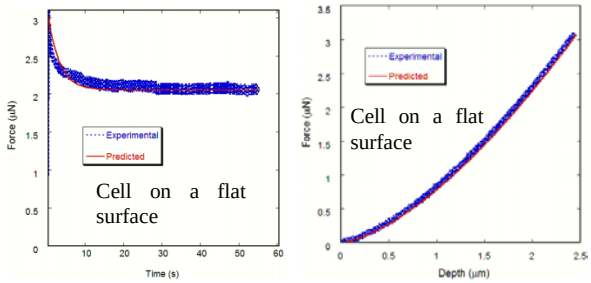

Fig.3: Comparison of force-time and force–depth relations between experimental measurement [5] and new predictive model [6].

DISCUSSION & CONCLUSIONS: The new predictive models are in good agreement with FEA and recent experimental data [5]. The new model has proven to enable a more consistent and accurate determination of the viscoelastic properties of the cells. In contrast, when the Hertz– Heaviside model was utilized, the Young's modulus obtained from the ramping period was nearly 60% higher than that determined from the stress relaxation [5], which is unreasonable. The models developed here are also applicable to nanoindentation on other viscoelastic spherical solids such as encapsulates for drug delivery.

REFERENCES: [1]M. Lekka, M., et al (2001) *Biochi. Biophys. Acta*. **1540**:127-136. [2]W.R. Trickey, et al. (2000) *J. Orthop. Res*.**18**: 891-898. [3]M.N. Starodubtseva (2011) *Ageing Res. Rev*.**10**:16-25. [4]Ng, L., et al. (2007) *J. Biomech*. **40**:1011-1023. [5]E.M.Darling, et al (2006) Osteoarthr. Cartil. **14**: 571-579. [6] J. Chen and G.X. Lu (2012) *J Biomech* **45**: 2810-2816.

Prediction of *in vivo* outcome of new dermal scaffolds by a novel *in vitro* model of 3D cell ingress

E García-Gareta[1], N Ravindran[1], V Sharma[1], S Samizadeh[1], JF Dye[1]

[1] *The RAFT Institute of Plastic Surgery, Mount Vernon Hospital, Northwood, UK*

INTRODUCTION: The commercially available collagen-based dermal reconstruction scaffolds Integra® (I) and Matriderm® (MD) are not widely used in major trauma because of variable integration and equivocal outcomes. Smart Matrix (SM) is a new fibrin based scaffold which shows rapid integration and vascularisation *in vivo*.
The **aim** of this study was to create a novel *in vitro* model of 3D cell ingress into dermal scaffolds to predict *in vivo* outcome. Cell proliferation, apoptosis, matrix contraction, cytokine/growth factor profile, α-smooth muscle actin (α-SMA) expression and cell morphology were studied for SM, I & MD.

METHODS: Normal primary human dermal fibroblasts ($0.5x10^6$) from 3 donors were cultured on coverslips (C-), contractile collagen gels (CCGs, C+ in apoptosis), I, MD and SM for 2 or 7 days.
SEM of unseeded scaffolds was performed to compare their morphology. Matrix contraction was monitored for the duration of the study. Cell proliferation was assessed by alamarBlue® assay and Ki67 immunostaining. Apoptosis was detected by AnnexinV staining. α-SMA expression was assessed by immunostaining. Cell morphology was studied by SEM and H&E staining of cross-sections. Cytokine/growth factor expression (TNFα, IFG1, VEGF, IL-6, FGFb, TGFβ, EGF and leptin) was profiled by ELISA.

RESULTS: SEM revealed the three dermal scaffolds used present micro-porosity. I shows no nano-features while MD and SM have nano-fibers, densely packed in Smart Matrix, as well as nano-pores (*Fig. 1*). The 3 dermal scaffolds did not contract over time.
Cell proliferation on SM was higher than on the collagen matrixes (*Fig. 2*), corroborated by Ki67 immunostaining.
Morphology (cross-sections) showed marked differences: cells in SM were elongated compared to stellate in CCGs or cuboidal in both I and MD, confirmed by α-SMA immunostaining. SEM showed cell-matrix adhesion on all the scaffolds. Apoptosis levels were very similar between the 3 dermal scaffolds.
Cytokine/growth factors profile was similar for all the scaffolds, except in SM VEGF increased, TNFα & TGFβ decreased.

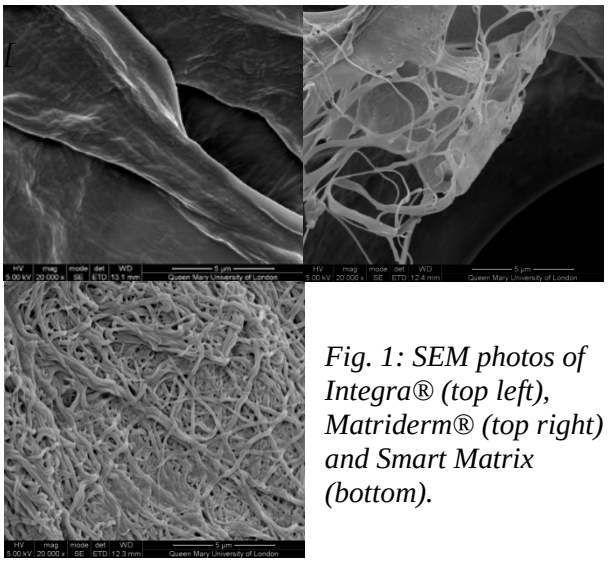

Fig. 1: SEM photos of Integra® (top left), Matriderm® (top right) and Smart Matrix (bottom).

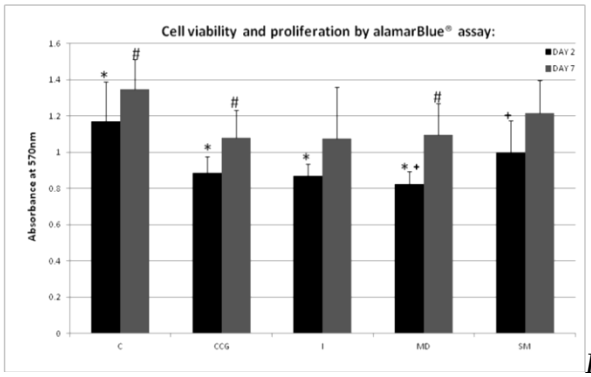

Fig.2: Cell viability and proliferation by alamarBlue® assay showing higher cell proliferation on SM compared to I and MD.

DISCUSSION & CONCLUSIONS: We proposed a novel *in vitro* model of 3D cell ingress into dermal scaffolds to predict *in vivo* outcomes such as integration, cellularisation and contraction. Differences seen in cell proliferation, α-SMA expression and cytokine/growth factor profile between scaffolds using the *in vitro* model are indicative of the extent of *in vivo* integration response rather than quantitatively representative. Particularly pro-angiogenic and cellular properties of SM are demonstrated.

Surface functionalization of electro-spun poly(L)lactic acid scaffolds to improve angiogenesis for surgical treatment of pelvic organ prolapse

Giulia Gigliobianco[1], Sabiniano Roman[1], Nadir I. Osman[2], Anthony J. Bullock[1], Chuh K. Chong[1] and Sheila MacNeil[1]

[1]*Kroto Research Institute, University of Sheffield, Sheffield, S3 7HQ, UK*

[2]*Department of Urology, Royal Hallamshire Hospital, Sheffield, S10 2JF, UK*

INTRODUCTION: Pelvic Organ Prolapse consists of a collapse in the vagina that causes displacement of the pelvic organs. Effects on the women include incontinence, pain and mental distress. Commonly, synthetic meshes are surgically put in place to support the prolapsed organs. However, better biomaterials are needed to treat pelvic organ prolapse because current treatments have a high failure rate (Maher et al., 2010). It is believed that a better integration of the material within the host would result in a better surgical outcome. Specifically, biomaterials can be functionalized to improve their angiogenic activity once implanted. The ultimate goal of this study is to improve biointegration of electro-spun PolyLactic Acid (PLLA) scaffolds (Fig.1) to improve angiogenesis post-implantation. This study deals with the initial scaffold functionalization and characterization *in-vitro*.

METHODS: Electrospun PLLA scaffolds were plasma polymerized with PolyAcrylic Acid (PAA). Afterwards, they were coated with alternative layers of PolyEthyleneImine (PEI) and PAA or PEI and Heparin for a total of seven layers, in a layer-by-layer (LBL) coating approach. Coated scaffolds were dipped in heparin solution, dried and immersed in Vascular Endothelial Growth Factor (VEGF) solution to prove that VEGF would bind to the heparin on the scaffold. The surface chemistry was verified by X-Ray Photon Electron Spectroscopy (XPS). An ELISA kit was used to quantify the amount of VEGF bound onto the scaffolds.

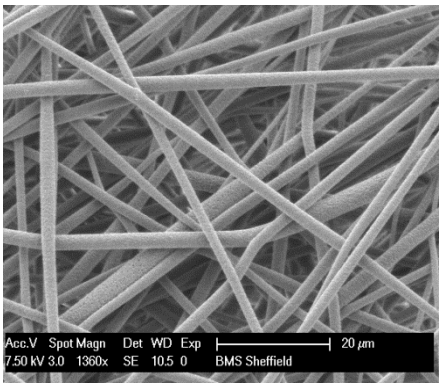

Figure 1. SEM picture of a poly(L)lactic acid electrospun scaffold

RESULTS: XPS showed that plasma polymerization of the scaffold with PAA was successful. Heparin bound well to LBL-coated scaffolds, compared to non-functionalized scaffolds, showing an increase in VEGF binding.

Table 1. Atomic ratios of elements present on the surface of different scaffolds, normalized by the amount of carbon atoms present (C= carbon, N=Nitrogen, S=Sulphur, O=Oxygen).

	Atomic Ratios		
Type of Scaffold	**O/C**	**N/C**	**S/C**
Not-functionalized PLLA	0.375	0.011	0.000
1 layer functionalized PLLA	0.468	0.128	0.052
5 layers functionalized PLLA	0.542	0.155	0.076
7 layers functionalized PLLA	0.546	0.149	0.082

DISCUSSION & CONCLUSION: Heparin binding to electro-spun PLLA scaffolds is greatly improved by plasma polymerization and layer-by-layer coating. This is probably due to an increase in surface charge. Heparin bound onto the scaffold is able to bind VEGF in solution, as an ELISA assay showed. These are the first step to design an electrospun material with improved angiogenic activity. Future work will involve testing the pro-angiogenic effect of the heparin-coated scaffolds both *in vitro* and *in vivo*. Experiments would include endothelial proliferation and migration assay and chorionic allantoic chick membrane assay.

REFERENCES: MAHER, C., FEINER, B., BAESSLER, K., ADAMS, E. J., HAGEN, S. & GLAZENER, C. M. A. 2010. Surgical management of pelvic organ prolapse in women. *Cochrane Database of Systematic Reviews*.

Identification of mechano-regulated genes following non-invasive murine knee joint loading *in vivo*.

SJ Gilbert[1], LB Meakin[2], DJ Mason[1], VC Duance[1], EJ Blain[1].

[1] Arthritis Research UK Biomechanics and Bioengineering Centre, School of Biosciences, Cardiff University, CF103AX [2] School of Veterinary Sciences, University of Bristol, Bristol, BS40 5DU.

INTRODUCTION: Abnormal mechanical loading modifies articular cartilage and bone structure and contributes to osteoarthritis (OA). We have used an *in vivo* non-invasive joint loading model [1] to investigate signalling mechanisms that control the response of cells to mechanical loading, and in particular the development of arthritis in response to abnormal loading.

METHODS: Loads (9N, 40 cycles [1]) were applied to the right knees of 12-week-old C57Bl6 mice on 3 occasions, 2 days apart; mice moved freely between loading sessions. Left knees served as unloaded controls. All procedures were in compliance with the Animals (Scientific Procedures) Act 1986. Knees were assessed 48 hours after the last loading episode for joint degeneration (histology) and changes in gene expression (RT^2 Profiler PCR arrays; SABiosciences).

RESULTS: Histology demonstrated surface fibrillation and loss of proteoglycan in the lateral compartment of the loaded knee (figure 1).

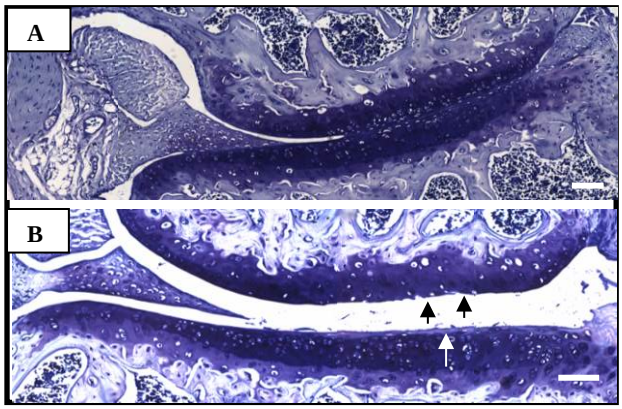

Fig. 1. Toluidine Blue stained sections from the unloaded (A) and loaded (B) knee. Evidence of surface fibrillation (black arrows) and loss of proteoglycan (white arrow) in the lateral compartments was observed in the loaded knee. Scale bar = 10µm.

Type I interferon response PCR array: A number of genes involved in the immune response were upregulated by load including CCL2 (2.64-fold), CCL5 (10.6-fold), and Cd86 (10.6-fold). In addition, interferon stimulated genes OAS1a, Gbp1, and Ifi30 were upregulated 2.6-fold. Genes switched on by load included TLR 3, 7, and 8, and Cxcl10. Interferon inducible genes down-regulated by load included Ddx58 (6-fold), PKR (3-fold), Ifit1 (6-fold), Ifnar1 (6-fold), and Tap1 (12-fold).

Wnt signalling PCR array: A number of genes involved in Wnt signalling were either up-regulated by load, *e.g.* Dab2 (16-fold), DKK3 (4-fold), Wnt5b (4-fold) and Rhou (16-fold), or down-regulated, *e.g.* DKK1 (16-fold), Myc (8-fold) and WISP1 (4-fold). Genes switched on by load included Fzd6, Sfrp1, Lef1 and Vangl2.

DISCUSSION & CONCLUSIONS: We have replicated an *in vivo* tibial loading model [1] in Cardiff, whereby murine knee joints are subjected to a defined loading regime (9N, 40 cycles) with three episodes over one week. Our preliminary results show that application of this regimen with a peak load of 9N results in OA-like cartilage lesions in the lateral compartment of the knee in agreement with previous reports [1]. Previous studies using micro-CT have shown that there is close apposition across the lateral compartment with compression [1].

Analysis of gene expression revealed regulation in both the interferon and Wnt signalling response pathways. Molecules involved in recruitment of immune cells to sites of inflammation [2] and in the pathogenesis of OA [3] were up-regulated following load. In addition, Wnt signalling pathway components essential for cartilage homeostasis and implicated in osteoarthritis progression [4] were also regulated. Identification of mechanically-regulated genes in a model of joint degeneration will aid our understanding of the molecular processes that contribute to OA progression.

REFERENCES: [1] B. Poulet, R.W. Hamilton, S. Shefelbine, et al (2011) *Arthritis Rheum* **63**:137-47. [2] C.H. Tang, C.J. Hsu, Y.C. Fong (2010) *Arthritis Rheum* **62**:3615-24. [3] X. E, Y. Cao, H. Meng et al (2012) *Cell Physiol Biochem* **30**:23-32. [4] R.S. Thomas, A.R. Clarke, V.C. Duance et al (2011) *Arthritis Res Ther* **13**:R203.

ACKNOWLEDGEMENTS: This work was funded by a grant from Arthritis Research UK (18461).

Engineering a mimetic basement membrane: integration of laminin into plastic compressed collagen gels

F Godarzi, NS Tan, RA Brown

University College London, UCL Tissue Repair & Engineering Centre, Institute of Orthopaedics & Musculoskeletal Sciences, Stanmore Campus, London, HA7 4LP.

INTRODUCTION: Basement membranes (BMs) are present in almost every tissue of the human body. BMs are amorphous, dense, matrix sheets commonly found at the junction of epithelial-stromal. They contact with cells providing cytoskeletal support and regulation of cell behaviour [1]. Laminin is one of the key components of basement membrane, important for a number of cell activities, such as anchorage, division, differentiation and polarisation [2]. Plastic compression (PC) of collagen gel [3] has previously engineered a biocompatible extracellular matrix. Our aim here is to design and fabricate a 3D model form of basement membrane by incorporating laminin into this basic collagen stroma to investigate the effects of key basement membrane proteins on cellular activities.

METHODS: Rhodamine-labeled laminin was diluted in PBS to a final concentration of 0.01 mg/ml. 75 µl of this solution was pippeted at the bottom of a well plate and air dried for 5 minutes. HaCaT cells (Keratinocyte cell line) were trypsinised and added to neutralised collagen gel solution at 3.33×10^5 cells/ml. To each of the coated wells 1.5 ml of the collagen mixture was added. The well plate was centrifuged for 5 minutes to get the cells to the bottom and to place the HaCaT in contact with the laminin layer; the plate was incubated for 30 minutes at 37°C to gel the collagen. The samples were compressed for 5 minutes using the absorbent plunges, fixed and processed for histology. Position of cells was assessed by Haematoxylin and eosin (H&E) staining while localisation of laminin was detected using fluorescence microscope.

RESULTS: Histological evaluation (Figure 1A) showed that by centrifugation, cells were placed at the bottom line of the construct. Images taken by fluorescence microscope (Figure 1B) verified the presence of laminin at the bottom of the constructs.

DISCUSSION & CONCLUSIONS: Present work validates two points: firstly, cells can be easily and quickly localised at the bottom of the gel by centrifuging. Secondly, laminin could be trapped into the gel by coating a thin layer at the bottom of the well. Further work will characterize HaCaT morphology and behaviour in the presence of laminin over time, potentially with other basement membrane proteins such as type IV collagen. This will model the need for greater protein complexity in these pseudo-basement membrane models.

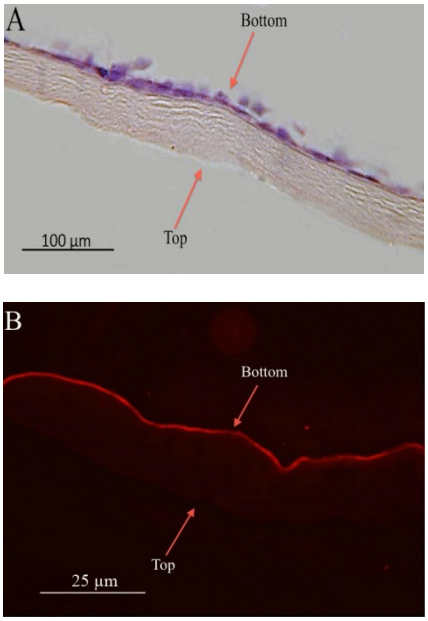

Fig. 1: Bright field (A) and fluorescence (B) microscopy results of HaCaT on collagen gel coated with Rhodamine-labelled laminin. Arrows indicate top and bottom of the constructs.

REFERENCES: [1] M. Paulsson (1992) *Basement membrane proteins: structure, assembly and cellular interactions*, Crit. Rev. Biochem. Mol. Biol. **27**, 93-127. [2] R. Fleischmajer, A. Utani, E. Douglas MacDonald II, et al (1998) *Initiation of skin basement membrane formation at the epidermo-dermal interface involves assembly of laminins through binding to cell membrane receptors*, J Cell Science **111**, 1929-40. [3]RA Brown, M. Wiseman, CB Chuo, et al (2005) *Ultra-rapid engineering of biomimetic materials and tissues*, Adv. Funct. Mater. **15**, 1762-70.

Tissue engineering bone: assessment of growth factor delivery within novel Stro-1+ MSC seeded alginate/bone ECM hydrogel constructs

D Gothard[1], EL Smith[1], JM Kanczler[1], JA Wells[1], CA Roberts[1], LJ White[2], O Quatachi[2], KM Shakesheff[2], MM Stevens[3] and ROC Oreffo[1]

[1] *Bone and Joint, Centre for Human Development, Stem Cells and Regeneration, Institute of Developmental Sciences, University of Southampton*

[2] *Wolfson Centre for Stem Cells, Tissue Engineering and Modelling, Centre for Biomolecular Sciences, University of Nottingham*

[3] *Centre for Biomedical Materials and Regenerative Medicine, Institute for Biomedical Engineering, Imperial College London*

INTRODUCTION: Demand for new reparative approaches to bone damage resulting from trauma and disease is growing within an increasingly aged population. Bone tissue engineering provides opportunity to create new tissue directly *in vivo*, or indirectly *in vitro* as transplantable constructs. Here we investigate the potential of a novel cell/biomaterial construct loaded with appropriate growth factors for bone tissue formation within an *in vivo* subcutaneous mouse model.

METHODS: Stro-1+ MSC populations were immuno-selected from human bone marrow via MACS [1]. BMP-2 and TGF-β3 were chosen for their osteochondral induction potency and encapsulated within PLGA/triblock (PLGA-PEG-PLGA co-polymer) microparticles [2]. Slow release BMP-2 (20-30um, 100ng/mL) and fast release TGF-β3 microparticles (50-100um 15ng/mL) were used to enable dual release profiles. Both cells and microparticles were suspended within an alginate and bovine bone ECM hydrogel scaffold (60:40% respectively) [3]. Hydrogel cylinders were formed through pastette extrusion into calcium chloride to set the construct. Constructs were subsequently cultured overnight before being cut into 5mm length segments.

Hydrogel constructs were subcutaneously implanted within the peritoneal cavity of MF1 nu/nu mice. Mice were euthanized after 28 days and samples harvested by dissection. Retrieved implants were fixed in 4% PFA and bone formation was assessed by micro-CT analysis. Fixed samples were then processed for histological analysis via Alcian blue/Sirius red stain.

RESULTS: Hydrogel constructs exhibited mineralised bone formation following *in vivo* implantation demonstrating potential for ectopic ossification (Fig 1A). Incorporation of Stro-1+ MSCs appeared to enhance bone formation. Histological analysis revealed higher collagen deposition correlated with implanted cells, although host-derived cell/tissue invasion was observed (Fig 1B).

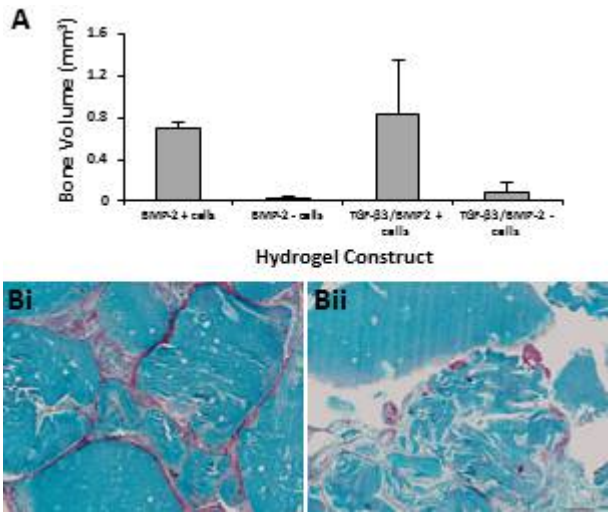

Fig. 1: *Micro-CT (**A**) and histological analysis (construct + cells (**Bi**); - cells (**Bii**)) of hydrogel constructs loaded with single and dual loaded microparticles following 28 days in vivo culture.*

DISCUSSION & CONCLUSIONS: The current study investigates the potential of novel constructs comprising Stro-1+ MSCs and growth factors within alginate/bone ECM hydrogel, for *in vivo* osteoinduction and bone formation.

REFERENCES: [1] R. S. Tare, *at al* (2012) *Methods Mol Biol* **816**: 83-99. [2] L. J. White, *et al* (2013) *Mater Sci Eng C* 33 (**5**) 2578-2583. [3] M. J. Sawkins, *et al* (2013) *Acta Biomater* Epub: 24th Apr.

ACKNOWLEDGEMENTS: Thanks to Mr Douglas Dunlop for provision of human bone marrow. This work was funded by the BBSRC (BB/GO10579/1).

Engineered neural tissue constructs retain aligned structure and cell viability following injection through a hypodermic needle

AL Gray[1], M Georgiou[1], JB Phillips[1]

[1] *Life, Health & Chemical Sciences, The Open University, Milton Keynes, UK*

INTRODUCTION: Fluid-filled cavities that form at the site of a spinal cord injury can potentially be filled with supportive cells and materials. Cells injected in suspension have been shown to be beneficial [1], but the lack of a matrix scaffold means cells are not organised to achieve optimal density and alignment for guidance of regeneration. Conversely, implantation of a solid cellular biomaterial construct would require surgical excision and a risk of damaging surviving tissue. Here the aim was to investigate whether an aligned cellular biomaterial construct could potentially be delivered to a cystic cavity within the spinal cord via minimally invasive injection.

METHODS: Sheets of engineered neural tissue (EngNT) were produced by self-alignment of Schwann cells in a tethered collagen gel, followed by plastic compression, to produce robust aligned cellular biomaterials. EngNT was then rolled to form cylindrical rods, potentially suitable for injection. Individual EngNT rods were either maintained as controls, or passed through hypodermic needles of various gauges with internal diameter less than that of the rods. Survival of cells was assessed using propidium iodide to identify % cell death, overall rod dimensions were measured before and after injection, and anisotropic cellular architecture was assessed using immunostaining and confocal microscopy.

RESULTS: Cells within EngNT rods survived being passed through hypodermic needles (G19, G21 and G23) and showed no significant reduction in viability after 1h with a G19 needle (Fig. 1), and no additional cell death at 24h. The diameter of the rods returned to their previous size following injection through a G19 needle, and the cells within them remained aligned parallel to the rod longitudinal axis (Fig. 2).

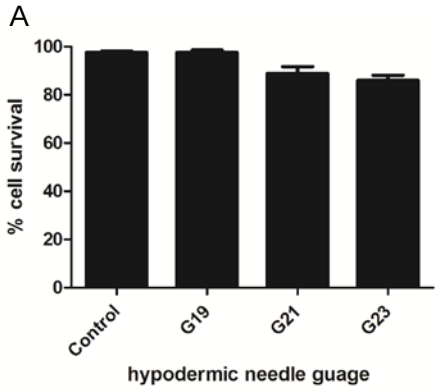

Fig. 1: Cells within rods of EngNT survive being passed through hypodermic needles

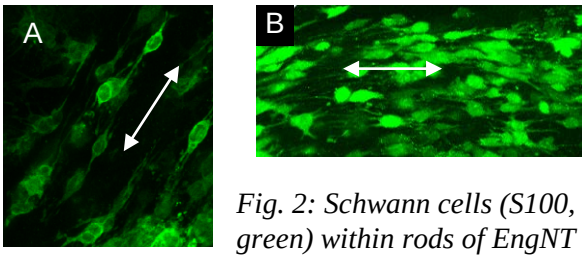

Fig. 2: Schwann cells (S100, green) within rods of EngNT remain aligned parallel to the rod longitudingal axis (white arrows) after being passed through a G19 needle.

DISCUSSION & CONCLUSIONS: EngNT constructs have the ability to pass through a hypodermic needle without loss of cell viability and with the potential for preservation of cellular alignment. These shape-memory properties could potentially be exploited to develop therapeutic versions of EngNT that could be delivered, via minimally-invasive injection, to a cystic cavity following spinal cord injury in order to support neuronal regeneration.

REFERENCES: [1]B. Sandner, P. Prang, FJ Rivera, et al (2012) *Cell Tissue Res* **349**: 349-62

Oral mucosa lamina propria-progenitor cells (OMLP-PCs) and OMLP-induced pluripotent stem cells (iPSCs) as potential sources of neurons for regenerative medicine

R Howard-Jones[*1], L Davies[1], A Mondini[2], N Allen[2], PJ Kemp[2], P Stephens[1]

[1]*Wound Biology Group, Cardiff Institute of Tissue Engineering and Repair, Tissue Engineering and Reparative Dentistry, School of Dentistry, Cardiff University, Cardiff;* [2]*School of Biosciences, Cardiff University, Wales.* *(howardjonesRA1@cardiff.ac.uk)

INTRODUCTION: Over the past few decades stem cells have been extensively investigated due to their potentially invaluable therapeutic use. Embryonic stem cells (ESCs) have wide-ranging therapeutic applications in tissue repair and regeneration due to their pluripotent properties and their ability to self-renew indefinitely. However, ethical concerns surround their use and hence alternatives are sought. Adult stem cells (ASCs) have been isolated from various adult tissues including the OMLP. This study aims to isolate ASCs from the OMLP, reprogram these cells to iPSCs and determine the potential for both to differentiate into functional neurons due to the limited regeneration of neurons following damage to the central nervous system.

METHODS: OMLP-progenitor cells (OMLP-PCs) were isolated by differential adhesion to fibronectin. OMLP-PCs were reprogrammed with two plasmids containing pluripotency factors (*oct-4*, *sox-2*, *nanog*, *klf-4*, *lin-28*, *c-myc*) to iPSCs[1]. Emerging colonies were stained for alkaline phosphatase or pluripotency markers. Cells were expanded in ESC medium as neurospheres[2] and differentiated in DMEM/F12 with brain derived neurotrophic factor, nerve growth factor and neurotrophin-3 (all at 10ng/mL)[3]. Immunocytochemistry was performed on cells to determine the proportion expressing neural markers and Ca^{2+} imaging was employed to determine the presence of functional Ca^{2+} and ligand-gated ion channels.

RESULTS: Nucleofection of OMLP-PCs resulted in colonies similar to ESCs (*Fig 1*) which demonstrated alkaline phosphatase staining and positive staining SSEA-4, SSEA-5, TRA-1-60 and TRA-1-81 suggesting that these were iPSCs. These iPSCs also demonstrated formation of embryoid bodies and differentiated down all three germ layers. Differentiated OMLP-PCs demonstrated expression of neural markers; microtubule-associated protein-2 (≈93% +ve), neurofilament medium (≈67% +ve) and βIII tubulin (≈88% +ve). Treatment with 50mM KCl or 300μM GABA resulted in Ca^{2+} influx, whilst application of 100μM ATP evoked rapid Ca^{2+} influx through P2X purinoceptors (*Fig 2*). Work is ongoing to confirm the potential of the oral-iPSCs to also form functional neurons.

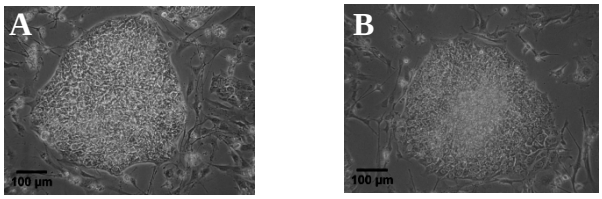

Fig. 1: ***(A)*** *Human ESCs.* ***(B)*** *OMLP-iPSCs*

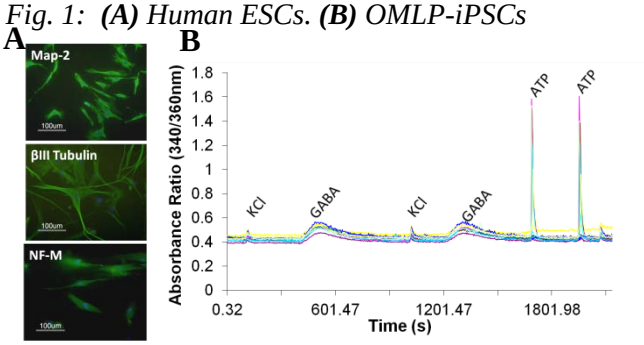

Fig. 2: ***(A)*** *OMLP-PC derived neurons positive for Map-2, βIII Tubulin and NF-M.* ***(B)*** *Ca^{2+} influx as a response to GABA & KCl (through voltage sensitive calcium channels) and an additional response to ATP (via P2X purinoceptors) confirms the functionality of neurons from OMLP-PC clones.*

DISCUSSION & CONCLUSIONS: OMLP-PCs can be reprogrammed to iPSCs which demonstrate pluripotent properties. Differentiated OMLP-PCs express neuronal markers, respond appropriately to certain ligands and depolarize suggesting that these cells have a functional neuronal phenotype. Together, these data suggest that OMLP-PCs have a future potential for regenerative medicine applications.

REFERENCES: [1] Yu et al (2009) *Science* **324**:797-801. [2] Li et al (2005) *Biotechno Bioeng* **91**:688-98. [3] Fernandes et al (2004) *Nat Cell Biol* **6**:1082-93.

In vitro biomimic niche *via* near-field electrospinning of polystyrene fibres

Xia Li[1] and Yan Yan Shery Huang [1,2*]

1Department of Physics, University of Cambridge, UK

*2*Department of Chemical Engineering and Biotechnology, University of Cambridge, UK.*

yysh2@cam.ac.uk

INTRODUCTION: Natural extracellular matrix (ECM) consists of well-defined architecture and spatial patterns formed by fibril features ranging from nanometre to micrometre scale. Recapitulating the key characteristics of such a cell-specific niche is important for *in vitro* studies as well as for tissue engineering. The development of controlled patterning in the nano- micro scale will therefore open the possibilities to direct cellular organisation and development using mechanisms such as contact guidance and mechanobiology. Here, the interaction between the NFES (near-field electrospinning) polystyrene fibre patterns and a cancer cell line or an endothelium cell line is demonstrated.

METHODS: Near-field electrospinning[1,2] was utilised to pattern polystyrene fibres. Prior to cell seeding, plasma treatment and gelatine coating were applied to improve initial cell attachment. *In-vitro* studies were performed using human breast cancer cell line (MB231), and an endothelium cell line (EA.hy926), to investigate the effects of fibre patterns on cell behaviours. Live-cell imaging was performed using a Leica fluorescence microscope over a time period of 12 hours.

RESULTS: Different types of fibre morphologies were fabricated (see Fig.1) where the fibre diameters can be fine-tuned between 100s of nanometre to a few microns. Patterns of straight or curling conformations can be formed, mimicking the naturally occurring ECM fibrils. Cells were found to favourably interact with the fibre patters, and displaying very different behaviours depending on the cell type. The MB231 cells were found to track and migrate along the fibre pattern, whereas the EA.hy926 cells were found to form flat sheet bridging the gap between the fibres (Fig.2).

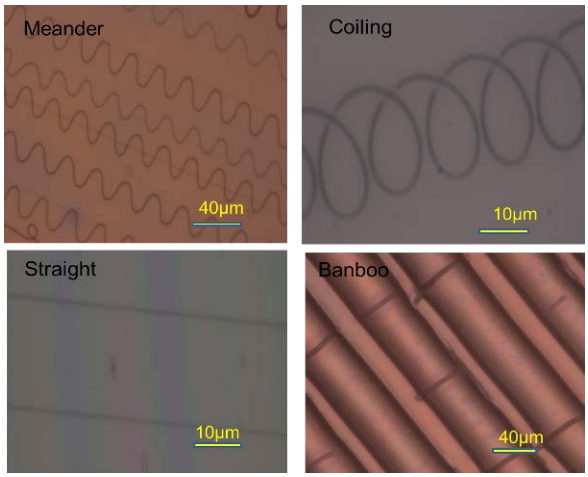

Figure 1. NFES fibre patterns.

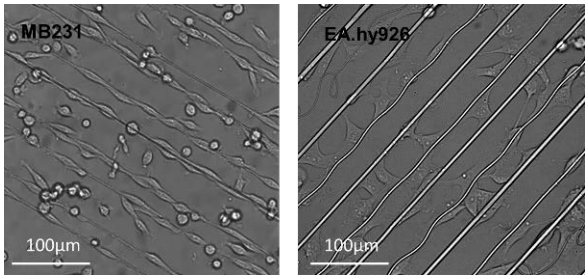

Figure 2. Cellular interaction with patterned fibres.

DISCUSSION & CONCLUSIONS: Ordered polystyrene fibre patterns of varied morphologies were fabricated using near-field electrospinning. The resulted patterns illustrate a cell-type dependent behaviour, which seem to reflect the invasive or biological function of the cells.

REFERENCES: [1] Huang *et al.* (2012) Nanotechnology 23 105305. [2] Sun *et al.* Nano Lett. (2006) 6 839

ACKNOWLEDGEMENTS: The authors would like to thank the Oppenheimer Fellowship and the Homerton College Research Fellowship for funding.

Targeting Wnt-loaded nanoparticles to skeletal stem cells for bone regeneration.

AA Janeczek[1], RS Tare[1], I Moreno[1], GS Attard[3], TA Newman[2], ROC Oreffo[1], ND Evans[1]

[1] *Bone and Joint Research Group, Centre for Human Development, Stem Cells and Regeneration,* [2] *Clinical Neurosciences,* [3] *Chemistry Department; Southampton University, SO16 6YD.*

INTRODUCTION: Bone-related illnesses are among major public health problems, with osteoporosis treatment costing the UK ~£2 billion each year. Furthermore, 10% of all bone fractures fail to heal properly, resulting in non-unions. To address these problems with bone tissue homeostasis and regeneration, we hypothesise that delivery of therapeutic agents targeted specifically to stem cell populations within the bone, called skeletal stem cells (SSCs), may represent a promising therapeutic approach. As the Wnt signalling pathway has been shown to be involved in regulating SSCs biology, our aim is to deliver Wnt proteins or agonists, entrapped in liposomes, to these cells, using the SSC marker STRO-1.This will ensure the specificity and safety of our approach.

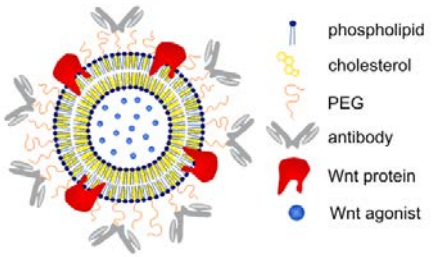

Fig. 1: Proposed therapeutic liposome design.

METHODS: We have tested the influence of Wnt signalling induction by different concentrations (25-100ng/ml) and time exposures (1 or 14 days) to Wnt3A protein on heterogeneous and STRO-1-sorted (progenitor enriched) bone marrow cell populations, cultured in basal or osteogenic media. Progenitor/osteogenic commitment were measured by FACS analysis for STRO-1 as well as colony forming assays (CFU-F and CFU-O) and alkaline phosphatase (ALP) assay. The validity of using STRO-1 as an epitope for targeted delivery of liposomes was tested by measuring its internalisation by FACS, triggered by antibody binding. We fabricated 100nm liposomes via extrusion and tested the suitability of different lipid components in our formulations (DSPE-PEG, DSPE, DPPC, DMPC, DOPC and cholesterol) and the stability of the preparations over a 12 day period via dynamic light scattering (DLS). The size distribution of nanoparticles was also confirmed by transmission electron microscopy (TEM).

The activity of Wnt protein entrapped within the lipid bilayer of our different liposome formulations is now being tested on a Wnt responsive cell line.

RESULTS: The results showed that short-term Wnt exposure increased the osteoprogenitor population whereas long-term inhibited differentiation. We have also looked at the STRO-1 marker as a delivery target and showed by FACS that it internalises rapidly upon binding (*Fig 2.*).

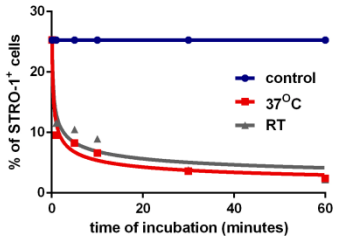

Fig. 2: Binding of the STRO-1 epitope results in its rapid internalisation (within 1h at 37°C; red line) indicating that antibody tagged nanoparticles will be taken up by cells.

Currently we are proceeding with the preparation of liposome nanoparticles *(Fig 3.)* and testing their binding specificity to SSCs as well as the effectiveness of liposome-entrapped Wnt protein.

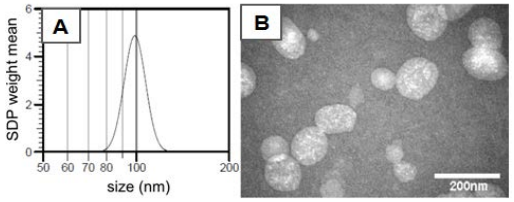

Fig. 3: Liposomes had a size distribution of 100±20nm measured by DLS (A) and TEM (B).

DISCUSSION & CONCLUSIONS: Induction of Wnt signalling increased the population of stem cells (marked by STRO-1) and promoted generation of osteoprogenitors in heterogeneous BMMNCs. Moreover, the STRO-1 antigen is rapidly taken up by cells after ligand binding, and therefore might be a suitable marker of SSCs for the targeted delivery of therapeutic liposomes. 100nm DMPC-PEG and DOPC-PEG liposome preparations are stable over 12 days and are now being tested for suitability for targeted delivery of Wnt signalling-inducing agents.

Superparamagnetic iron oxide labeling of mesenchymal stem cells for tracking in a sheep model of intra-thecal tendon injury

MR Khan, RKW Smith, R DeGodoy, S Dakin, F David, AE Goodship, J Dudhia

Clinical Sciences and Services, Royal Veterinary College, Hawkshead Lane, North Mymms, AL9 7TA London, United Kingdom

INTRODUCTION: Release of extracellular matrix (ECM) components from tendon injuries located within a synovial compartment is thought to cause chronic synovial inflammation resulting in poor ability of the tendon to heal. We propose that autologous mesenchymal stem cells can enhance healing due to their immunomodulatory function and/or by adhering to and sealing the defect to halt the loss of ECM components. Autologous bone marrow mesenchymal stem cell (BM-MSCs) transplantation can enhance repair in extra-synovial tendon injuries[1.] In addition, synovial membrane (SM) contains MSCs that can be isolated in large numbers from diseased joints[2], display similar characteristics to BM-MSCs, and offer the possibility of an alternative cell source for cell therapy. In this study we have developed a novel sheep model of intra-synovial tendon injury to the digital flexor tendon sheath (DFTS) to track BM- and SM-MSCs labeled with Molday-ion iron-oxide nanoparticles (MIONs) injected into the lesion, by MRI.

METHODS: Stromal cells were isolated from sheep BM aspirates taken from the iliac crest and SM biopsies from the DFTS. Cells were selected for adherence to tissue culture plastic and characterised by trilineage differentiation and CFU-F assays. Cells were labeled with MIONs (BioPal, USA) according to supplier's conditions; label uptake was confirmed by confocal microscopy. The sensitivity of MRI to detect different densities of cells, either clustered or evenly dispersed, was conducted. $5x10^6$ labeled cells were injected into the DFTS of the right forelimb in which the lateral deep digital flexor tendon bore a longitudinal defect created tenoscopically 7 days earlier (n=4). Cells were tracked in the forelimbs at 7 days post-injection with a 1.5 Tesla MRI scanner (Philips). Control sheep had PBS injected (n=2).

RESULTS: A 10 ml aspirate of ovine BM would yield ~$1x10^6$ cells after 7 days in primary culture. By comparison, $2x10^5$ SM-MSCs were obtainable by mild overnight digestion of ~ 50 mg SM biopsy. Both populations exhibited a mean CFU count of 25 % as well as tri-lineage capacity. Uniform MION labeling of cells, assessed by confocal microscopy, occurred in all instances. Addition of protamine sulfate did not enhance MION uptake, which could be detected by MRI in ~$3x10^4$ cells suspended in low-melting point agarose. Label was detectable in cells for up to five population doublings. MION labeling did not significantly affect clonogenic replication, population doubling time or tri-lineage capacity of cells compared to control medium. MRI showed both MSC types were distributed unevenly throughout the tendon sheath, mostly to the synovial membrane in clusters. This was confirmed by histology, which showed areas of cellular distribution within the synovium and superficial DFT tendon. One sheep showed generalised inflammatory reaction around the sheath but this was not reflected by impairment in mobility or discomfort

DISCUSSION & CONCLUSIONS: MSCs isolated from both bone marrow- and synovium membrane readily take up nanoparticles, whose intracellular presence did not affect MSC viability or characteristics. Although the labeled cells could be detected by MRI, its sensitivity was found to depend on high density as well as relative localisation as dispersed cells exhibited poor contrast.

REFERENCES: [1]E.E. Godwin, N.J. Young, J. Dudhia, I.C. Beamish, and R.K.W. Smith (2012) *Equine Vet J* **44**: 25-32. [2]T. Morito, T. Muneta, K. Hara, Y.J. Ju, T. Mochizuki, A. Umezawa, and I. Sekiya (2008) *Rheumatology (Oxford)* **47**(8):1137-43. [3]P.Becerra, M.A. Valdés Vázquez, J. Dudhia, A.R. Fiske-Jackson, F. Neves, N.G. Hatman, and R.K. Smith et al *J Orthop Res* (2013 Mar 18:0. doi: 10.1002/jor.22338. [Epub ahead of print]).

ACKNOWLEDGEMENTS: This work was funded by the MRC.

Isolation and characterisation of adult and foetal tenocytes

J. K. Kular[1], M. J. Ellis[1], R. I. Sharma[1]

[1] *Department of Chemical Engineering, University of Bath, Bath, BA2 7AY UK*

INTRODUCTION: Tendon tissue is primarily composed of extracellular matrix (ECM) and tenocytes. Tenocytes are a specialised fibroblast cell type that play a role in managing the conservation and modification of the tissue[1]. The aim of this study was to successfully isolate and characterise tenocytes from adult and foetal sources. This initial work will supply evidence towards understanding the age-related differences that cause the variation between reparative healing in adults and regenerative healing in foetuses, with the aim to aid better design of scaffolds to promote scarless healing of tendon in adults.

METHODS: We examined three different isolation techniques for adult and foetal tenocytes, to optimise outgrowth from the Achilles tendon using primary explant culture. In the first approach, tendon tissue was placed in tissue culture vessels under glass coverslips. The second method involved scoring the bottom of the culture disk, to make grooves, and adding the tissue. The third method used trypsin treatment of the tissue, with air-drying before adding media. Following cell outgrowth, adult and foetal tenocytes were trypsinised and subcultured in 6 well plates. Cell morphology assays were performed by culturing cells on tissue culture plastic, then fixing and staining with FITC conjugated phalloidin for the actin cytoskeleton and nuclei labelled with DAPI. Images of the stained cells were taken with an upright Olympus microscope at 10x magnification. Using Image J, average area of the cells and circularity were measured to indicate how spread cells were on the substrate. Circularity values range from 1.0-0.0 indicating a perfect circle, to a progressively elongated cell shape. Circularity was calculated using the equation:

$$Circularity = 4\pi r^2/Perimeter^2$$

RESULTS: Outgrowth of cells from foetal tissue was achieved when the tissue was air dried with a coverslip on top. The outgrowth rate was faster by up to two weeks than cells from adult tissue, which was best when the tissue was trypsinsed, air-dried, and secured under a glass coverslip. Cytoskeletal staining (*Fig. 1*) showed that foetal cells were larger compared to the adult cells, with the foetal cells displaying well defined stress fibres and filopodia projections. Quantifying the data for cell area and circularity (*Fig. 2*) corroborated the image findings: foetal cells were on average five times larger in surface area, and less circular, with an average circularity of 0.13. ANOVA analysis confirmed significant differences between the adult and foetal cells, with p values below 0.05.

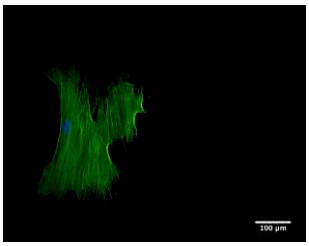

Fig. 1: Staining of actin fibres (green) and cell nuclei (blue) of an adult tenocyte (left) and a foetal tenocyte (right).

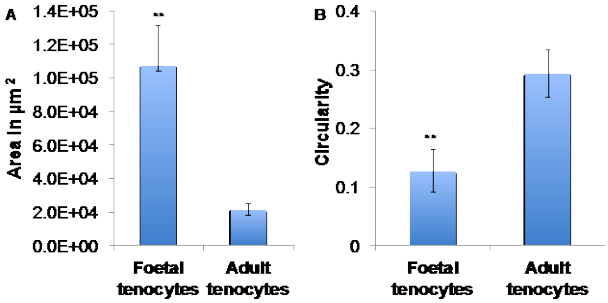

Fig. 2 (a) Average area of the adult and foetal cells (p =0.002) (b) Average circularity of adult and foetal cells (p = 0.006).

DISCUSSION & CONCLUSIONS: The data highlights physical characteristics of cells, and cell responses to a substrate can change with age. Outgrowth of both adult and foetal tenocytes from tendon tissue was successfully observed, using different pre-treatments prior to executing the explant culture. Staining the actin cytoskeleton showed dramatic differences in cell shape and the organisation of the actin cytoskeleton as a function of the cell age. Future work will involve evaluating differences of cell interactions and functional studies of adult and foetal tenocytes.

REFERENCES: [1]O Haddad et al. (2011) *Exp. Cell Res.* July; 317(12): 1726-35

ACKNOWLEDGEMENTS: This research is funded by a University Research Scholarship (URS) by the University of Bath. We thank Dr. Robert Williams from Biology and Biochemistry for providing tendon tissue.

Development of in vitro systems for investigating spinal cord cellular responses to wear debris from metal on metal total disc replacements

H. Lee[1], R.M. Hall[1], J.B. Phillips[2] J. Tipper[1]

[1] *Institute of Medical and Biological Engineering, University of Leeds, Leeds, LS2 9JT UK..*

[2]*Department of Life, Health and Chemical Sciences, The Open University, Milton Keynes, MK76AA, UK*

INTRODUCTION: Motion preservation devices including Metal on Metal Total Disc Replacements and fusion instrumentation (rods, plates, hooks and screws) are a valuable intervention to treat back pain and restore motion in the spine. The longevity of these devices is thought to be compromised by wear debris and there are growing concerns within the orthopaedic community regarding the exposure to both metal debris and ions from spinal devices and instrumentation. It has been hypothesised that such metal debris may impact upon and alter the functionality of periprosthetic tissues including the spinal cord.

This project aims to provide an insight into the responses of specific neurological cell populations (astrocytes, microglia, oligodendrocytes and neurons) to clinically relevant wear particles and their ions

METHODS: Cobalt Chrome wear particles were generated using a six station pin on plate friction rig. Here smooth (Ra 0.01-0.02µm) high carbon Cobalt Chrome pins articulate against high carbon smooth Cobalt Chrome plates, with water as the lubricant under a force of 80N for 80 hours[1](fig 1). The nanoparticles were then isolated from simulator serum using an enzyme digestion protocol and the debris imaged and characterised using Field emission gun scanning electron microscopy (FEGSEM). The effect of debris on cell viability was determined using both and ATP-Lite and MTT assays which were optimized using a cell line.

RESULTS: Initial studies to compare ATP-Lite and MTT assays using indicated that ATP-Lite was a reliable way to detect ten-fold differences in cell number (Fig. 2). Two rat neural cell lines; NG108 and C6 (glial cells) were used to determine the effect of Cobalt Chrome wear debris prior to experiments using primary cells.

Fig. 1: Six station pin on plate friction rig, for nano-scale wear debris generation.

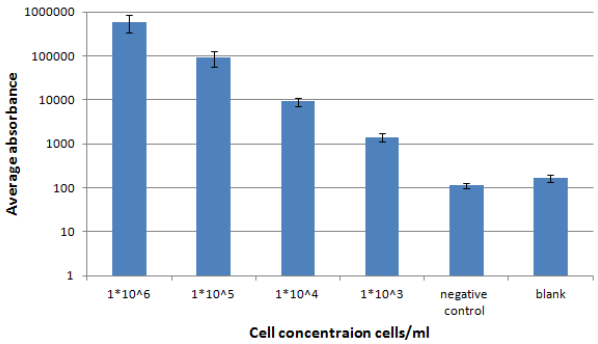

Fig. 2: Optimised ATP-Lite assay detected differences in L929 cell concentrations.

DISCUSSION & CONCLUSIONS: Methodology has been developed for testing the potential cytotoxic effects of Cobalt chrome debris on neuronal cells in a 2D culture system. This will form the basis for future work.

FUTURE WORK: To Determine the effect of Cobalt Chrome debris on cell viability and neurite outgrowth. This will include using tissue engineered 3D cell culture models

REFERENCES: [1] B Behl, I Papageorgiou, C Brown et al (2013) *Biomaterials* Vol 34, 14. 3547-3558

ACKNOWLEDGEMENTS: This work was supported by the Institute of Medical and Biological Engineering and is funded by the EPSRC.

Nanotopographical direction of adult mesenchymal stem cell growth and differentiation

LCY Lee[1], N Gadegaard[2], S Yarwood[3], RMD Meek[4], MJ Dalby[1]

[1]Centre for Cell Engineering, Institute of Molecular, Cell and Systems Biology, University of Glasgow, [2]Department of Bioengineering, University of Glasgow, [3]Institute of Molecular, Cell and Systems Biology, University of Glasgow, [4]Department of Orthopaedics, Southern General Hospital, Glasgow

INTRODUCTION: Generation of a large number of stem cells that can be differentiated into osteogenic cell types is a greatly anticipated future therapy in orthopaedic research. A nanotopographical strategy offers the advantage of not requiring soluble chemical factors. Established nanopit nanotopographies that direct adult mesenchymal stem cells (MSCs) to undergo osteogenic differentiation[1] or self-renewal[2] are transferrable between different polymers, and here we describe the optimisation procedures implemented to make best use of MSCs and nanopatterned polycarbonate substrates with regards to cell seeding density. In-house isolation of patient-derived MSCs from bone marrow allows for clinically applicable studies to be carried out, to better understand how MSC self-renewal and differentiation is regulated by nanotopography. Further application of nanotopographies were explored for efficient long-term culture of MSCs and expansion *in vitro*.

METHODS: STRO-1$^+$ or CD271$^+$ MSCs were seeded onto an ordered arrangement (SQ) of 120 nm diameter pits with 100nm depth (300 nm centre-centre spacing) and an arrangement incorporating ±50 nm displacement (NSQ). Resulting cell phenotypes were assessed by immunostaining and image analysis (CellProfiler) or Western blotting with appropriate stem cell/bone marker antibodies.

RESULTS: Cultured MSCs on SQ and NSQ polycarbonate showed best results at a lower density than used in previous work, when seeding directly onto the surface of the substrates. Similar results were seen for both STRO-1 and CD271 isolated cells. Image analysis of fluorescence images revealed (figure 1) a significantly higher expression of stem cell marker in MSCs seeded on nanopatterned tissue culture plastic.

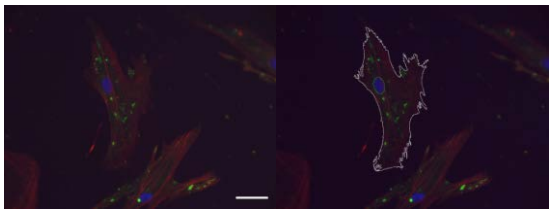

Figure. 1: CellProfiler image analysis. Cells are detected from fluorescence microscopy images, and required measurements can be obtained.

DISCUSSION & CONCLUSIONS: MSCs were successfully isolated from patient bone marrow using magnetic separation techniques. The seeding density of MSCs was found to have varying effects on the efficiency of the nanotopographies and an optimal density was determined in order to best use these surfaces. Stem cell marker expression in MSCs seeded onto SQ patterned tissue culture polystyrene was maintained at greater efficiency in comparison to a flat (planar) surface, showing a potential for nanotopographies to be applied in novel MSC culture products.

REFERENCES: [1] M. Dalby *et al* (2007) The control of human mesenchymal cell differentiation using nanoscale symmetry and disorder. *Nature Materials*. 6; 997-1003. [2] RJ McMurray *et al.* (2011) Nanoscale surfaces for the long-term maintenance of mesenchymal stem cell phenotype and multipotency. *Nature materials*. 10; 637-644

ACKNOWLEDGEMENTS: CD271 MSCs were isolated from surplus bone marrow from the Southern General Hospital, Glasgow. STRO-1 MSCs were provided by the University of Southampton. Polycarbonate substrates were made by the department of Bioengineering, University of Glasgow. LCYL is funded by an MVLS scholarship, University of Glasgow. MJD is funded by grants from BBSRC, EPSRC and MRC.

Modelling the mesenchymal stem cell niche *in vitro* using magnetic nanoparticles

E.E.L.Lewis[1], M.J.Dalby[1], C.C.Berry[1]

[1]*Centre for Cell Engineering, Institute of Molecular Cell and Systems Biology, University of Glasgow, Glasgow*

INTRODUCTION: Mesenchymal stem cells (MSCs) reside in localised areas in the bone marrow termed the 'niche'.[1] The niche environment controls the fate of MSCs; whether they retain their self-renewal characteristics or differentiate and commit to a lineage.[2] There is a current drive towards understanding the regulatory mechanisms in the niche *via in vitro* model systems, as this may then allow for external manipulation of stem cell populations to increase stem cell numbers for therapy, or to stimulate cells to regenerate specific tissues. We have developed a simple MSC niche *in vitro* by pre-labelling MSCs with magnetic nanoparticles (mNPs). Once labelled, we magnetically levitate our MSCs (*via* an external magnetic field), creating a distinct 3D MSC spheroid exhibiting excellent cell viability and maintenance of STRO-1 expression compared to parallel MSCs cultured in monolayer.

METHODS: Human MSCs (hMSCs) were either purchased (Promocell) or isolated from surgical bone marrow samples using a $CD271^+$ selection process. The PEA coated mNPs (200 nm diameter, Fe_3O_4) are labelled with a FITC fluorescent tag (Chemicell). Magnets comprised of a NdFeB core (13 mm diameter, 350 mT).

MSC Labelling. The MSC labelling with mNPs was initially optimised (0.1 mg/mL mNPs; 30 minutes + magnetic field). Uptake of mNPs within MSCs was analysed by ICP-MS, TEM and fluorescence microscopy.

Spheroid Culture. Labelled MSCs were suspended in media. A single magnet was placed on the top or bottom of the well and the plate was incubated for 24 hours and 72 hours. MSCs were assessed for viability (calcein and ethidium homodimer), cell architecture (actin) and phenotype (STRO-1) using fluorescence microscopy.

RESULTS: MSCs were successfully labelled with mNPs, and retained the label in successive passages (figure 1). When an external magnetic field was placed above the well, the MSCs were levitated towards the field and formed a spheroid structure within several hours. MSCs are adherent cells and previous studies have shown the formation of these spheroid balls, which have very strong cell-cell interactions provide a better representation of the natural niche environment.[3] Furthermore, the MSCs remained strongly viable over 72 with strong marker expression.

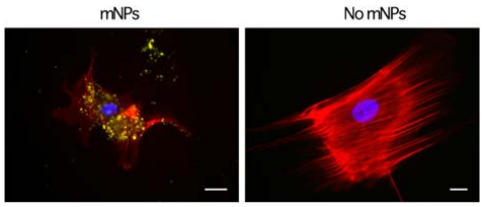

Figure 1. MSCs tagged with fluorescent mNPs as compared to control cells (red: actin, blue: nucleus). Scale bar:20 μm.

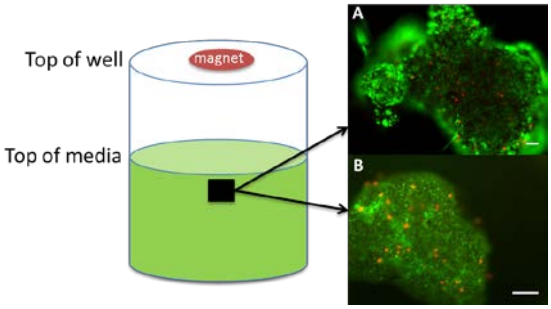

Fig. 2: Schematic of the culture system. MSCs labelled with mNPs incubated for 24 hours (A) and 72 hours (B) within media assessing cell viability (green: live cells, red: dead cells). Scale bar:50 μm.

DISCUSSION & CONCLUSIONS: Spheroid culture is being recognised as an excellent method of stem cell culture whilst maintaining phenotype. A simple, quick and highly efficient method has been developed to use mNP-labelled MSCs to form spheroid 3D cultures. Our system is novel in the use of mNPs, which allows for rapid spheroid formation (hours compared to days). The MSC spheroids remained viable and retained their multipotency potentials over 72 hours compared to conventional 2D cultures.

REFERENCES: [1]T. A. Mitsiadis, O. Barrandon, A. Rochat, et al (2007) *Exp Cell Res*, **313,** 3377-85. [2]J. M. Weber, & L. M. Calvi, (2010) *Bone*, **46,** 281-5. [3]W. Wang, K. Itaka, S. Ohba, et al (2009) *Biomaterials*, **30,** 2705-15.

ACKNOWLEDGEMENTS: David Stirling (UWS) & Margaret Mullin (GU).

Microparticles as building blocks for tissue engineering

KA Luetchford[1], JB Chaudhuri[2], PA De Bank[1]

[1] Department of Pharmacy and Pharmacology, University of Bath, UK. [2] Department of Chemical Engineering, University of Bath, UK.

INTRODUCTION: In vivo, the extracellular matrix provides cells with a scaffold, providing mechanical strength as well as biochemical cues. When approaching the challenge of artificially recreating organs in vitro, it is necessary to supply cells with an alternative matrix. This work explores the use of microcarriers produced from blends of silk fibroin (SF) and gelatin (G) as cell scaffolds. Silk is a material of interest for bone tissue engineering because of its strength, biocompatibility and wide range of processing options. The use of small particles allows a 'bottom up' approach to assembling a tissue construct, by moulding the microparticles into a larger structure. The 'bottom up' approach facilitates the introduction of hierarchy within the final construct, for example by layering different microparticles carrying different cell types.

METHODS: SF was extracted from the cocoons of *Bombyx mori* [1]. Briefly, the cocoons were boiled in 0.02 M Na_2CO_3 before rinsing in distilled water. The dried silk was dissolved in 9 M LiBr before dialysis against distilled water for two to three days. Type A gelatin was dissolved in water at 60°C, and maintained at 37°C before use. 3T3 fibroblasts were maintained in DMEM with 10% (v/v) fetal bovine serum, 100 U/mL penicillin and 100 µg/mL streptomycin, at 37°C in a 5% CO_2 atmosphere. A microfluidic flow-focussing device was used to process SF and SF/G blends into spherical microparticles. Cell adhesion to the particles was assessed by seeding $3x10^6$ cells with approx. 4000 particles in a volume of 500 µL, in agar-coated 24 well plates. Seeding efficiency was calculated by filtering the suspension and counting unattached cells after 24 hours. Confocal microscopy was used to obtain images of LIVE/DEAD stained cells on the microparticles.

RESULTS: Microparticles were produced from SF and gelatin blended volumetrically at ratios of 25:75, 50:50 and 75:25. Cells were successfully seeded onto all of the blended SF/G microparticles with high efficiencies (figure 1). Seeding efficiencies of the blended microparticles were significantly higher than for SF alone. Cell seeding and viability was confirmed using confocal microscopy (figure 2). A high proportion of cells remained viable after culture on the SF/G microparticles.

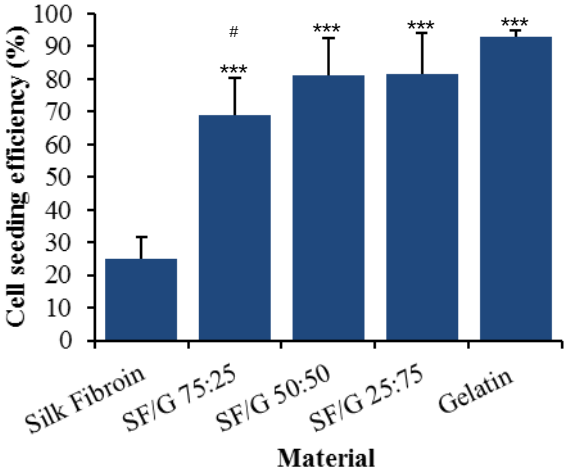

*Fig. 1: Seeding efficiency (percentage of cells seeded adhered to microparticles) of SF, SF/gelatin and gelatin microparticles. Bars show mean + standard deviation, n=5. *** $p<0.001$ versus SF alone. # $p<0.05$ versus gelatin.*

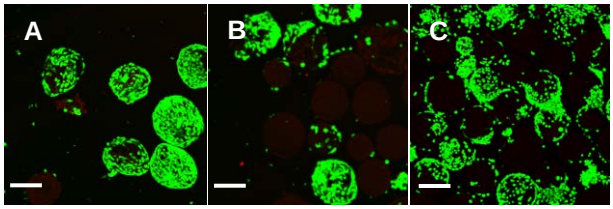

Fig. 2: 3T3 fibroblasts seeded on A) SF/G 75:25, B) SF/G 50:50 and C) SF/G 25:75, stained with LIVE/DEAD to indicate viability. Scale bar represents 200 µm.

DISCUSSION & CONCLUSIONS: Fibroblasts were successfully seeded on novel microparticles created from blends of SF and gelatin. This work creates a platform for the development of three-dimensional tissues, by moulding the cell carriers described here into macroscopic constructs. Including different combinations of cell types on the microparticles could prove an essential tool in the development of complex tissue constructs.

REFERENCES: [1] X. Wang, E. Wenk, A. Matsumoto, et al (2007). *Journal of controlled release* **117(3)**:360-370.

ACKNOWLEDGEMENTS: Funding from the MRC is gratefully acknowledged.

Designing peptide based biomaterials for influencing mesenchymal stem cell behaviour

A Macintyre[1], R Ulijn[2], K Burgess[3] and M Dalby[1]

[1] Centre for Cell Engineering, University of Glasgow, [2] West Chem, University of Strathclyde, [3]Metabolomics Facility, University of Glasgow

INTRODUCTION: Stem cells have two defining properties, the ability to differentiate and the capacity to undergo a process of self-renewal. Mesenchymal stem cells (MSCs) are derived from the bone marrow and are termed multipotent as they hold the potential to differentiate into a number of cell types.

Self-assembling peptide based hydrogels comprised of Fmoc diphenylalanine (FF) and Serine (S) have been discovered to self- assemble under physiological pH. The Fmoc group attached to the peptides aids in π-π stacking of these peptides which result in long nanofibres of Fmoc FF with Fmoc Serine.

This cell type is being studied as after a period of time in culture, the MSCs lose their defined stem cell properties. By culturing MSCs on a hydrogel mimicking the stiffness of bone marrow, we aim to maintain MSC multipotency in culture, as well as promote differentiation to a cell type corresponding to the stiffness of the hydrogel material and architecture.

METHODS: MSCs were isolated from human bone marrow and then positively selected for the MSC cell surface marker CD271. They were cultured upon Fmoc FF-S hydrogels with varying molarity. To detect gene expression on the hydrogels at given time points, qPCR was performed and metabolomics was employed alongside to provide insight into the cellular behaviour of the MSCs in response solely to the stiffness of their hydrogel substrate. The pre-hydrogel solution was imaged by TEM and SEM in order to analyse the fibre widths and nanofibre networking respectively.

RESULTS: A pool of hydrogels with stiffnesses ranging from 0.2 to 12 kPa has been created in order to mimic the elastic modulus of a variety of human tissues. The hydrogels aim to mimic the architecture of the extracellular matrix as the Fmoc peptides self assemble to form nanofibres, which are locked in a gelated state. MSCs can be cultured on the upper surface of the hydrogel (in 2D) or within the gels (in 3D). Fig.1 illustrates TEM and SEM imaging of a hydrogel, which corresponds to a stiffness of 0.2 kPa.

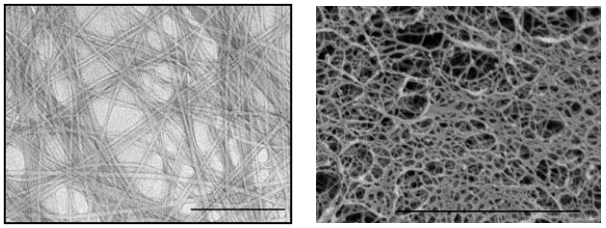

Fig. 1: TEM (A) and SEM (B) imaging of a hydrogel peptide solution which results in formation of a 0.2 kPa hydrogel. Fibre width is 21 nm in A and scale bar denotes 500 nm. In Image B, scale bar denotes 5 μm.

DISCUSSION & CONCLUSIONS: MSCs were cultured upon a 0.2kPa hydrogel and through qPCR found that the stem cell marker (CD271) was lost after day 1. The adipogenic marker PPARG was predominant at day 1, and expression diminished as time course continued. Therefore, the data suggests that adipogenic differentiation is occurring on this 0.2kPa gel, which correlates to the stiffness of this adipogenic tissue.[1] Metabolites were identified and normalised within samples and data illustrates an up regulation of metabolites found in amino acid and nucleotide metabolism at days 1 & 3, suggesting cells are active on this gel and differentiating. Lipid metabolism was explored as PPAR-γ was the predominant marker detected by qPCR and is associated with adipogenic differentiation. Therefore this hydrogel does not support MSC multipotency.

REFERENCES: [1]A.J Engler *et al* (2006) Matrix elasticity directs stem cell lineage specification Cell. **126**:677-89.

Culture of muscle derived cells from SOD1^{G93A} mice in monolayer and tissue engineered constructs

N.R.W.Martin[1], V.Mudera[2], K.Baar[3], L.Greensmith[4], M.P.Lewis[1]

[1] Musculoskeletal Biology Research Group, School of Sport, Exercise and Health Sciences, Loughborough University, UK. [2] Institute of Musculoskeletal Sciences, University College London, UK, [3] Division of Neurobiology, Physiology and Behaviour, University of California Davis, California, USA, [4] Sobell Department of Motor Neuroscience and Movement Disorders, University College London, UK.

INTRODUCTION: Amyotrophic lateral sclerosis (ALS) is a disease in which both the upper and lower motor neurons degenerate, leading to muscular atrophy, paralysis and death. Approximately 20% of familial ALS and 2% of all cases of ALS are caused by a mutation in the SOD1 gene. Transgenic mice expressing a mutant SOD1 gene express many characteristics of ALS, and are widely used to model this disease and further understand its progression (1).

Previously, we have created *in vitro* 3-D co-cultures of myotubes and motoneurons derived from rats, and showed interactions between the cells types indicative of early neuromuscular junction (NMJ) formation (2). We now aim to create a similar system that models ALS as a means of creating a test-bed for clinical screening of potential therapies for this disease. To this end, it was firstly necessary to obtain and culture muscle derived cells (MDCs) from mice expressing both endogenous and mutant human forms of the SOD1 gene, and determine if they can fuse to form multinucleate myotubes and be cultured in 3-D.

METHODS: Transgenic SOD1^{G93A} mice were maintained by breeding male heterozygous carriers with female (C57BL/66 SJL) F1 hybrids. The presence of the SOD1^{G93A} mutation was confirmed by PCR on DNA extracted from tail snips taken when pups (P0) were culled. Once culled, the hind limbs of each litter mate were removed and muscle dissected away from bone before being digested using 0.1% collagenase at 37°C to release MDCs. MDCs were plated at 2×10^5 per well in 12 well plates or 2×10^5 per 35mm dish and cultured in DMEM containing 20% Foetal bovine serum until confluence, and thereafter in DMEM containing 2% horse serum to induce differentiation.

RESULTS: Each pup yielded similar numbers of total MDCs between conditions, with 735,278 ± 330,423 cells isolated per SOD1^{G93A} pup compared with 935,889 ± 393,589 cells isolated per Wild type (WT) pup (n=9 per group). Similarly, there were equivalent levels of myoblast fusion between conditions, as morphologically there was the appearance of multinucleate myotubes in both conditions 3 days after the media was changed to induce differentiation (see fig. 1).

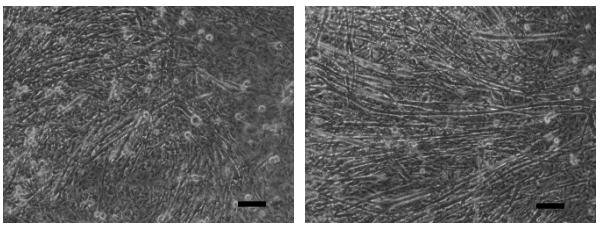

Fig. 1: Extensive myotube formation is evident in muscle derived cells from both WT (left) and SOD1^{G93A} (right) mice.

MDCs from both WT and SOD1^{G93A} mice have been cultured in preliminary experiments on fibrin based hydrogels, and show survival and self-assembly of the constructs to form 3-D constructs.

DISCUSSION & CONCLUSIONS: MDCs from mice expressing mutant SOD1 transgene can be successfully isolated and cultured *in vitro*, in both monolayer and in engineered fibrin constructs. This forms the first step in developing a test bed for future ALS research. Further work will attempt to optimise these cultures and subsequently co-culture the myotubes with mutant SOD1 expressing motoneurons.

REFERENCES: [1] P.McGoldrick, P.I.Joyce, E.M.C.fisher et al. (2013) *BBA-Mol Basis Dis* In Press. [2] S.L.Passey, A.S.T.Smith, N.R.W.Martin et al. (2012) *Eur Cells Mater* 23 Suppl. 4 pp21.

ACKNOWLEDGEMENTS: The authors wish to thank J.Dick and CH.Lu for maintenance of the SOD1^{G93A} colony. This research was funded by NC3R's grant code G0900762.

Tissue models for studying host-parasite interactions with salmon lice *Lepeophtheirus salmonis* (Copepoda, Caligidae)

HC McDonald[1], AP Shinn[1], K Thompson[1], KF Muir[1], SJ Monaghan[1], CM McNair[1], JE Bron[1]

[1] *Institute of Aquaculture, University of Stirling, Stirling, FK9 4LA*

INTRODUCTION: The parasitic copepods known as salmon lice cause serious problems in salmon aquaculture, which have a detrimental economic impact. These crustacean ectoparasites infect salmonids, attaching to hosts and feeding on host surface mucus, which can result in large lesions appearing on the surface of infected fish and in fish mortality. A range of existing strategies have provided some control of the parasite, but a better, environmentally friendly approach would be vaccination that could be used commercially to prevent/minimise infection. Current studies of parasite-host interactions require the use of fish but it would be ideal to develop a method that could reduce the number of animals used. Available fish tissue culture methods have proven unsuitable for the maintenance of the infecting copepodid stage and promotion of moulting to the next stage. Previous attempts [(1)] found that, although the sea lice attached to artificial tissue, moulting did not occur and grazing extensively damaged the tissues.

This PhD project aims to develop *in vitro* tissue models (including skin / epithelial analogues as well as perfused and non-perfused explants from Atlantic salmon (*Salmo salar*) and rainbow trout (*Oncorhynchus mykiss*)) that may be used to examine host-parasite interactions and which could also serve to reduce the use of animals in research for this and other salmonid diseases.

METHODS: It has been proposed that using scales with attached epithelium, either as part of an artificial tissue or as an explant, could provide the support and stability needed for maintenance of sea lice. However, there have been limited studies into culture from scales or culturing of scale-associated cells [(2,3,4)], so primary investigations into culturing from Atlantic salmon scales were carried out, looking at different conditions for optimal culture. For this, individual scales were taken from both seawater and freshwater Atlantic salmon, plated in plastic tissue culture dishes in a range of states with EMEM and incubated under CO_2 conditions. For studies into different scale location sources, the same protocol was used but scales from 4 distinct areas of the fish were investigated: caudal, midline, pectoral and dorsal.

RESULTS: Results from the initial trials suggested that individual scales (no coverslips) performed more successfully in culture than those in a non-coated glass coverslip sandwich. In these wells, outgrowth of new epidermal cells was observed after 24 hours and showed good adherence of both the scale and new cells to the plate. After 48 hours, the new outgrowth of cells surrounded the scales, whereas wells with coverslip sandwiches had no new cells. From subsequent experiments, it has been suggested that placing multiple scales per well aids outgrowth of new cells and by comparing different areas of the fish, it was suggested that scales from the dorsal and caudal regions of the fish provided better outgrowth of new cells than others.

DISCUSSION & CONCLUSIONS: From initial results, the use of scales as explants or as part of an artificial tissue seems promising and experiments are continuing to optimise the culturing of cells. The conditions needed for sea lice maintenance must also be taken into account to determine the ideal conditions needed and whether it is possible for moulting to occur. When a potentially viable culture technique is obtained, it can be used to maintain sea lice and can be altered to provide optimum conditions for investigation into host responses..

REFERENCES: R. Butler (2000) PhD Thesis, University of Stirling. [2]K. Akimoto *et al.* (2000) Zoological Science, **17**(1): 61-63. [3]R. Matsumoto *et al*. (2007) Cell and Tissue Research, **327**: 249-265. [4] S. Rakers *et al*. (2011) European Journal of Cell Biology, **90**: 1041–1051.

ACKNOWLEDGEMENTS: This PhD is funded by TSB as part of the work being undertaken for the development of a novel sea louse vaccine.

Age-associated loss of fibroblast differentiation is rescued by microRNA-7 inhibition

AC Midgley[1], T Bowen[1], AO Phillips[1], R Steadman[1]

[1] *Institute of Nephrology, Institute of Molecular & Experimental Medicine, School of Medicine and Cardiff Institute of Tissue Engineering & Repair, University of Cardiff, Heath Park, Cardiff, CF14 4XN, Wales, UK*

INTRODUCTION: During wound healing the remodelling of the extracellular matrix and restoration of tissue integrity are essential steps. Fibroblasts are central to this and when activated by Transforming Growth Factor-β1 (TGF-β1), they differentiate into α-smooth muscle actin-positive, contractile myofibroblasts (1) responsible for wound closure and scar formation. We have previously shown that aging fibroblasts are resistant to myofibroblast differentiation, through the loss of hyaluronan (HA)-dependent modulation of CD44 interaction with epidermal growth factor receptor (EGFR) (2).

MicroRNAs are small 18-23 nucleotide RNA molecules that function as regulators of gene expression. The microRNA, miR-7 has been shown to regulate EGFR expression and functionality (3, 4). Whether or not miR-7 is implicated in age-associated loss of EGFR and fibroblast differentiation is not yet known. Our hypothesis is that age-related miR-7 upregulation may be central to the loss of the HA-dependent EGFR signalling pathway.

METHODS: Young (P6-8) and aged (P14-15) fibroblast cells were cultured and transiently transfected with pre-miR-7 and miR-7 LNA respectively before further analysis.

To determine EGFR promoter activity, cells were transfected with the firefly luciferase plasmid; PGL3basic containing a 200bp EGFR promoter insert. Co-transfection of a renilla luciferase-containing plasmid was used for data normalisation and to determine transfection efficiency.

RT-PCR and QPCR were used to evaluate miRNA and mRNA expression of cells. Western blotting was used to assess the expression of EGFR protein and immunocytochemistry was used to stain for α-SMA.

RESULTS: Age-associated loss of EGFR was on both the genetic and protein levels. The activity of the EGFR promoter was not significantly different between young and aged fibroblasts and therefore it was hypothesised that there was an additional factor responsible for the loss of EGFR mRNA and protein, and receptor expression.

In silico analysis identified the highly conserved seed site for miR-7 on the 3'UTR of the EGFR mRNA; upregulated levels of miR-7 reflected the downregulated EGFR mRNA present in aged fibroblasts. Through miR-7 overexpression in young fibroblasts we were able to produce results similar to those observed in aged fibroblasts. The inhibition of miR-7 in aged fibroblasts was able to significantly induce EGFR mRNA and protein. Additionally, in response to TGF-β1 treatment, there was successful upregulation of α-SMA fibril formation and α-SMA mRNA, indicating differentiation to myofibroblasts.

DISCUSSION & CONCLUSIONS: In this study we show that miR-7 affects the cellular expression and functionality of EGFR implicating a role in the cellular resistance to differentiation. Through transient transfection of pre-miR-7 we were able to demonstrate the consequences of miR-7 suppression of EGFR. In addition, we demonstrated that inhibition of miR-7 can rescue the differentiation response in aged fibroblasts. This report highlights how miR-7 can regulate the TGF-β1-mediated mechanism central to differentiation and wound healing and identifies a possible therapeutic target for promoting the wound healing of chronic non-healing wounds in the elderly.

REFERENCES: [1] G. Gabbiani (2003) *J Pathol*, **200**:500-3. [2] A.C. Midgley, M. Rogers, M.B. Hallett, et al (2013) *J Biol Chem*, In press. [3] B. Kefas, J. Godlewski, L. Comeau, et al (2008) *Cancer Res*, **68**:3566-72. [4] X. Li and R.W. Carthew (2005) *Cell*, **123**:1267-77.

ACKNOWLEDGEMENTS: This research wa funded by RiA and AgeUK grant awarded to AM and RS. The authors thank Kidney Wales Foundation for financial support.

Alterations to sub-lamellar corneal collagen organisation in an in-vivo animal model of microwave keratoplasty

SR Morgan[1], S Hayes[1], J Hiller[2], NJ Terrill[2], Y Nakai[3], O Hieda[3], S Kinoshita[3], A Quantock[1], C Boote[1], KM Meek[1]

[1]School of Optometry and Vision Sciences, Cardiff University, Wales. [2]Diamond Light Source Ltd, Didcot, United Kingdom. [3]Ophthalmology, Kyoto Prefectural University of Medicine, Kyoto, Japan.

INTRODUCTION: Microwave keratoplasty is an emerging thermo-refractive procedure for correcting mild to moderate myopia and treating corneal ectasia. The method works by applying microwave energy to an annulus of tissue in the anterior stroma of the corneal mid-periphery, causing frictional heating and raising stromal collagen to axial shrinkage temperatures. This results in localised shrinkage of anterior mid-peripheral lamellae and central corneal flattening. However the potential effects of the treatment on collagen structure at the sub-lamellar level have not yet been evaluated. The current study was designed to assess ultrastructural changes to the stromal matrix following the procedure in an in-vivo rabbit model.

METHODS: Under anaesthesia, 4 adult NZ White rabbits received 915 MHz of unilateral microwave treatment as a 3.8mm (inner) to 4.3mm (outer) diameter annulus with a Vedera KXS machine (Avedro Inc. USA). Untreated contralateral eyes served as controls. Animals were euthanized after 3 weeks by intravascular injection of pentobarbital sodium and the corneas harvested and fixed in 4% paraformaldehyde to preserve collagen ultrastructure. Small-angle x-ray scattering (SAXS) was carried out using Beamline I22 at the Diamond Light Source, Didcot, UK. SAXS patterns were recorded at 0.25 mm intervals along linear scans across each specimen from limbus to limbus, using a 6 m long x-ray camera and monochromatic x-ray beam with wavelength 0.1 nm and cross-sectional diameter 0.2 mm (Fig. 1).

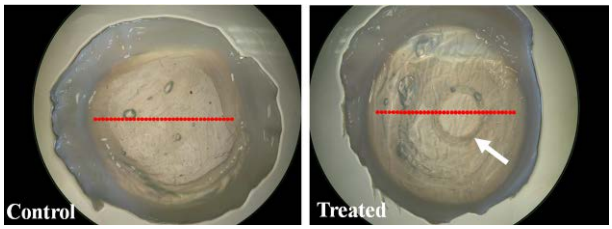

Fig. 1: X-ray beam sampling locations (red circles) on control (left) and microwave treated (right) rabbit corneas. The microwave region is visibly demarcated in the treated specimen (arrow).

Data analysis provided quantitative profiles of collagen fibril spacing, diameter, axial period and spatial disorder index at 0.25 mm intervals across each corneal specimen.

RESULTS: Microwave treatment did not produce significant measurable change in intra-fibrillar parameters (fibril diameter, axial D-period), while inter-fibrillar measures (fibril spacing, spatial order) were markedly altered (Table 1). These modifications were confined to the microwave treated region, which also exhibited a discernible increase in opacity. The absence of significant change in diameter and axial period in the treated tissue may be due to the fact that these parameters become un-measurable by SAXS as a result of fibrils becoming thermally denatured in the anterior, radiation-affected, portion of the tissue.

Table 1. Comparison of collagen fibril disorder, spacing, diameter and axial D-period within the treatment annulus and corresponding location in controls.

Fibrillar parameter	Control (n=3) mean (±SD)	Treated (n=4) mean (±SD)	P-value
Disorder (a.u.)	18.75 (±0.14)	25.36 (±1.56)	0.004
Spacing (nm)	62.96 (±0.33)	66.39 (±3.02)	0.110
Diameter (nm)	39.45 (±0.29)	38.75 (±0.45)	0.069
D-period (nm)	66.24 (±0.04)	66.16 (±0.07)	0.109

DISCUSSION & CONCLUSIONS: Microwave keratoplasty may impact on peripheral vision by introducing spatial disruption of stromal collagen that results in localised corneal opacity in the microwave treatment area. Loss of fibrillar structure and order within the treated tissue could also have further implications for corneal biomechanics and shape.

Engineering of microfluidic chambers for high throughput compound screening in neuromuscular cell biology

E. Matas[1], C. Jenkins[1], A. De La Iglesia[2], X. Tonellier[2], S. Marson[2], D. Player[3], N.R.W. Martin[3], M. P. Lewis[3] and S. Cellek[1]

[1]Cranfield Health, Cranfield University, UK; [2]School of Applied Sciences, Cranfield University, UK; [3]School of Sport, Exercise and Health Sciences, Loughborough University, UK

INTRODUCTION: There is an unmet need to engineer cell-based assay technologies that can quantify axonal and neuromuscular junction biology in high throughput formats. Our aim was therefore to develop a microfluidic chamber in a multi-well well format to study axonal growth and neuromuscular junction formation.

METHODS: A photolithographic technique using epoxy-based resin SU-8 was used to mould the microfluidic device with poly-dimethylsiloxane (PDMS), a biocompatible, optically transparent polymer. The PDMS device was covalently bonded on a glass slide. In one of the channels of the microfluidic chamber a human neuroblastoma cell line (SH-SY5Y) was cultured in Dulbecco's Modified Eagle Medium (DMEM) containing D-glucose (1g/L), L-Glutamine (580 mg/ml), foetal bovine serum (10%), 10,000 units/ml penicillin, 10 mg/ml streptomycin and differentiated by treatment with retinoic acid to model human neurones. In the opposite channel of the chamber human primary skeletal muscle cells were cultured in DMEM containing D-glucose (4.5g/L), L-Glutamine (580mg/L), sodium pyruvate (110mg/L), sodium bicarbonate (3.7g/L), 20% foetal bovine serum, 10,000 units/ml penicillin and 10 mg/ml streptomycin.

RESULTS: We have identified the optimum conditions required to grow and differentiate human neuroblastoma cells and grow human primary skeletal muscle cells in the microfluidic devices manufactured. We have also identified the optimum dimensions of the channels and the microgrooves that will allow the single axonal growth but prevent the migration of the cell bodies. In the figure below, growth of a single axon through one of the microgrooves can be observed.

DISCUSSION & CONCLUSIONS: PDMS substrate has allowed us to test several different dimensions and configurations in order to identify the optimum conditions and design. Our aim is now to adapt this optimum design into a multi-well format which can then be utilised for high throughput compound screening. It is envisaged that such a technology to study axonal and neuromuscular biology in a high throughput format will enable us to interrogate known targets and identify novel compounds and targets for diseases such as spinal cord injury in a relatively short period of time.

ACKNOWLEDGEMENTS: This project is fully funded by Dr Hadwen Trust for Humane Research (DHT) which is the UK leading medical research charity that funds and promotes exclusively human-relevant research that encourages the progress of medicine with the replacement of the use of animals in research.

Osteogenesis of Mesenchymal Stem Cells by Nanoscale Mechanotransduction

Habib Nikukar,[1, 3] Stuart Reid,[2] Monica P. Tsimbouri,[1] Mathis O. Riehle,[1] Adam S. G. Curtis,[1] and Matthew J. Dalby[1]

[1]Centre for Cell Engineering, Institute for Molecular, Cell and Systems Biology, College of Medical, Veterinary and Life Sciences, University of Glasgow, Glasgow G12 8QQ, United Kingdom. [2]SUPA, Thin Film Centre, University of the West of Scotland, Paisley PA1 2BE, United Kingdom, and [3]Shahid Sadoughi University of Medical Sciences, Yazd, I. R. Iran.

INTRODUCTION: It is likely that mesenchymal stem cells will find use in many autologous regenerative therapies. However, our ability to control cell stem growth and differentiation is presently limited. Here we give a first demonstration of using nanoscale sinusoidal mechanotransductive protocols (10-14 nm displacements at 1 kHz frequency), "nanokicking", to promote osteoblastogenesis in human mesenchymal stem cell cultures[1].

METHODS: By developing a simple protocol for the stimulation of cells in nanoscale Z-axis where Piezo actuators were connected to cell culture dishes allowing controlled vertical displacements (Figure 1). Human mesenchymal stem cells seeded at 10^4 cells per dish. After 4 hours seeding and cell settlement, the cells were stimulated for 24 hours, 1 week, and 2 weeks with 10 nm displacements at 500 and 1000 Hz. PCR, immunofluorescence and gene microarray were used to assess osteogenesis.

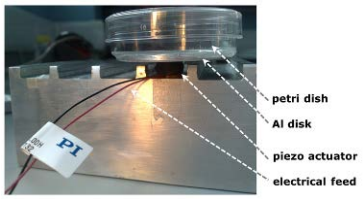

Fig 1. Mechanical nanostimualtion set up showing aluminium block to ensure displacement is transferred upwards, Al coin under the petri dish to ensure faithful transfer of mechanical signal across the base of the petri dish and piezo ceramic used to provide 10 nm high displacements.

RESULTS: Data demonstrated high levels of osteogenesis at 1000 Hz and less osteogenesis at 500 Hz. Array data showed that gene grouping were similar between cells stimulated at 500 and 1000 Hz suggesting a signalling threshold point between these two frequencies where osteogenesis is initiated. Arrays implicated a role for RhoA as being central to osteoblastic differentiation in agreement with materials-based strategies e.g.[2]. We validated this with pharmacological inhibition of RhoA kinase (Figure 2).

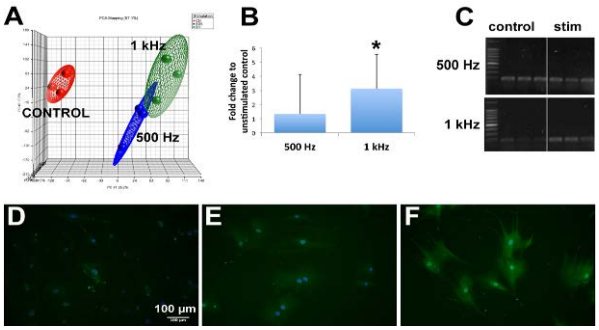

Fig. 2: Transcriptional analysis: (A) Microarray principle component analysis showing large shifts of gene regulation from MSCs on control after 1 week of culture. (B) PCR of BMP2 expression showing increased expression in response to 1 kHz stimulation but not 500 Hz after 24h of culture. (C) PCR showing similar RUNX2 expression between control and 500 Hz stimulation, but up-regulation after 1 kHz stimulation for 1 week. Looking at protein expression of the osteoblast marker, osteocalcin, after 14 days showed increased expression in response to 1kHz stimulation (F) compared to control (D) and 500 Hz (E) (green = osteocalcin, blue = nucleus).

DISCUSSION & CONCLUSIONS: Human MSCs are responsive to vertical nanoscale mechanical excursions. This osteoblastogenic response was ROCK-dependent, in agreement with previous materials-based strategies for osteoinduction. It is easy to envisage up-scale of such simple protocols to allow development of large scale osteoblast bioreactors.

REFERENCES: [1]. Nikukar, H. *et al.* Osteogenesis of Mesenchymal Stem Cells by Nanoscale Mechanotransduction. *ACS nano* **7**, 2758–2767 (2013).

[2]. McBeath, R. *et al.* Cell shape, cytoskeletal tension, and RhoA regulate stem cell lineage commitment. *Developmental cell* **6**, 483–95 (2004).

ACKNOWLEDGEMENTS: Thanks to all the members of CCE, the Iranian Ministry of Health for funding HN and BBSRC, EPSRC and MRC for funding MJD.

Transferable cell micro-patterns for hydrogel engineering in Three-Dimensions

Rebeen H. Othman*, Disheet A. Shah, Lee D. Buttery,
Kevin M. Shakesheff and James E. Dixon

Wolfson Centre for Stem Cells, Tissue Engineering, and Modelling (STEM), Centre for Biomolecular Sciences, School of Pharmacy, University of Nottingham, Nottingham, UK

INTRODUCTION: Correct cell organisation and patterning within three-dimensional (3D) matrices is a major goal for authentic tissue engineering and in applications for regenerative medicine. We describe a novel method to micro-pattern cells on thermo-responsive surfaces and directly transfer these to hydrogels. This transfer (with downstream manipulation of the patterned hydrogel sheets) allows 3D cell patterning at microscopic resolution with a macroscopic scale. We demonstrate fabrication of thermoresponsive culture substrates by coating poly(N-isopropylacrylamide) (PNIPAAm) on non-tissue culture polystyrene (NTCP) dishes. In addition, the use of micro-stencils for selective deposition of foetal calf serum (FCS) or extracellular matrix (ECM) proteins creates a selective surface for cell interaction[1]. Cells attach at 37°C and the entire pattern can be released by decreasing temperature below 32°C (lower than the critical solution temperature [CST] of PNIPAAm)[2]. By overlaying and crosslinking a variety of hydrogels before detachment we were able to faithfully transfer all patterned cells to hydrogels and encapsulate these to allow the production of 3D patterned structures.

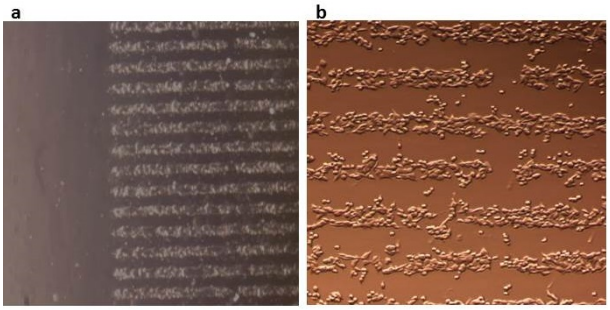

Fig. 1: Bright field images of micro-patterns on PNIPAAm-coated NTCP dish. a) FCS micro-patterns on PNIPAAm-coated NTCP dishes after airbrushing and 20mins attachment, (area is 1mm^2) b) 20mins post-seeding with NIH3t3 cells (area is 0.5mm^2)

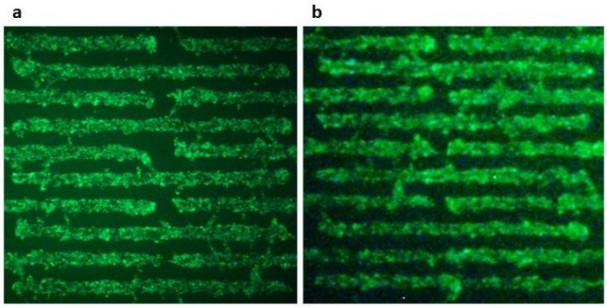

Fig. 2: Fluorescent Images of GFP-labelled NIH3t3 cells micro-patterns a) Cells after culturing o for 50 minutes at 37°C b) Alginate hydrogel with the patterned cells after direct transferring from PNIPAAm-coated micro-patterned surface (area is 0.75mm^2).

METHODS: NTCP dishes were successfully coated with poly(N-isopropylacrylamide) by airbrushing aerosols of the polymer. Then, FCS or ECM proteins were micro-patterned using micro-stencilling technology we have previously described[1]. Genetically labelled NIH3t3 cells[1] were cultured on the substrate at 37°C. Hydrogels were directly overlaid on the pattern and crosslinked. To detach patterned hydrogels surfaces were incubated sub-CST of PNIPAAm and removed.

RESULTS: NIH3t3 cells attached to FCS/ECM-adsorbed regions on the PNIPAAm-coated plates and cell patterns are faithfully achieved (Fig 1, 2a). and transferred to thin layer of alginate film (Fig 2b).

DISCUSSION & CONCLUSIONS: Here we demonstrate a powerful technique for rapid macro scale/micro-resolution cell patterning in which 2D patterns can be transferred to 3D matrices. Our technique is not only used for patterning of various cell types in different configurations (such as those in our previous study[1]) and transfer to sheets of hydrogels, but also as a tool for patterning cells within more complex geometries. This approach could be useful for construction of 3D tissues with multiple cell layers and will allow more biologically relevant hydrogel constructs to be fabricated.

REFERENCES: [1] Paik, et al. (2012) *Biotech Bioeng* **109**:2630-41. [2] Nash, et al. (2012) *J Materials Chemistry* **22**:19376-89.

3D Micro-Printing of Nerve Guides for Peripheral Nerve Repair

CJ Pateman[1], R Plenderleith[2], M Daud[1], A Harding[3], C Christmas[3], F Boisannade[3], S Rimmer[2], F Claeyssens[1] & JW Haycock[1]

Departments of [1]Materials Science & Engineering, [2]Chemistry and [3]Clinical Dentistry, University of Sheffield, UK.

INTRODUCTION: Nerve Guidance Conduits (NGCs) presently have a limited regenerative capacity, mainly due to the absence of physical guidance cues and materials, which do not ideally support the regeneration of injured neuronal and Schwann cell growth [1]. A need exists to fabricate more accurate NGC structures from more biocompatible materials to improve nerve regeneration following injury. The broad aims of this work are therefore to develop NGCs with improved bulk properties, physical design and surface chemistries to better support neuronal and Schwann cell growth, for surgical applications of nerve injury repair.

METHODS: The use of 3D structuring via laser stereolithography and micro-fibre electrospinning is reported for the fabrication of perineurial and epineurial mimicking scaffolds. Caprolactone, trimethylenecarbonate and polyethylene glycol pre-polymers were microwave synthesised, methacrylate functionalised and characterised by THF-GPC, MALDI-TOF, MS and NMR. Pre-polymers were UV cured into 2D sheets and 3D structures via stereolithography [2]. Electrospinning of aligned PCL was undertaken using condition previously determined for making 5µm parallel fibres inserted in to NGCs [3].

RESULTS: Characterisation revealed accurate reliable production methods. *In vitro* testing using neuronal, Schwann [4] and dorsal root ganglion culturing, cell viability testing and immuno-fluorescence labelling of ß-tubulin-III (for neuronal cells) and S100ß (for Schwann cells) demonstrating cellular adhesion and neurite outgrowth on these materials. Early *in vivo* implantation results of control microSL NGCs without lumen structures in to a mouse YFP common fibular model reveals axon regeneration which is equivalent to autograft. This work is continuing with the implantation of intraluminal - structured conduits.

DISCUSSION & CONCLUSIONS: In summary, photocurable degradable polymers with 3D structures have considerable potential for the manufacture of a new generation of NGCs, with improved physical, biochemical and biological properties.

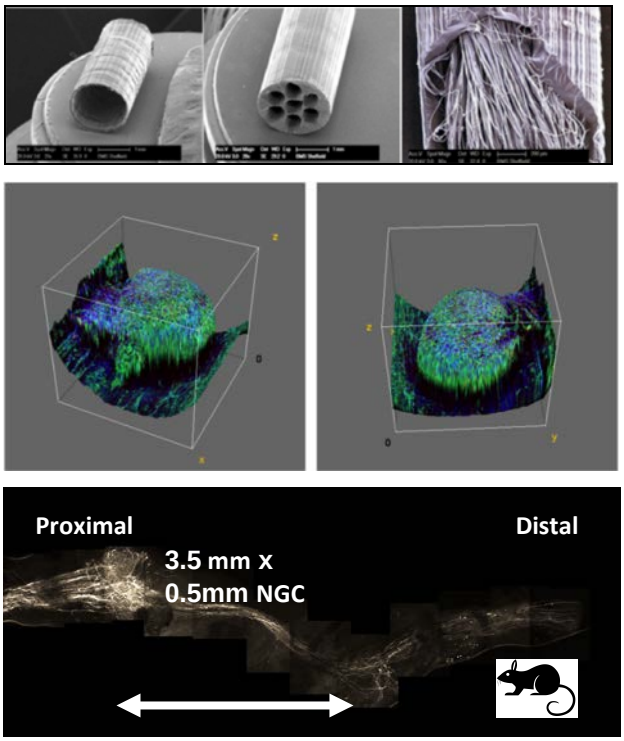

*Fig. 1: Prototype nerve conduits fabricated by microSL and electrospinning demonstrating an ability to manufacture devices with: **top left**) an internal diameter of 1.2mm and wall thickness of 50µm; **top centre**) parallel channel diameters of 250µm and **top right**) an outer conduit wall thickness of 200µm with parallel aligned fibres of 5µm diameter. **Middle**) 3D 2-photon microscopy of a DRG growing in vitro in an NGC. **Bottom**) In vivo axon regeneration through a microSL NGC in a mouse common fibular injury model.*

REFERENCES:

1. Bell JHA, Haycock JW (2012). **Tissue Engineering** 18(2): 116-128.
2. Koroleva A, Gill AA, Ortega I, Haycock JW, Schlie S, Gittard SD, Chichkov BN, Claeyssens F (2012). **Biofabrication.** (2012) 23;4(2):025005.
3. Daud MFB, Pawar KC, Claeyssens F, Ryan AJ and Haycock JW (2012) **Biomaterials** 33(25) 5901-5913.
4. Kaewkhaw R, Scutt AM, Haycock JW (2012). **Nature Protocols** 7: 1996-2004.

ACKNOWLEDGEMENTS: EPSRC for funding.

Developing a co-culture model of the small intestine using poly ethylene terephthalate fibre scaffolds

J D Patient[1], C Roberts[1] P Williams[1], A Ghaemmaghami[2], K Harris[3], C Tannergren[4], B Ambrahamson[4], FRAJ Rose[1]

[1] School of Pharmacy, University of Nottingham, Nottingham UK [2] School of Molecular Medical Sciences, University of Nottingham, Nottingham, UK [3]Astrazeneca, Alderly Park, Cheshire, UK [4]AstraZeneca, Mölndal, Sweden.

INTRODUCTION: Assessing drug permeability using cultured epithelial cells is fundamental during drug development. Current *in vitro* models of the intestinal tract fail to accurately simulate the dynamic 3D multicellular tissue environment. We hypothesize that a more complex *in vitro* model will allow for greater correlation between *in vitro* and *in vivo* drug and drug formulation performance. We have currently developed a co-culture model of intestinal epithelial cells (Caco-2) grown in co-culture with intestinal fibroblasts (CCD-18co) on 3D nano-scale poly ethylene terephthalate (PET) electrospun fibre scaffolds.

METHODS: Cell scaffolds with fibre diameters in the nanofibre range were manufactured by electrospinning 10% w/v PET dissolved in a 1:1 solution of dichloromethane and trifluoroacetic acid. Nanofibre scaffolds, secured in Snapwell™ cell inserts, were then utilised as a cell culture substrate.

CCD-18co cells were seeded at a density of $5x10^4$/0.2 mL on the underside of the nanofibre scaffold for 4 days. Subsequently $2x10^5$ Caco-2 cells were seeded on the top of the cell scaffold and cultured for 15-21days.

Samples were then fixed in formalin or 3% v/v glutaraldehyde and prepared for electron microscopy and immunocytochemistry.

RESULTS: Caco-2 and CCD-18co cells showed good attachment to the PET nanofibre scaffolds by scanning electron microscopy. Histological analysis of the co-culture revealed two distinct layers of cells either side of the polymer scaffold. Figure 2 illustrates the Caco-2 cells cultured on nanofibre scaffolds retained tight junction forming capability. Comparable staining for tight junction protein ZO-1 is visualised using fluorescence microscopy regardless of culture substrate.

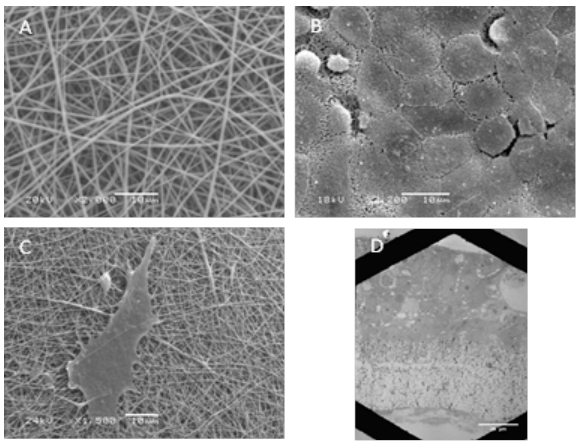

Fig. 1: Electron micrographs of A) nanofibrous polymer cell scaffolds for cell culture B) Caco-2 cells cultured for 21 days c) CCD-18co cells cultured for 2 days. D) Caco-2/CCD-18co co-culture after 21 days of culture

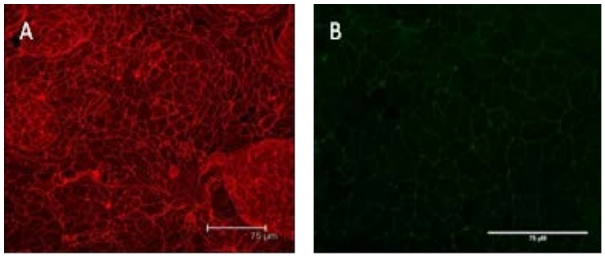

Fig. 2: ZO-1 staining for Caco-2 cells grown on A) nanofibre PET cell scaffolds and B) Transwell® cell culture inserts.

DISCUSSION & CONCLUSIONS: A protocol is now in place to culture intestinal epithelial cells alongside fibroblasts on 3D nanofibre PET scaffolds. We now seek to investigate whether such a model confers greater similarity with the in-vivo epithelial barrier and whether data generated using this model provides greater correlation for drug and formulation development.

ACKNOWLEDGEMENTS: Funding from EPSRC (EP/I01375X/1) and AstraZeneca.

Study the effect of antibody density on binding strength with AFM

E. Pulleine[1], D. Marshall[2], M. Baradez[2], H.B.Yin[1]

[1] *College of Science and Engineering, School of Engineering, University of Glasgow, Glasgow, UK*

[2]*Department of Molecular and Cell Biology, LGC, Queens Road, Teddington, United Kingdom*

Email: e.pulleine.1@research.gla.ac.uk

INTRODUCTION: The current gold standard for diagnosis of cell type is fluorescently activated cytometery[1]. It is based on the binding of antibodies to antigen (CD markers) on cells. In order to understand the effect of antibody density on the binding strength, we have developed a method to control antibody and antigen binding density using a model horse radish peroxidase (HRP) and anti-HRP system. We further studied the binding strength using atomic force microscopy (AFM).

METHODS: Antibodies were immobilised on 5µm silica beads with oriented or randomly oriented configurations. Epoxy silanisation, followed by incubation with NTA-lysine gave a rich carboxyl surface coating. Antibodies were then immobilised at different densities using EDC/NHS methods, with different concentrations of antibodies. AFM was performed using these 5µm antibody functionalised silica beads as indenter probe. Adhesion was measured between these probes, two HRP surfaces and a PEG surface.

RESULTS: Figure 1 shows quantification of the amount of antibody attached on beads using tetramethylbenzidine (TMB) - HRP assay.

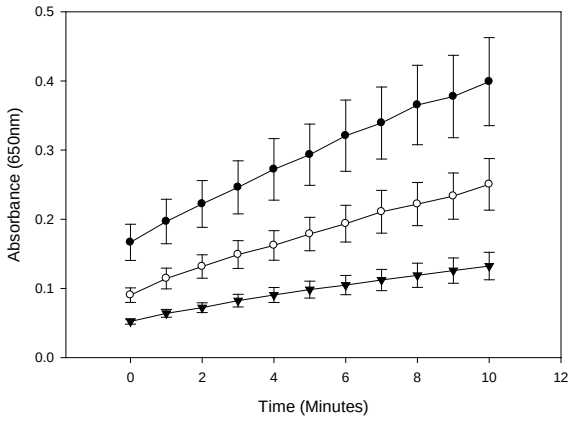

Fig. 1: Absorbance of TMB catalysis by HRP bound to anti-HRP functionalised beads. The beads were incubated with anti-HRP solutions at the concentrations of 2.5µg/ml (black circles), 0.25µg/ml (white circles) and 0.025µg/ml (black triangles).

Figure 2 shows the force required to remove anti-HRP functionalised beads (i.e. anti-HRP probe) from different surfaces: HRP surface, HRP with a polyethylene glycol (PEG) linker and a PEG surface.

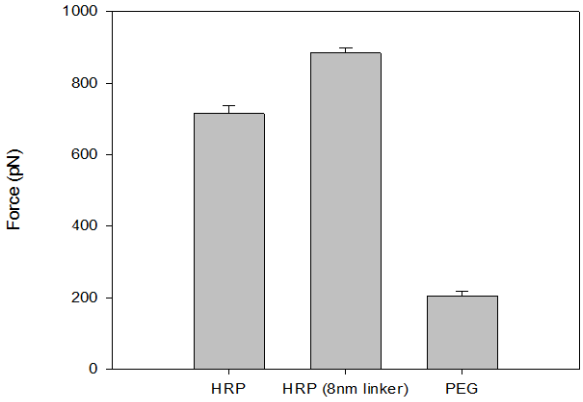

Fig. 2: Initial rupture force required to remove an anti-HRP probe from three different surfaces in PBS buffer (pH 7.4) .

DISCUSSION & CONCLUSIONS: As shown in Figure 1, the amount of anti-HRP bound to the functionalised beads increases with the increase of anti-HRP concentrations, indicating a simple way to control the density of antibodies on beads. The AFM force measurement illustrates the ability to differentiate between surfaces on the basis of adhesive strength. PEG surfaces are well known for their excellent protein resistance. This agrees well with the low adhesion force (~200 pN) between the anti-HRP probe and PEG surface found in this study. These results suggest a background force threshold could be identified that is associated with nonspecific binding. Further work will focus upon identifying individual binding events.

REFERENCES: Bonner, WA, Hulett, HR, Sweet, RG and Herzenberg, LA. Fluorescence activated cell sorting. Review of Scientific Instruments, 43(3):404–409, 1972.[1]

ACKNOWLEDGEMENTS: The authors would like to thank EPSRC and LGC for their financial help.

An alginate capsule for organotypic *ex vivo* chick femur segmental defect

O.Qutachi, Rebeen Othman, L.D. Buttery, K.M. Shakesheff

Wolfson Centre for Stem Cells Tissue Engineering and Modelling, Centre of Biomolecular Sciences, School of Pharmacy, University of Nottingham, Nottingham, U.K

INTRODUCTION: Although healing with normal bone fractures can be seen with no delay, however, a different scenario can be evident with segmental defect. Depending on the defect size impaired bone healing leaves a gap due to failure of bone bridging[1]. Promoting bone bridging can be studied by using alginate capsule containing defined combinations of cells and growth factor-loaded MPs (BMP-2 and /or TGF β3). In this study as a proof of concept, 3T3cells were mixed with fluorescently labeled MPs in an alginate gel capsule to bridge a segmental femoral defect in an ex vivo chick model.

METHODS: PLGA MPs were fabricated by the emulsion method in which 20% (w/v) PLGA polymer (52 kDa) in DCM was homogenized in 200ml of 0.3% PVA at 9000 RPM [2] [1]. The created MPs were vortexed overnight before harvesting via a series of by centrifugation (at 1500 rpm for 5 min and repeated 3 times with washing with distilled water. The MPs were freeze dried and stored at -20°C. The alginate capsule was prepared by mixing alginate gel (0.5, 1 and 2%) with 3T3 cells and PLGA MPs loaded with green fluorescent coumarin-6. The alginate gel / cell / MPs mixture was pipetted gently into a 135 mM calcium chloride solution to allow cross linking of the alginate gel. Different cell (66x 10^3 - 2.6x 10^6 cell/ml) and MPs (0.6-6mg/ml) concentrations were tested. The resultant cross linked gel were harvested and incubated in cell culture media for further 10 days.

RESULTS: Among the different alginate concentrations under test, the 2% appears to provide a reliable capsule with reasonable integrity that can withstand processing (Figure 1). In terms of cell/MPs distribution, 3.3mg/ml MPs and 1.33x 10^6 cell per ml showed a homogenous distribution within the capsule (Figure 2).

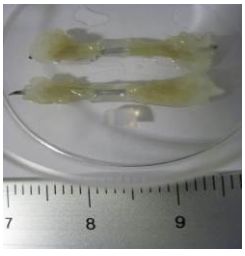

Fig. 1: Segmental defect for check femur with 2% cross-linked alginate capsule fitted with a pin.

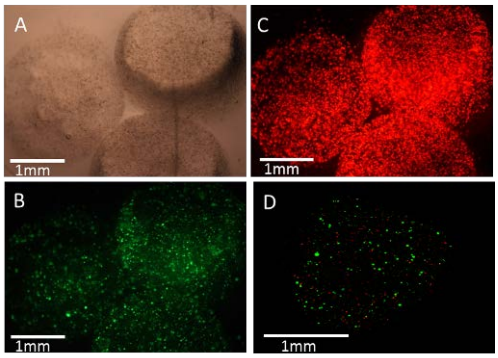

Fig. 2: Alginate capsule containing 3.3mg/ml MPs plus 1.33x 10^6 cell/ml. A-bright field image; B- Green fluorescence showing MPs labelled with Coumarin-6; C-Red fluorescence showing 3T3mr cells. D- merged confocal image for cells and MPs.

DISCUSSION & CONCLUSIONS: The alginate capsule provides the right consistency for handling with segmental defect. Homogenous distribution of cell and MPs as well as maintaining cell growth is expected to provide a reliable microenvironment for induced osteogenesis via an efficient material/cell/growth factors interaction. This model and approach can provide new insights into promoting healing of segmental defects in bone tissues. Future evaluation for the model is recommended.

REFERENCES: [1] Mills, L.A. and A.H. Simpson, *In vivo models of bone repair.* J Bone Joint Surg Br, 2012. **94**(7): p. 865-74. [2] Bible, E., et al., *Neo-vascularization of the stroke cavity by implantation of human neural stem cells on VEGF-releasing PLGA microparticles.* Biomaterials, 2012. **33**(30): p. 7435-46.

ACKNOWLEDGEMENTS: This work is funded by a BBSRC LoLa grant entitled "Combining stem cell science and tissue engineering to study the development and repair of human skeletal tissues" Grant No BB/G010617/1. Thanks to Dr. David Gothard from Bone & Joint Research Group, Institute of Developmental Sciences at University of Southampton for providing the chick femurs.

Protein binding functionalisation of plasma-derivatized silicone surfaces.

V Sharma [1], KA Blackwood[2], D Haddow[3] & JF Dye[1]

[1] RAFT Institute/UCL, UK. [2] RAFT Institute/Queensland University of Technology, AUS. [3] Altrika Ltd, UK

INTRODUCTION: A major concern related to large area wounds is loss of barrier function. Silicone is a versatile material for medical applications, but is essentially bio-inert. The ability to bind proteins will allow functionalisation of silicone surfaces which may benefit wound healing and other biocompatible medical device applications. This study aimed to characterise target protein binding to derivatised silicone surfaces.

METHODS: Silicone sheets were derivatized with acrylic acid (AcA) or oxygen (O2) by plasma polymerisation (supplied by Altrika). Non-blocked polystyrene wells (PS) without any discs were used as reference. Discs of silicone sheets with fibrinogen (5-250 µg/ml) were incubated in pre-blocked ELISA wells. In some cases, the silicone surfaces were crossed linked with 2% glutaraldehyde (GTA). Bound fibrinogen (FBG) was detected by using an ELISA system. Total protein was measured using Bradford Ultra reagent (Novexin).

RESULTS: Optimal primary and secondary antibody concentrations were determined and FBG binding affinity and capacity to PS, O2 & AcA surfaces determined. FBG-silicone binding curves were characterized by saturation at around 150 µg/ml to all types, with the highest binding to AcA. Binding for PS samples saturated at around 50 µg/ml. GTA cross linked FBG was detected by a polyclonal anti-fibrinogen antibody. From total protein measurements approximate values for FBG binding were 1.27 µg/mm^2 (all of the silicone surfaces); 0.74 µg/mm^2 (PS). Release of protein by trypsinisation and slot-blot assay provided an alternative estimate of total bound protein. Silicone surfaces show 2x protein binding capacity than PS but with lower affinity. Bound protein was not removed from either surface, but binding could be reduced by co-incubating with non-ionic surfactant.

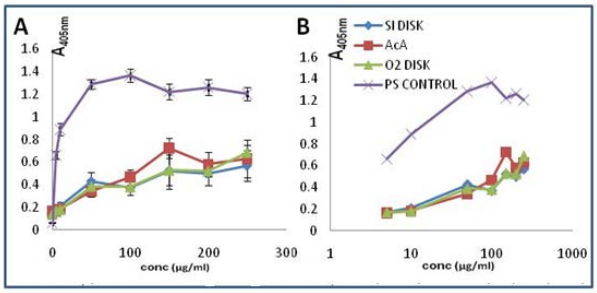

Fig. 1: ELISA characterisation of protein absorption on various silicone sheets coated with acrylic acid (AcA DISC), oxygen (O2 DISC) and non polymerized silicone (Si DISC). Non- blocked polystyrene wells without any discs were used as reference (PS CONTROL).

DISCUSSION & CONCLUSIONS: Silicone surfaces show nearly twice protein binding capacity than PS but with lower affinity. Currently, we are relating this to plasma resonance spectroscopic surface. Studies with surface extraction solutions to examine the robustness of this surface binding for practical functionalisation, and the effect of GTA crosslinking stabilisation are underway.

ACKNOWLEDGEMENTS: This work is supported by a TSB grant.

A novel, whole femoral head wash process produces an acellular, biocompatible and mechanically stable bone scaffold suitable for use in tissue engineering.

CA Smith[1], P Rooney[2], T Board[3], SM Richardson[1], JA Hoyland[1]

[1]Centre for Regenerative Medicine, Institute of Inflammation and Repair, The University of Manchester, [2]NHS Blood and Transplant, Liverpool, [3]Wrightington Hospital, Wigan

INTRODUCTION: Unlike "gold standard" autograft material, allografts are devoid of a viable osteogenic cell source. However the remaining marrow tissue may increase the risk of immune response and disease transfer whilst preventing proper infiltration by osteogenic cells. While sterilization of the allograft can improve graft safety, it may alter the biocompatibility of the bone material. To overcome this, a novel wash process has been developed by the National Health Service Blood and Transplant (NHSBT) department which uses mechanical and chemical means to wash (sterilize) such material. This study aims to assess the biomechanical and biological properties of the washed bone and ascertain its use as a potential scaffold for bone tissue engineering.

METHODS: Fresh frozen femoral heads (n=13) were washed using a 14 stage process and wash solutions were subsequently assayed for DNA (Picogreen), soluble protein (Bradfords) and haemoglobin (Drabkins) content to assess removal from tissue. Fresh frozen and washed bone samples (n=5) were also assayed to assess DNA retention. Fresh frozen (N=5) and washed (N=6) bone was powdered, and used to condition media to assess biocompatibility. Mesenchymal stem cells (MSCs) were cultured in conditioned media for 24 hours, and cell viability (WST-1) and number (LDH) assessed. Seeding of $1x10^6$ MSC onto washed bone was undertaken to determine seeding efficiency, with the sustained vitality of cells tested by alamarBlue at time points: 0, 7, 14, 21 and 28 days. Uni-axial compression testing was conducted on $1cm^3$ bone cubes from washed and fresh-frozen material.

RESULTS: Washing of the bone removed 99.5% of immunogenic material. DNA content of the bone was reduced from 140ng/mg in fresh frozen to 16.4ng/mg in washed bone. Culture of MSCs with washed bone conditioned media caused no significant decrease in cell viability or number. In contrast fresh-frozen bone conditioned media caused a significant decrease in cell viability and cell number (Figure 1).

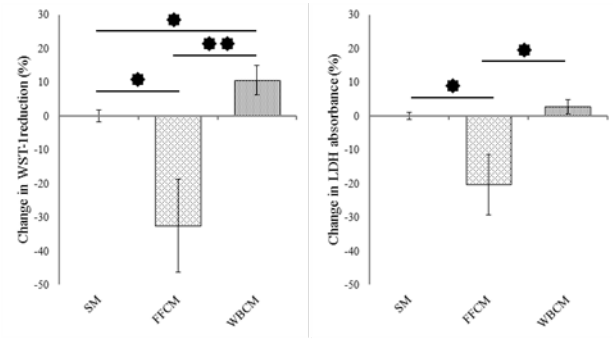

Figure 1: Histogram displaying the relative changes in cell viability and cell number (● $p \leq 0.05$, ●● $p \leq 0.01$)

MSC seeding onto washed bone demonstrated a cell retention efficiency of 91% after 60 minutes incubation, with alamarBlue indicating proliferation of MSCs on the bone over 28 days. Mechanical compression testing indicated no significant change in the strength of the washed bone compared to fresh frozen samples.

Discussion & conclusions: Utilization of the novel wash process resulted in an acellular material with no loss of biomechanical properties.
Unlike fresh-frozen bone, the washed bone was not cytotoxic and was able to support cell attachment and proliferation, suggesting the wash process removed cytotoxic agents found within the bone marrow of fresh-frozen bone allograft material. Importantly, this study indicates that washed allograft bone has potential as a scaffold in tissue engineering. Further research is being conducted to determine the latent osteoconductive and osteoinductive abilities of this matrix, and the effect the material has on osteogenesis of human MSCs.

ACKNOWLEDGEMENTS: Funding for this work was provided by the Wrightington Foundation and Joint Action.

Enhancement of skeletal tissue formation with dual growth factor release – evaluation in a novel *ex vivo* chick femur organotypic model

EL Smith[1], D Gothard[1], CA Roberts[1], JM Kanczler[1], LJ White[2], O Qutachi[2], KM Shakesheff[2], MM Stevens[3], ROC Oreffo[1]

[1]*Bone & Joint Research Group, Centre for Human Development, Stem Cells and Regeneration, University of Southampton.* [2]*The Wolfson Centre for Stem Cells, Tissue Engineering & Modelling (STEM), University of Nottingham.* [3]*Department of Materials and Institute for Biomedical Engineering, Imperial College London.*

INTRODUCTION: Development of alternative tissue engineering strategies to augment bone repair and regeneration is dependent on suitable animal models. *Ex vivo* model systems allow for more complex interactions to be studied while addressing the 3Rs, thus bridging the gap between simpler *in vitro* cell systems and complex *in vivo* models. We have developed a 3D *ex vivo* culture system of embryonic chick femora[1], adapted in this study to investigate effects of novel gel scaffolds containing growth-factor releasing microparticles and skeletal stem cells on bone repair and regeneration. Modification of the system to analyse older mature chick femurs, or combination with a chick chorioallantoic membrane (CAM) system to assess angiogenesis, further widens the potential of the model.

METHODS: Alginate/bovine ECM gel scaffolds[2] were loaded with PLGA/Triblock (10-30% PLGA-PEG-PLGA copolymer) microparticles[3], either small (20-30µm) loaded with 100ng/ml BMP-2, or large (50-100µm) loaded with 15ng/ml TGF-β3, to allow for slow or fast growth factor release respectively. Human serum albumin (HSA) was used as a control loading protein. Gel scaffolds were also loaded with human adult Stro-1 selected bone marrow stromal cells (BMSCs). Following cross-linking in calcium chloride, 2mm cylindrical gel segments were created and placed into 2mm central segmental defects in freshly isolated embryonic day 11 chick femurs. Chick femurs were placed into organotypic cultures for 10 days in basal media, and analysed by micro-computed tomography (µCT), and histologically for proteoglycan (Alcian blue) and collagen production (Sirius red), as well as expression of bone and cartilage markers (collagen I/II).

RESULTS: Cultured alginate/ECM gels loaded with HSA control protein, with or without BMSCs, displayed minimal matrix or expression of bone or cartilage markers. Addition of growth factor-releasing microparticles into the gel, either BMP-2 alone or a combination of TGF-β3 and BMP-2, increased Sirius red-stained matrix and collagen I / II expression within the gels, although the matrix was disperse and disordered. Addition of BMSCs into the gels containing BMP2-releasing microparticles resulted in a more structured bone matrix being deposited into the gel. This effect was significantly enhanced with addition of BMSCs to gels containing combined dual TGF-β3/BMP-2 releasing microparticles, with formation of a highly-structured bone matrix within the gels.

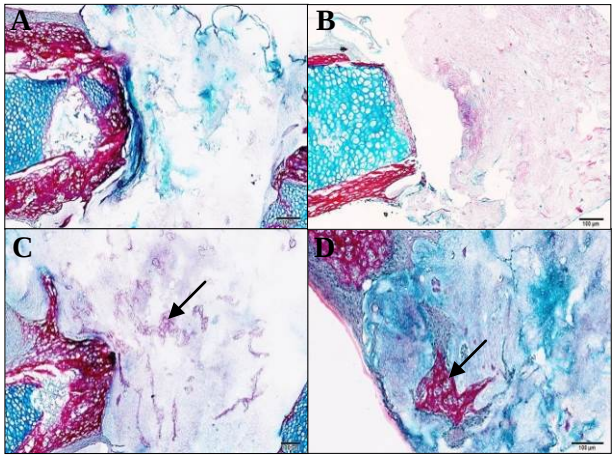

Fig. 1: HSA control gels demonstrated limited cell / matrix activity (A,B). TGF-β3/BMP2-releasing microparticles increased deposition of Sirius red stained bone matrix (C), and addition of Stro-1 BMSCs significantly enhanced deposition of highly structured bone matrix within gels (D).

DISCUSSION & CONCLUSIONS: This study demonstrates the successful use of organotypic chick femur cultures as a high-throughput test model for scaffold/cell/growth factor therapies for regenerative medicine. Temporal release of dual growth factors, combined with BMSCs, improve formation of a highly structured bone matrix compared to single release modalities.

REFERENCES: [1]J.M. Kanczler, E.L. Smith et al. (2012) *Tissue Eng Part C: Methods* **18**(10): 747-760. [2]M.J. Sawkins et al. (2013) *Acta Biomater* Epub Apr 24. [3]L.J. White et al. (2013) *Mater Sci Eng C* **33**(5): 2579-83.

ACKNOWLEDGEMENTS: This work was supported by the strategic longer and larger grant (LOLA) from the BBSRC, UK-grant number BB/G010579/1.

Tissue engineering a 3D culture model to investigate cellular responses to mechanical loading in spinal cord injury

JT Smith[1], RM Hall[1], JB Phillips[2], JL Tipper[1]

[1] *Institute of Medical and Biological Engineering, University of Leeds, Leeds, LS2 9JT*
[2] *Department of Life, Health and Chemical Sciences, The Open University, Milton Keynes, MK7 6AA*

INTRODUCTION: Spinal cord injury (SCI) affects approximately 1,000 people a year in the UK and up to 12,000 in the US [1]. The biological and biomechanical factors that might interfere with the regeneration of spinal cord tissue are not fully understood. This project aims to investigate the responses of specific spinal cord cell populations – neurons, astrocytes, microglia and oligodendrocytes, to tensile and compressive forces in both 2D & 3D culture. Tissue engineered constructs will be subjected to normal physiological loading and loads simulating trauma. The ultimate goal is to develop a cellular model of spinal cord injury using tightly controlled loads within defined laboratory environments to study the cellular response.

METHODS: In order to assess cell viability changes in response to mechanical loading, two cell viability assays were compared using the L929 fibroblast cell line before generating spinal cord models using neural cells. The sensitivity of the MTT and ATPlite assays in the detection of differences in cell concentration was assessed in a 96-well plate after 24 hours. The cells were seeded at concentrations ranging from $1x10^3$ to $1x10^6$ cell/ml, with a ten-fold increase between densities.

RESULTS: The absorbance profile for the ATPlite assay (Fig. 1) showed that the increase in cell concentration causes an increase in absorbance, as expected.

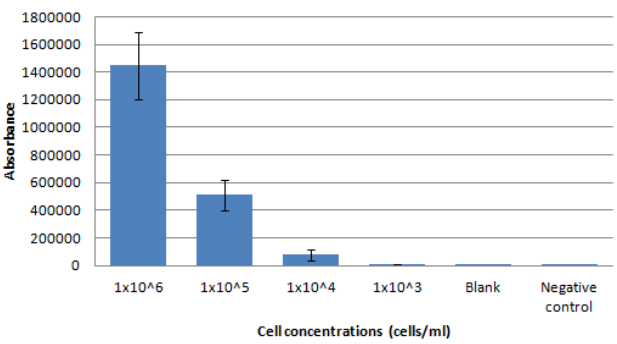

Fig. 1: ATPlite assay showing absorbance change in response to cell concentration.

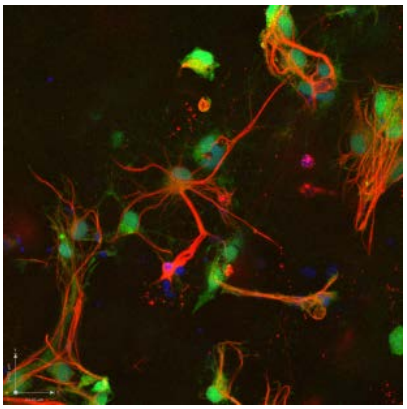

Fig. 2: Astrocytes in a 3D culture model labelled with GFP and stained for GFAP (red).

DISCUSSION & CONCLUSIONS: Using the L929 cell line, the ATPlite assay was found to be an effective measure for future assessment of changes in cell viability following mechanical loading of neural cells. Future work will combine cell viability assays with neural cell culture models (Fig. 2) in order to investigate differences in sensitivity of specific neural cell populations to mechanical loading scenarios.

REFERENCES: [1]The National Spinal Cord Injury Statistical Centre (2011) Spinal Cord Injury facts and figures at a glance. https://www.mscisc.uab.edu February 2011 [2]Short, D. J., Masry, W. S., Jones, P. W. (2000) High dose methylprednisolone in the management of acute spinal cord injury ± a systematic review from a clinical perspective. Spinal Cord **38** 273-286

ACKNOWLEDGEMENTS: This work was supported by the Institute of Mechanical and Biological Engineering at the University of Leeds and the EPSRC.

Comparison of senescence state of patient-matched bone marrow and adipose derived mesenchymal stem cells and its effect on multipotentiality

KL Swinton[1], JA Hoyland[1], SM Richardson[1]

[1] *Centre for Regenerative Medicine, Institute of Inflammation and Repair, University of Manchester, UK.*

INTRODUCTION: Mesenchymal stem cells (MSCs) are multipotent cells which can differentiate towards the osteogenic, adipogenic and chondrogenic lineages, therefore providing the opportunity to regenerate damaged and diseased musculoskeletal tissues. While bone marrow is a common source of MSCs (BM-MSCs), it has been shown that adipose tissue contains a high frequency of MSCs (AD-MSCs) and evidence, although conflicting, suggests a higher proliferative capacity and maximal lifespan compared with BM-MSCs. For clinical use, MSCs are required in large numbers; therefore *in vitro* expansion is necessary. However, it is not clear whether different sources of MSCs exhibit similar states of cellular senescence upon isolation. The focus of this study was to investigate the senescent state of patient matched BM-MSCs and AD-MSCs and its subsequent effect upon population kinetics and differentiation potential during *in vitro* expansion. Results will identify the optimal source and suitability of autologous cells in cell-based tissue engineering and regenerative medicine therapies for musculoskeletal diseases.

METHODS: Patient-matched BM and AD-MSCs (mean age 44; range 28-55 years), were expanded in monolayer with population kinetics assessed throughout the culture period. Cell senescence was assessed following isolation and during *in vitro* culture. Expression of pluripotency markers was also assessed using quantitative real-time PCR (qPCR). Multipotentiality of both BM and AD-MSCs was assessed by differentiation using established methodologies for 21 days. Osteogenic, adipogenic and chondrogenic differentiation was assessed using qPCR for standard lineage markers and histological staining.

RESULTS: Patient-matched BM and AD-MSCs initially demonstrated similar population kinetics (figure 1); however AD-MSCs reached a higher number of population doublings (PDs) compared to BM-MSCs which rapidly slowed in proliferation rate with extended time in culture. Expression of the senescence associated gene, $p16^{ink4a}$ was significantly higher in BM-MSCs at an early life span compared with AD-MSCs. Expression increased for both cell types with time in culture although continued to be higher in BM-MSCs. Conversely expression of the pluripotency marker, Nanog was consistently greater in AD-MSCs. BM-MSCs and AD-MSCs displayed similar differentiation potential along the chondrogenic, osteogenic and adipogenic lineages at early passage. However, with time in culture BM-MSCs showed a decline in their differentiation potential along all 3 lineages tested, while AD-MSCs appeared to retain their osteogenic and chondrogenic potential.

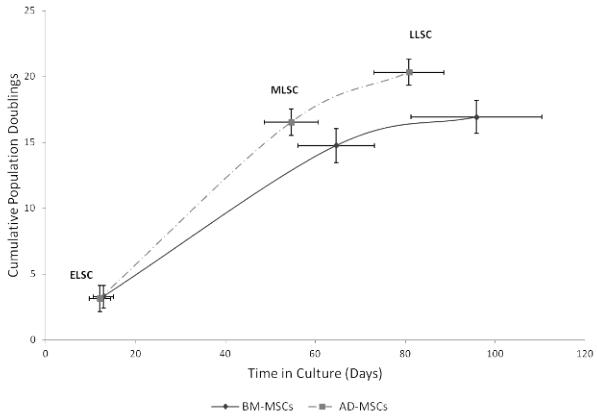

Fig. 1: Population kinetics analysis demonstrating significantly higher PDs over time in culture in AD-MSCs compared to BM-MSCs.

DISCUSSION & CONCLUSIONS: These results demonstrate that AD-MSCs have a higher proliferative capacity and undergo replicative senescence later than patient-matched BM-MSCs. AD-MSCs also demonstrated significantly lower expression of the senescence marker $p16^{ink4a}$ and higher expression of Nanog throughout culture and their multipotentiality appeared to be less affected by monolayer expansion. This data suggests that for autologous MSC therapies where *in vitro* expansion is required AD-MSCs may be the more appropriate cell population.

ACKNOWLEDGEMENTS: The authors wish to thank Research Council UK and Orthopaedic Research UK for funding this research, together with Mr. Tim Board and staff at Wrightington Hospital for the acquisition of samples.

Tissue engineered amniotic membrane substitute for drug delivery to the ocular surface

NS Tan[1], N Bedi[2], D Ossipov[3], J Hilborn[3], NL Tint[4], IF Uchegbu[2] and RA Brown[1]

[1] University College London, Tissue Repair & Engineering Centre, Institute of Orthopaedics & Musculoskeletal Science, Stanmore Campus, London, HA7 4LP, United Kingdom. [2]Department of Pharmaceutics, UCL School of Pharmacy, 29-39 Brunswick Square, London WC1N 1AX, United Kingdom. [3] Department of Chemistry-Angstrom, Angstrom Laboratory, Uppsala University, Lägerhyddsvägen 1, Box 538, SE-751 21, Uppsala, Sweden. [4] Moorfields Eye Hospital and UCL Institute of Ophthalmology, University College London, 11-43 Bath Street, London, EC1V 9EL, United Kingdom.

INTRODUCTION: Many infections and inflammatory conditions of the cornea require frequent and prolonged topical administration of medication due to poor drug penetration and high clearance rate. In addition to direct topical drug application, amniotic membrane (AM) patches have been used for adjuvant management of eye injuries or infections, however, the AM is biochemically variable, hard to handle and carries the risk of disease transmission. The aim here was to test the use of dense plastically compressed (PC) collagen, loaded with drug-encapsulated nanoparticles (NPs) as an AM substitute that may be utilised for ocular surface drug delivery.

METHODS: Quaternary palmitoyl glyol chitosan (GCPQ) nanoparticles (NPs) were prepared as previously reported [1]. In the first instance, nile red (NR) was encapsulated in GCPQ NPs, and hyaluronan was tagged with fluorescein isothiocyanate (FITC) for retention and distribution studies. Plastically compressed collagen scaffolds were prepared as previously described [2]. Collagen gels containing the GCPQ-NPs were subjected to PC, rapidly removing most of the fluid to form dense NP-loaded collagen scaffolds. Entrapment efficiency was determined by fluorometry following collagenase digestion of compressed constructs. Spatial distribution of hyaluronan-NP was determined by fluorescence microscopy of 8 µm sections of the constructs. The antibiotic, Sparfloxacin, was encapsulated in GCPQ for loading into scaffolds for drug release studies and to test their antibacterial activity.

RESULTS: Trapping efficiency of HA-NP was 18.5-31.1% depending on configuration. Similarly, the entrapment efficiency of chitosan (quaternary ammonium palmitoyl glycol chitosan (GCPQ)) nanoparticles loaded with nile red (NR) was 18.8-36.2%. GCPQ particles carrying a cargo of Sparfloxacin were used to test effective drug release by this system. Sustained release of active Sparfloxacin was demonstrated to be capable of killing target microorganisms.

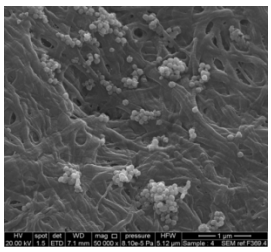

Fig.1: SEM micrograph of GCPQ-NR particles in a compressed collagen scaffold.

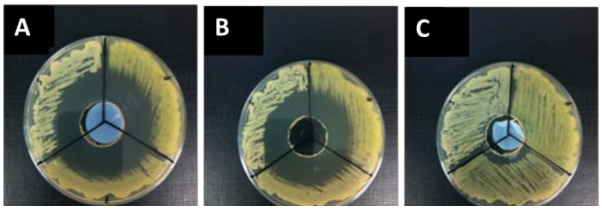

Fig. 2: Digital images demonstrating bacterial inhibition by GCPQ-Spar-loaded scaffolds 24 H post inoculation. A: GCPQ-Spar-loaded scaffold; B: 60 µg Sparfloxacin solution; C: Unloaded scaffold. For each petri dish, the left regions were inoculated with Staphylococcus aureus, the right with Pseudomonas aeruginosa and the bottom with Escherichia coli.

DISCUSSION & CONCLUSIONS: Thus this mass-produced, reproducible nanoparticulate-scaffold system allows for the controlled release of drug directly at the target site, with the capability of use with alternative drugs for other therapeutic applications.

REFERENCES: [1] I.F. Uchegbu, L. Sadig, M. Arastoo, A.I. Gray, W. Wang, R.D. Waigh and A.G. Schätzlein (2001) *Int. J. Pharm.*14;224(1-2):185-99. [3] R.A. Brown, M. Wiseman, C.-B. Chuo, U. Cheema and S. N. Nazhat (2005) *Adv. Func. Mater. 15, 1762-1770.*

ACKNOWLEDGEMENTS: Biodesign, EU Commision Framework 7.

Fabrication of cellular pre-crosslinked collagen based hydrogel

JPF Wong[1], DF Baptista[1], RA Brown[1].

[1 1]UCL, Institute of Orthopaedics- TREC, Stanmore Campus, London, UK

INTRODUCTION: Natural, protein-based scaffolds, such as collagen, are commonly subjected to cytotoxic cross-linking procedures to improve their mechanical properties. However, this prevents the initial incorporation of cells which must then be seeded later. Polymeric collagen offers a solution by having naturally cross-linked collagen fibrils, which can be blended with monomeric, acid-soluble collagen to give cell compatible hydrogels.

METHODS: Polymeric collagen from calf tendons was expanded in 0.5M acetic acid following EDTA treatment (Steven, 1967). Hydrogels were made by blending up to 50% polymeric collagen with monomeric, acid-soluble collagen. The blended collagen hydrogel was developed as a cellular ready-cross-linked material. Human dermal fibroblasts were added to neutral blended collagen solutions (0%, 20% 40% and 50% polymeric collagen; 15,000cells/2.5ml gel), and gels were set at 4°c for 24 hours. The hydrogel was then plastically compressed (Brown et al, 2005) to produce dense collagen constructs. Rate of compression for blended gels was measured as a function of the fluid expelled from the hydrogel (weight) during compression. Cell activity and proliferation within the gel (alamar blue and total DNA assays) was measured for up to 14 days of incubation. Additional cell viability assay was used to determine compatibility of polymeric collagen with interstitially seeded cells.

RESULTS: Rate of hydrogel compression was dependent on percentage polymeric collagen present within the gel. Compression of monomeric collagen gels 0% polymer was slowest at 19 minutes with an initial compression rate of 0.72 $g.min^{-1}$. 40% or 50% polymeric collagen samples have a doubled initial compression rate, and were completely compressed by 7 minutes. 20% polymeric collagen gels were compressed by 10 minutes and have an initial rate of 0.96 $g.min^{-1}$. Hence fluid expulsion was faster as PC content increased.

40% and 50% gels showed n initial reduction in total DNA suggesting early cell death. At day 7, all samples displayed marked increase in metabolism, coupled with a significant increase in total DNA within 50% polymeric collagen. Total DNA in 0%, 20% and 40% polymeric collagen samples displayed only a modest changes. Cell viability imaging indicated extensive cell death in 40% and 50% polymeric collagen samples after compression; but by day 7, this had recovered to 96.3±5.2% and 97.51±1.7% live cells respectively. 0% and 20% samples had good cell viability after compression (day 1) and day 7.

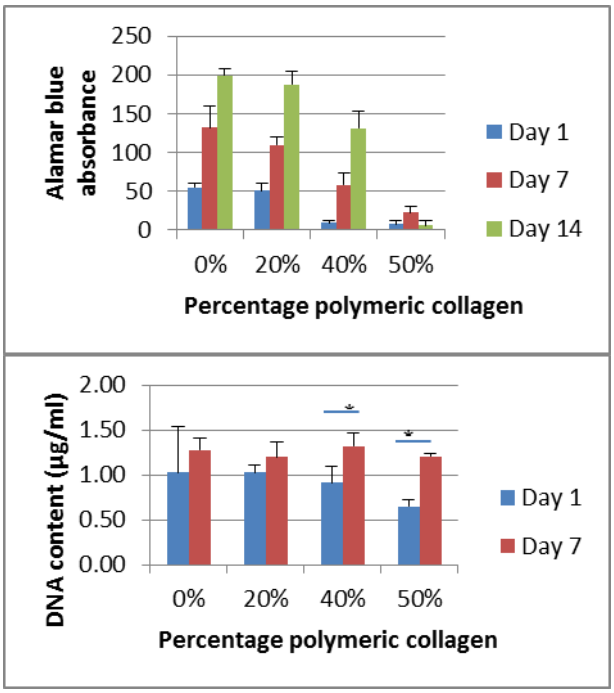

Fig. 1: Fibroblast metabolism and total DNA within blended gels (up to 14 days of incubation)

DISCUSSION & CONCLUSIONS: Hydrogels based on a blend of polymeric and monomeric collagen, resulted in non-aligned, but more importantly, cross-linked, cellular and 3D hydrogels. Initial, cell viability within the polymeric blended gels was reduced, probably by faster fluid flow during the compression; however, the material demonstrated good cell compatibility with incubation.

REFERENCES: [1] R. Brown, et al (2005) *Adv. Funct. Mater*. **15**, 1762-1770. [2] F. Steven (1967) *Biochim. Biophys. Acta.* **140**, 522-528.

ACKNOWLEDGEMENTS: Funded by European Union Framework 7 ‘‘BIODESIGN’’ programme.

Fabrication of vascularised tissues using 3D printing

Jing Yang[1], Kevin Shakesheff[1]

[1] *Tissue Engineering group, School of Pharmacy, The University of Nottingham, UK*

INTRODUCTION: Metabolically active tissues must reside within 200 μm of a capillary lumen to gain sufficient oxygen and nutrients for survival. Incorporation of a perfusing blood supply in tissue engineering design is vital for the scalability, survival and integration of almost all tissues with the exception of a few poorly vascularised tissues such as skin epidermis and cartilage. Promising results have been reported, in which delivery of angiogenic growth factors, genes and regenerative cell types as well as combination therapies were employed to promote vascularisation. However, the integration of these engineered tissues with the host remains a monumental challenge. To meet this challenge, the establishment of functional vasculature in engineered tissue constructs is likely to be required before transplantation. To this end, a recent research highlight has been the use of a sacrificial lattice of carbohydrate fibres to fabricate vascular-like tubule networks.[1] Here, we demonstrate a novel method for engineering vascularised tissues using 3D printing. A construct with an embedded tubule network in a hydrogel matrix has been successfully printed at cell-compatible conditions. The tubule network was then perfused with endothelial cells to form vasculatures.

METHODS: A Fab@Home™ printer was used to print the tubule network and the hydrogels. Human umbilical vein endothelial cells (HUVECs) were loaded in an ECM-like material, and then printed into a tubule network between two layers of printed hydrogels. For the sacrificial tubule network forming, a thermo-responsive material is printed into a pre-designed network structure, and then it was dissolved away at physiological conditions. Cells within the construct were imaged using a fluorescent microscope. Cells were stained by a live/dead or labelled by a red cell tracker. A tile scan was carried out to image an area larger than a single field of view.

RESULTS: HUVECs after 8 days culture were stained with live/dead (Figure 1). A tubule network facilitating the perfusion of HUVECs was printed within a hydrogel (Figure 2).

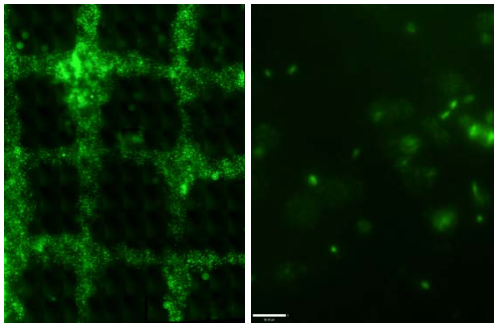

Fig. 1: A stitched image of a printed tubule network with HUVECs embedded in an ECM-like material (Left). An image of encapsulated HUVECs showing spreading of some cells (Right).

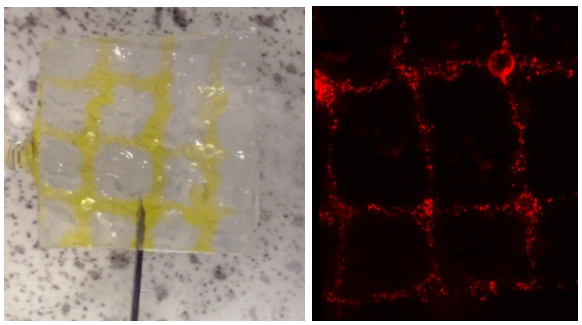

Fig. 1: Images of tubule networks embedded in a hydrogel perfused with a protein solution (Left) and HUVECs (Right)

DISCUSSION & CONCLUSIONS: The method reported here allows the fabrication of a vascular network at physiological conditions, a significant advance compared to carbohydrate fibre lattice which was printed at elevated temperature unsuitable for cells and biological materials. The cell-compatible printing environment would permit the simultaneous patterning of the tubule networks, hydrogel matrices and multiple cell types, which facilitates the mimicry of complex tissue structures in a single printing process. Future work will look to improve, measure and validate the architecture and function of the engineered vasculature.

ACKNOWLEDGEMENTS: The authors would like to thank the Nottingham Research Fellowship scheme and the ERC Advanced Grant (227845) for supporting this work.

REFERENCES: [1] Miller, et al (2012) *Nat Mater* **11**:768-774.

Compressed collagen hydrogels- An *in vitro* tissue model for decompression sickness

C. Walsh[1,2,3], N. Ovenden[3], E. Stride[4], U. Cheema[2]
[1]Centre for Mathematics and Physics in the Life Sciences and Experimental Biology (CoMPLEX), UCL, London UK.
[2] UCL Institute of Orthopaedics and Musculoskeletal Science, London, UK.
[3] Department of Mathematics, University College London, London, UK
[4]Institute of Biomedical Engineering, Old Road Campus Research Building, University of Oxford, Oxford UK.

INTRODUCTION: Decompression sickness (DCS) is a potentially fatal condition caused by the formation of inert gas bubbles in tissues following a rapid reduction in ambient pressure.
Despite having been recognized for over 100 years little is known about the formation and dynamics of these bubbles; or how this may vary between tissues and individuals. Difficulties in collecting relevant experimental data are a major impediment to this understanding.

METHODS: Plastic compression[1] of Collagen type I hydrogels provides a controllable system for studying bubble dynamics in tissue models.
This technique has been used to make a selection of biomimetic tissue constructs with varied tissue parameters such as diffusivity, cell type and density. A miniature pressure vessel, with optical access allows for the microscopic observation of bubble dynamics in these constructs during a dive simulation of up to 100m in depth.

A computational model has also been developed alongside the tissue model. This model simulates bubble dynamics in a block of tissue, over a dive profile. The experimental results are used to validate and refine the model.

RESULTS:
The computational model in this work is the extension of a 2D[2], to 3-dimensions. The model describes bubble dynamics via the following equations.

$$\frac{dm}{dt} = 4\pi R^2 D \frac{\partial c}{\partial r}\bigg|_{r=R} \quad (1)$$

Mass flux through the bubble wall, where m is mass, R is bubble radius and c is gas concentration.

$$c = kP \quad (2)$$

Henry's law for the concentration of gas dissolved in the tissue at a given pressure P; k is Henry's constant.

$$PV = m\alpha \quad (3)$$

The perfect gas law.

$$\frac{\partial c}{\partial t} = D\nabla^2 c \quad (4)$$

The diffusion equation, where D is the diffusion constant.

$$P_b = P_{amb} + \frac{2\sigma}{R} + \frac{4\pi}{3} R^3 \lambda \quad (5)$$

The Young-Laplace equation for the pressure inside the bubble, where σ is the surface tension and λ is the bulk modulus of elasticity.

DISCUSSION & CONCLUSIONS:

Current progress in the simultaneous development of a computational and 3D collagen tissue model for decompression sickness (DCS), is presented. Governing equations for the computational model are given.

REFERENCES: [1]Chappell, Michael. *Modelling and Measurement of Bubbles in Decompression Sickness*. Diss. University of Oxford, 2006.

[2] Jean-Pierre O'Brien (2013) Improved Characterisation and Modelling of Microbubbles in Biomedical Applications, Ph.D. Thesis, University College London.

Self-assembling peptide gels for intervertebral disc tissue engineering

S Wan[1], A Saiani[1], S Richardson[2], J Gough[1]

[1] *School of Materials, University of Manchester, UK.* [2] *Faculty of Medical & Life Sciences, University of Manchester, UK.*

INTRODUCTION: Low back pain (LBP) affects 80% of people in their lifetime and has been estimated to cost the UK economy £12 billion per annum[1]. LBP aetiology varies but intervertebral disc (IVD) degeneration is strongly associated with the condition[2].

IVDs are located in-between the vertebrae of the spine. Each consists of the tough, fibrous annulus fibrosus (AF) which surrounds the gel-like nucleus pulposus (NP). The IVD acts as a shock absorbing system, it also supports the axial body load and allows a range of movement in the spine. With age, the NP dehydrates and becomes more fibrous whilst the AF weakens and becomes disorganised[3]. This causes the IVD to degenerate and lose function, and often leads to LBP.

Current LBP treatments are symptomatic rather than curative. Also it is predicted that LBP prevalence will become more widespread, therefore a new strategy is urgently required for LBP management Cell-based therapies are regarded to hold particular promise in regards to LBP managment as they might be able to preserve, repair and even regenerate a degenerated IVD.

A self-assembling peptide hydrogel was investigated for its potential use as a NP tissue engineering scaffold due to its injectability, biocompatibility and the ease at which it can be modified to produce tunable properties.

METHODS: Two gel preparation protocols (A and B) were developed and compared to produce 30 mg ml^{-1} gels. The principal difference in gel preparation protocols was the final product homogeneity. The gels were characterised using atomic force microscopy (AFM) and rheology was used to test the mechanical properties. The behaviour of bovine NP cells (bNPCs) when encapsulated in the gels was investigated using various assays to determine cell morphology, viability and proliferation.

RESULTS: AFM was used to image the gels and showed that they consisted of a dense nanofibrous network. Rheology determined that gels produced using protocol A had comparable mechanical properties to the native NP (5.39 kPa[4]) however the gels weren't homogenous. Protocol B produced weaker but homogenous gels. Fluorescence microscopy showed that majority live cells were present throughout cell culture for both gel preparation protocols with cell viability between 70 - 90%. Crucially, bNPCs maintained their rounded morphology for the duration of the experiments which suggested that the cells preserved their NP phenotype when in 3D culture. A cell proliferation assay showed that there was no significant decrease in cell population for either gel preparation protocol. There was evidence of cell proliferation at later time points.

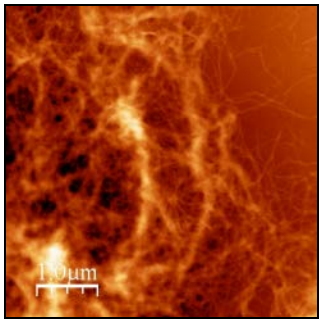

Fig. 1: Atomic force microscope micrograph (5x5 µm height mode scan) showing the nanofibrous architecture of the self-assembled peptide gel (0.25 mg ml^{-1}).

DISCUSSION & CONCLUSIONS: AFM micrographs showed that the gel network was on the nanofibrous scale. Separate fibres were of comparable size to individual collagen fibres whilst the observed larger assemblies were of similar scale to type II collagen found in the native NP. The hydrogel architecture likely mimicked the NP environment which allowed the bNPCs to preserve their phenotype. Evidence for the cells maintaining their NP phenotype was observed in fluorescent micrographs where bNPCs displayed rounded morphology. Results support the hypothesis that the peptide gel could act as a suitable scaffold for NP tissue engineering.

REFERENCES: [1] N Maniadakis, Gray A (2000) *Pain* **84**: 95-103 [2] K Cheung *et al* (2009) *Spine* **34**: 934-940 [3] J Urban *et al* (2003) *Arthritis* **5**: 120-131 [4] J Cloyd *et al* (2007) Eur Spine J **16**: 1892-1898

ACKNOWLEDGEMENTS: The authors would like to thank the EPSRC for providing financial support for this project.

Adipose-derived stem cells: isolation within the intraoperative timeframe and characterisation

A Wilson[1,2,3] , P Butler[1,3] , J Dye[2] , A Seifalian[3]
[1]*Department of Plastic and Reconstructive Surgery, Royal Free Hospital, Pond St, London NW3 2QG*
[2]*Restoration of Appearance and Function Trust, Mount Vernon Hospital, Northwood HA6 2RN*
[3]*Department of Surgery and Interventional Science, UCL, Royal Free Hospital, London NW3 2QG*

INTRODUCTION: The use of adipose-derived stem cells (ASCs) as an autologous and self-replenishing source of tissue provides much promise in reconstructive surgery[1,2]. Multiple methods of extraction of pluripotent adipose stem cells from lipoaspirated tissue have been described. The aim of this research was application of novel time- and yield- efficient ASC isolation protocol, which can be applied for use in the intraoperative timeframe to ameliorate results in reconstruction surgery.

METHODS: Six patients undergoing free fat transfer procedures donated surplus adipose tissue collected by the Coleman method from the abdomen for isolation and characterisation of ASCs. 10 grams of adipose tissue were washed, digested, centrifuged and filtered to obtain the ASCs pellet, which was cultured for 7 days. Cells were then FACS characterised using cell markers CD14, CD45, CD73, CD 90 and CD105 and HLA-DR.

RESULTS: Cells were isolated using a time-efficient protocol totalling two hours 30 minutes (Figure 1). Cultured cells (Figure 2) largely stained positive for CD73, CD90 and CD105, as expected from ASCs, and negative for CD14 and CD45.

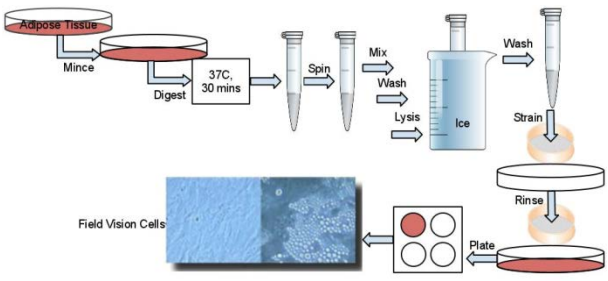

Fig. 1:Adipose-derived stem cell isolation protocol from Coleman-aspirated fat.

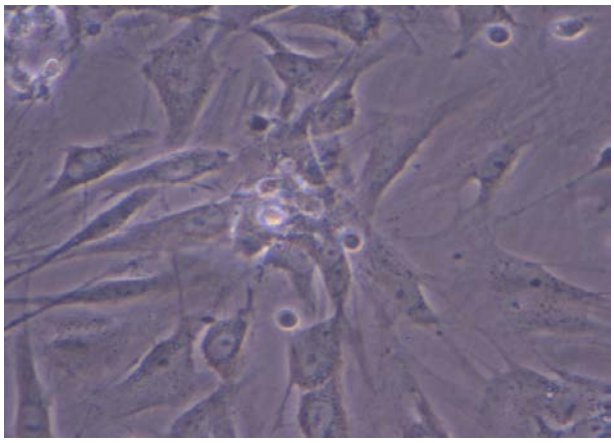

Fig. 2: Image of ASCs after 7 days of culture post-isolation.

DISCUSSION & CONCLUSIONS: An ASC isolation protocol suitable for use within the intraoperative timeframe has been identified. This may be further time-constrained from 2 hours 30 minutes to under one hour, by reduction of digest time of adipose tissue. Further manipulation of ASCs is advisable by directed differentiation, to demonstrate their multipotency.

1. **REFERENCES:** [1]Rigotti G, Marchi A et al. (2007) Clinical treatment of radiotherapy tissue damage by lipoaspirate transplant: a healing process mediated by adipose-derived adult stem cells. *Plast Reconstr Surg.* **119**, 1409-1422; [2] Zuk PA, Zhu M et al (2001) Multilineage cells from human adipose tissue: implications for cell-based therapies. *Tissue Eng.* **7**, 211–228; [3] Bunnell B, Flaat M et al (2008) Adipose-derived stem cells: isolation, expansion and differentiation. *Methods.* **45**, 115-120; [4] Lin CS, Xin ZC et al (2010) Defining adipose tissue-derived stem cells in tissue and in culture. *Histol Histopathol.* **25**, 807-815.

ACKNOWLEDGEMENTS: We would like to acknowledge the contribution of Adam Wilson.

Small-scale skeletal muscle constructs for *in-vitro* musculoskeletal junction pre-clinical testbed.

NM Wragg[1], DJ Player[1], Y Liu[2], MP Lewis[1]

[1]*Musculoskeletal Biology Research Group, School of Sport, Exercise and Health Sciences, Loughborough University*
[2]*Healthcare Engineering Group, School of Mechanical and Manufacturing Engineering, Loughborough University*

INTRODUCTION: Currently, musculoskeletal tissue damage is surgically repaired with the aim of restoring functionality over form. Any resulting tissue damage reduces utility and can increase the likelihood of further local injury. Therefore, more effective repair and regeneration techniques are needed.

By creating an in vitro musculoskeletal junction that closely replicates the form and function of the in vivo system, novel materials and chemical products could be tested for viability in a more representative manner.

In order to engineer a repeatable system capable of scaling-up, a small scale model of bone and muscle must be optimised.

METHODS: 0.75mL 3D type-1 rat-tail collagen (2.20mg/mL) neutralised constructs were seeded with C2C12 murine myoblast cells at $4x10^6$ cells/mL as previous described (*Sharples et al.* 2012) and set in a gelling area of 11mm x 14mm at 37°C, 5% CO_2 .The constructs were tethered at either end by bespoke polythene mesh floatation bars to create longitudinal lines of isometric tension *(Fig 1)*. Constructs were placed in 20% FBS high glucose DMEM for 4 days and then cultured in 2% horse serum high glucose DMEM to induce differentiation.

RESULTS & DISCUSSION: Immunohistochemical staining for the intermediate filament protein Desmin showed the capacity for alignment and differentiation of C2C12 myoblasts within the collagen system at this scale *(Fig 1)*. This replicates at a molecular level what is seen in larger constructs (*Sharples et al.* 2012).

CONCLUSIONS: Preliminary indications show that a small-scale tissue engineered muscle suitable for a preclinical test-bed is viable from a phenotypic standpoint. Myotubes are evident and aligned however genotypic considerations and co-cultured limitations with osteoblasts are yet to be taken into account.

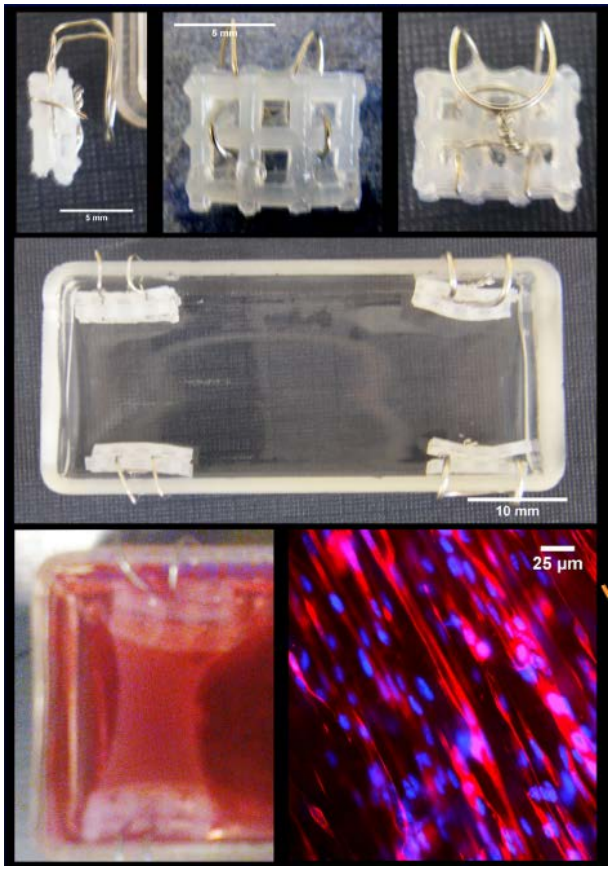

Fig. 1: Collagen Muscle System: 0.75ml collagen/cell hydrogel set between PTFE 'floatation bars'. Immunohistochemistry shows Desmin intermediate filament (red) and DAPI nuclear stain (blue) taken at edge of the gel (40x magnification).

REFERENCES: Sharples, A. P., Player, D. J., Martin, N. R. W., Mudera, V., Stewart, C. E., & Lewis, M. P. (2012). Modelling in vivo skeletal muscle ageing in vitro using three-dimensional bioengineered constructs. Aging cell, 11(6), 986–95.

ACKNOWLEDGEMENTS: With thanks to the EPSRC as the funding body.

Development of a novel polymer and cell source for a bioartificial liver

N Wung[1, 2], ZD Burke[1], MJ Ellis[2], D Tosh[1]

[1] Department of Biology and Biochemistry, University of Bath, UK. [2] Department of Chemical Engineering, University of Bath, UK.

INTRODUCTION: The primary treatment for liver failure is whole organ transplantation. However, there are fewer donor organs available than patients. Bioartificial liver (BAL) devices provide a potential interim therapeutic strategy for supporting a patient until a donor organ becomes available. BAL devices comprise a biological component (hepatocytes) with a bioreactor for replicating normal liver function within a 3D environment. The aim of this research is to develop a BAL using a novel polymer to construct hollow fibre bioreactors and to utilise an alternative source of hepatocyte-like cells (HLCs) created from the transdifferentiation (or conversion) of pancreatic cells. HLCs induced from the rat pancreatic cell line AR42J-B13 readily display normal liver cell functionality [1, 2].

METHODS: Flat sheet membranes were used for preliminary studies. Characterisation of the novel polymer (hereafter referred to as polymer X) was performed on flat sheet membranes. Membranes were cast through phase inversion of 20% w/w polymer X in NMP. Deionised water or 70% v/v industrial methylated spirits (IMS) in deionised water was used as the nonsolvent. Membranes were subsequently exposed to surface treatment for 1 min, 2 min or 5 min and the surface energy was analysed using the contact angle method by sessile drop. Statistical analysis of treatments was by a one-way ANOVA with Tukey's post-hoc tests using SPSS 20.

AR42J-B13 cells were seeded on to glass coverslips in 35mm culture dishes at a density of 30000 cells per dish. Cells were treated without or with 1μM dexamethasone (Dex) and 10ng/ml oncostatin-M (OSM) for 14 days and immunostained for the ammonia detoxifying liver enzymes glutamine synthetase (GS) and carbamoylphosphate synthetase (CPS).

RESULTS: Membranes undergoing surface treatment for 1 min showed significant reduction in the mean contact angle compared to the untreated control but thereafter showed no further significant change; this trend was seen for both nonsolvents (Fig. 1).

AR42J-B13 cells treated with Dex and OSM expressed GS and CPS (Fig. 2).

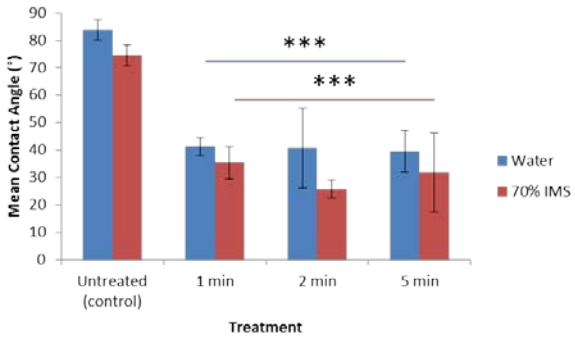

*Fig. 1: Surface treatment effect on polymer X surface energy on 3 randomly selected membrane sections. Error bars = ± 1 SD. ***p<0.005.*

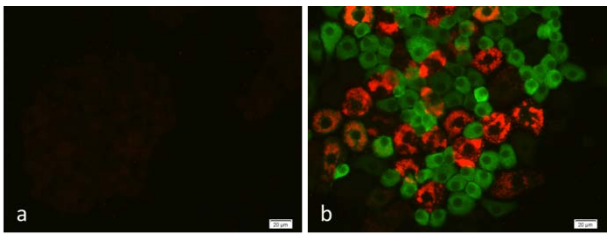

Fig. 2: Immunofluorescence of AR42J-B13 cells cultured on glass coverslips. Cells were treated without (a) or with (b) 1μM Dex and 10ng/ml OSM for 14 days and stained for GS (green) and CPS (red).

DISCUSSION & CONCLUSIONS: Surface treatment of the polymer demonstrated an increase in hydrophilicity compared to the control. The utility of AR42J-B13 cells to transdifferentiate to HLCs under Dex and OSM treatment has also been shown. Future work will assess the ability of the pancreatic cells to convert to HLCs on the novel polymer on both flat sheets and on the exterior of hollow fibre membranes.

REFERENCES: [1] Shen, C. N. *et al* (2000) *Nature Cell Biol* **2**: 879-887. [2] Burke, Z. D. *et al* (2006) *J Cell Physiol* **206**: 147-159.

ACKNOWLEDGEMENTS: We would like to thank the BBSRC and the University of Bath for funding.

Isolation and characterisation of mesenchymal stem cells from rat bone marrow and compact bone

N Yusop[1], AJ Sloan[1,2], R Moseley[1,2], RJ Waddington[1,2],

[1] *Tissue Engineering and Reparative Dentistry, School of Dentistry, Cardiff University, UK.*
[2] *Cardiff Institute of Tissue Engineering and Repair, Cardiff University, UK.*

INTRODUCTION: The application of mesenchymal stem cells (MSCs) for regenerative therapies and functional studies relies on establishment of reliable protocol for their isolation. The aims of this study were to compare the classical "stem cell" characteristics of MSCs from rat bone marrow and compact bone, by using different selection methods. Analyses allowed for comparisons to be made on clonal and non-clonal populations and MSCs successfully derived from different niche environments within the bone.

METHODS: MSCs were isolated from the femurs of 21 day old male Wistar rats by three different methods: Mononuclear marrow cells were isolated using histopaque density-gradient centrifugation [1] followed by fibronectin adherence selection of immature MSCs and isolation of clonal population expanded from a single cell colony [2] (FNA); Mesenchymal cells in bone marrow were separated from other cells by adherence and culture to plastic for 3 days followed by preferential selection of immature MSCs on fibronectin surfaces (PFNA); Derived from 3 day explant cultures of femoral bone chips previously cleared by collagenous digestion [3] (BCE). Cells were cultured in αMEM, 20% FBS, 100μM L-ascorbic acid 2-phosphate. Long term population doublings (PDs) were determined. Clones were analysed at 15, 50, 100PDs for a range of MSC markers by RT-PCR. Osteogenic / adipogenic potentiality was assessed.

RESULTS: *Cell isolation and cell morphology:* Isolation of heterogeneous populations (PFNA & BCE) was highly reproducible. For FNA, colony formation and successful clonal expansion was highly unpredictable. During early PDs heterogeneous populations exhibited cells with rounded or spindle morphology, but only spindle-like cells were observed after 50 PDs. Spindle cells only were observed in clonal FNA populations.

Stem cell characteristics: Heterogeneous populations, PFNA and BCE, demonstrated similar growth profiles with a noticeable increase in cell expansion noted after 5-10 PDs and 60 days in culture. Conversely, clonal FNA populations were more variable, with a slow PD until 70-125 days in culture, after which cell expansion rates were similar to heterogeneous populations. All MSC populations expressed MSC markers (Fig.2) which were maintained after 100 PDs. All were absent for CD45 and CD34 (haematopoietic cell marker) and differentiation markers for osteoblasts, adipocytes or chondrocytes. Additionally, all MSC populations demonstrated equivalent potentiality towards osteogenic and adipogenic differentiation.

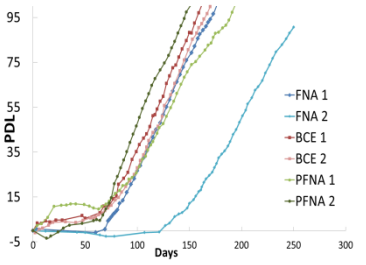

←*Fig 1: Growth profiles showing the sustained PDs of MSC and clonal variation*
↓Fig 2*: Continued expression of classical MSC markers.*

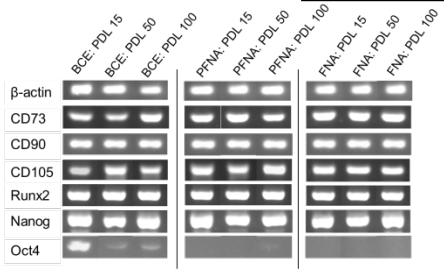

DISCUSSION & CONCLUSIONS: Regardless of the heterogeneity of the starting cell population, all methods allowed cell populations to be manipulated, yielding a predominant stem cell population after 10 PDs which demonstrated morphological uniformity, high and prolonged proliferative capacity, maintenance of stem cell markers and bi-potentiality. MSCs of equivalent characteristics were successfully isolated from the resident cells of bone marrow and endosteal niches. We propose that the support of other undefined cells in the heterogeneous populations allowed for the easier establishment of the MSCs compared to clonal lines.

REFERENCES: [1] J.H. Sung, H. M. Yang, J. B. Park, G. S. Choi, J. W. Joh, C. H. Kwon, *et al* (2008). *Transplant P.* 40:2649-2654. [2] R.J. Waddington, C.P. Lee, S.J. Youde, A.J Sloan (2008) *Cells Tissues Organs* 189:268-74. [3] H. Zhu, Z. K. Guo, X. X. Jiang, H. Li, X. Y. Wang, H. Y. Yao, *et al* (2010). *Nat protoc* **5**:550-560.

ACKNOWLEDGEMENTS: Supported by Ministry of Higher Education, Malaysia.